Wenmei Gai
Yunfeng Deng

Emergency Guidance Methods and Strategies for Major Chemical Accidents

Emergency Guidance Methods and Strategies
for Major Chemical Accidents

Wenmei Gai · Yunfeng Deng

Emergency Guidance Methods and Strategies for Major Chemical Accidents

Wenmei Gai
China University of Geosciences
Beijing, China

Yunfeng Deng
National Academy of Governance
Beijing, China

Preface

This book focuses on the optimization of public emergency behavior guidance strategies and methods for major chemical accidents. If the emergency guidance can help the public under the threat of accidents to understand the risks correctly and take reasonable emergency response actions in time, the whole emergency process will achieve good results. Taking toxic gas leaks and diffusion accidents as an example, it describes the characteristics of such accidents and the selection of public emergency guidance strategies such as sheltering in-place and evacuation, risk assessment, and characteristics of subregional evacuation. It has five chapters. Chapter 1 discusses the research background, basic concepts, and research development. Chapter 2 obtains the characteristics, development trend, and emergency evacuation level of hazardous chemical leaks through the statistical analysis of chemical leakage accidents in China from 2009 to 2018. In Chap. 3, the risk assessment method of sheltering-in-place for the blowout accident of high-pressure natural gas well containing hydrogen sulfide has been proposed. Apart from health consequences and accident probability under different protective measures, the method also considers the emergency response probability. In Chap. 4, a dynamic evacuation path planning model for major chemical accidents is proposed, which takes one or more factors in health consequences or transfer time as optimization objectives. Based on the above optimization objectives, it proposes a regional risk assessment method for emergency response, which also considers the regional population composition. In Chap. 5, based on simulation analysis, the subregional evacuation characteristics are studied.

The book summarizes the recent research outcomes achieved by the team of the first authors. The support and help from the first author's leaders and colleagues in China University of Geosciences (Beijing), as well as the students who participated in the research, are deeply appreciated. When composing the project research, Prof. Saïd Salhi, the tutor of the first author during her visit to the University of Kent, Prof. Cheng Wuyi, the colleague of the first author, Xi Xuejun, a professor-level senior engineer of China Academy of Safety Science and Technology, Jia Haijiang, the senior engineer of Beijing Municipal Institute of Labor Protection, and Li Jing, the senior engineer, have provided valuable opinions and suggestions. Moreover, Li Xin, the foreign-language scholar, and Hou Jie, Xu Ke, Shi Xiuli, Yue Yue, Jiang

Yanli, and Dong Hao, students of the first author, have all done a lot of work in format editing and manuscript proofreading. We feel grateful for all these efforts. Moreover, we have referred to research outcomes of scholars and researchers at home and abroad. Thus, heartfelt thanks to all who have helped.

Due to our limitations, there may be mistakes and weak spots. We welcome your corrections and suggestions.

Beijing, China   Wenmei Gai
                                                                                              Yunfeng Deng

Contents

Chapter 1
Why Do We Conduct the Study

1.1 Research Significance

Chemical industry is an important pillar of China's economy. With the rapid development of economy, the industrial cluster development in chemical industry is gradually increasing in China, and the number of construction projects and construction chemical industrial parks either planned or under construction is also rocketing year by year (Dou et al. 2019). By the end of 2017, chemical enterprises accounted for about 7% of the total number of industrial enterprises in China, and the output value of the chemical industry increased at an average annual rate of 18%. There were 502 national key chemical parks or industrial parks dominated by petroleum and chemical industry (Dong 2006). Although the chemical industry cluster promotes economic development, it brings serious safety problems. In the chemical industry cluster, various major hazard sources gather, involving dangerous materials and processes. Once a large number of accidental leakage or discharge of various types of flammables, explosive, and toxic gaseous and liquid substances produced, transported, stored, and used in the park due to human factors, equipment factors, production management, and environmental factors, a large amount of toxic gas may be released into the air and diffuse and form a toxic gas cloud, causing poisoning or casualties of personnel who have not been evacuated in time or have not taken effective protective measures near the leakage area (He et al. 2011). In recent years, there have been many serious toxic gas leaks and diffusion caused by the explosion, fire, and chemical leaks in China, most of which occurred in the chemical industry cluster area (as shown in Fig. 1.1). According to the summary and reflection on the emergency response of such accidents, the public in the accident scenes is the most direct harming object, meaning that the core disaster bearing body is exposed to the accident impact. When major toxic gas leaks and diffusion occur in the chemical industry cluster, guiding the public in the affected area to quickly and efficiently take protective actions (such as evacuation or sheltering in place) is crucial to reduce casualties and property losses (Georgiadou et al. 2010). The analysis of the regular pattern of public emergency
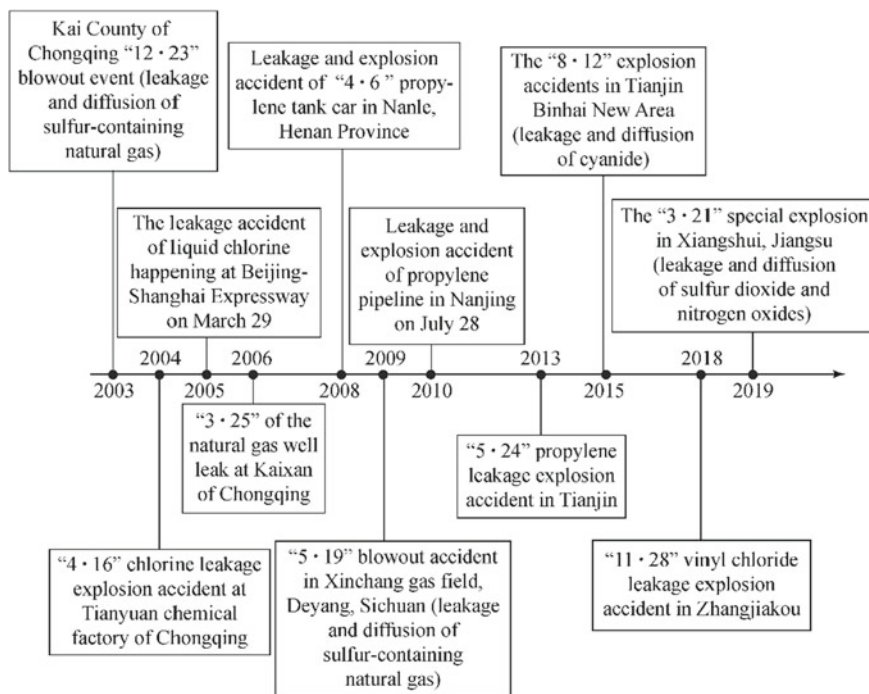
Fig. 1.1 Major toxic gas leaks and diffusion in China in recent years

behavior under such circumstances is a vital basis and premise for the optimization of public emergency behavior guidance strategy. Therefore, the purpose of this research topic is to meet challenges faced by chemical industry cluster in terms of safety production, improve the capacity of the authorities in mitigating, responding to, and making preparations for natural disasters, and ensure people's life and safety.

There are three characteristics of major toxic gas leaks and diffusion in the chemical industry clusters, which are significantly different from natural disasters (such as hurricane, earthquake) and building fire: ① All kinds of hazard sources gather in the chemical industry clusters, and there are many flammable, explosive, toxic, and harmful substances. Once a major toxic gas leak and diffusion occurs, there will be a large number of nonlinear dynamic relationships (such as secondary, derivative, and coupling) in the development and evolution of accidents, and the "chain reaction" is more serious; ② The scope of public emergency response may be expanded due to the evolution of accidents, which may result in the changes of the content and scope of warning information released by decision-makers accordingly (Take the explosion of liquid chlorine storage tank in Chongqing Tianyuan chemical factory on April 16, 2004, as an example. The field headquarters expanded the early warning range of 500−1000 m after 3 h in consideration of the possible explosion of 13 t liquid chlorine storage tank nearby); ③ There are obvious differences in the expansion model and the scope of geographical space of natural disasters (such as hurricanes, earthquakes,

etc.) or building fires and those caused by toxic gas leaks or explosion which causes the delivery of emergency information and the public's risk perception special when such accidents occur, and thus affecting the decision-making of individuals in terms of responses. From the above analysis, compared with natural disasters (such as hurricanes, earthquakes) and building fires, there are many differences in the evolution of disasters, the characteristics of responsible person's decision-making and the characteristics of individual risk perception. Thus, these differences also make public emergency actions for major toxic gas leaks and diffusion in the chemical industry clusters special, and they further affect the formulation of public guidance strategy in the accidents. However, according to the literature, the existing domestic and foreign researchers of public emergency behavioral regularity and optimization strategies discuss more of natural disasters (such as hurricanes, earthquakes) and building fires, which are not fully applicable to major toxic gas leaks and diffusions in chemical industry clusters.

Besides, there are some new characteristics and problems in emergency disposal and public protection of major toxic gas leaks and diffusion in chemical industry clusters over the years:

First, there are obvious diversification of emergency notification means and strategies. With the rapid development of science and technology, radio, television media, WeChat, and other network media have become possible emergency notification methods. Due to the organization of public evacuation and other public protection strategy implementation processes, the emergency scope may be expanded (Deng and Jiang 2009). Therefore, at different emergency response stages, the public may obtain emergency information through various channels and methods, such as face-to-face notification, telephone, radio, network, television, etc. The content of emergency information may vary from source to source and may also change with time, affecting the public risk perception and emergency response efficiency.

Second, the spread of rumors about the disaster through means of new media may bring about other negative social impacts. Once a major accident occurs, rumors of disasters usually spread quickly on social networks (Sahafizadeh and Tork 2018), which may cause adverse social effects. For example, after the accident occurs, a large number of public might take "shadow evacuation" behavior—meaning that the public in the area not affected by the accident may also carry out spontaneous evacuation, significantly pressuring on the traffic and affecting the efficiency of emergency evacuation and rescue.

Thirdly, taking emergency refuge does not limit to evacuation, while shelter-in-place can be used as an alternative. These two measures are the most important emergency protection for public protection in toxic gas leaks, and they help to reduce the loss and impact caused by the accident. At present, some enterprises have set up emergency shelters, and some residential buildings with good airtightness can also be used as temporary local shelters (Xi 2016). Therefore, after the major toxic gas leaks and diffusion occur in the chemical industry clusters, once the local refuge is ignored and the disordered evacuation is blindly selected, more avoidable casualties may be produced, which will affect public protection.

Fourth, the technical route in the relevant requirements and standards is not clear, so it is difficult to find applicable provisions. There are a lot of technical problems in the design of the emergency plan and the organization of emergency drills in chemical industry clusters. For example, the decision-making problems such as which way to take refuge, when the public shall start to evacuate, and what path evacuees shall follow to reach the destination (Dou et al. 2019).

To sum up, it has important theoretical and practical significances to conduct this research at present. This book shall deal with the major challenges faced by chemical industry clusters in terms of production safety and solve a large number of technical problems in handling and public protection of major toxic gas leaks and diffusions in such areas. It will help avoid the refuge risk caused by the mismatch between the emergency plan formulated by the designer and the actual public emergency behavior characteristics while trying to improve the disaster reduction and relief ability and ensure the people's life safety. The research results can improve the theoretical system of public protection and lay a scientific theoretical and methodological foundation for building a public emergency shelter guidance system.

1.2 Research Status and Development Dynamic Analysis

1.2.1 Research on the Law of Public Emergency Response Behavior

As early as in the 1950s, the characteristics of public emergency behavior have attracted people's attention. Early studies focused on the external behaviors (such as clustering, phototaxis, etc.) in the evacuation process (Killian 1952; Bryan 1957). Later, with the rise of the school of cognitive psychology, the characteristics of risk perception and its impact on individual behavior decision-making characteristics under information dissemination have also received extensive attention. In their research, Rogers and Sorensen (1993), Lindell et al. (2005), Klafft (2013), and other scholars pointed out that the dissemination of information in the emergency scenario is crucial to the public's risk perception. The source of information, communication channels, and content forms will greatly affect or even determine the public's risk perception of the event, thus affecting the decision-making of individual coping behavior. The above-mentioned research shows that there is a logical relationship among emergency information dissemination, risk perception and response behavior.

In terms of information dissemination, the traditional research methods mainly include information theory and communication science. The information field theory in information theory is an effective means to quantitatively study the evaluation of information influence. For example, Liu (2014) proposed to use the information field model to evaluate the information influence and apply it to citation analysis. The early information field theory was constructed based on the field theory to study the influence of information in the physical environment (Shannon 1948). In recent years,

many scholars have focused on the information field research based on social behavior (Fisher 2004). There is currently no public report on modeling and analyzing the information environment characteristics under an emergency based on information field theory. Most of the existing research on emergency information environment are based on communication studies to study the dissemination characteristics and influencing factors of early warning information or to analyze the communication strategies of early warning information (Wang et al. 2020, 2012), and do not involve quantitative research on the influence of emergency information.

Some scholars have studied the modeling of public emergency behavior decision-making from the perspective of sociology and psychology to explain how individuals understand the information and take corresponding actions after obtaining the relevant information of emergency. For example, Mileti and Sorensen (1990) studied the public response behavior under the effect of early warning information from the perspective of social psychology. They believed that the kind of behavior the public took after receiving the warning was the result of self-perception of danger. They also assumed the decision-making of individual emergency behavior as an orderly choice model. In addition to early warning information and their understanding of the situation, the public perception of the risk of emergency scenarios also depends on the behavior of people around (Wang et al. 2012). Lindell and Perry (2004) took the individual risk perception of environmental cues, social cues, early warning information as among the main influencing factors on public behavior decision-making, and put forward a decision-making model for the public to take protective actions under disaster conditions.

Mccaffrey et al. (2018) surveyed and analyzed the influencing factors of the public emergency behavior in wildfire disasters and pointed out that the public effectiveness in a particular response or action (evacuating, staying, or waiting), differences in risk attitudes, and the different emphasis on different emergency information (such as official warnings and environmental clues) are the key factors leading to different emergency behavior responses, and an emergency behavior decision model based on multiple logistic regression has been proposed. Sun (2018) built a public emergency behavior decision-making model with "information factors-public risk perception-response behavior" as the chain for typhoon disasters.

Based on sociological and psychological research, many scholars have studied the simulation model of public emergency behavior from the perspective of system dynamics. At present, the simulation model of emergency evacuation behavior or escape behavior characteristics is relatively in-depth, mainly based on microscopic evacuation models and multi-agent modeling techniques, tracking the details of the movement of each individual entity in the road network. These entities can be evacuated individuals or evacuated groups. For example, Wagner and Agrawal (2014) used multi-agent technology to establish a simulation model for evacuation of people in a fire scene in a concert venue. Targeting the evacuation problem of a school in Iquique, Chile during the tsunami. Zhao (2016) proposed a multi-agent-based cellular automata evacuation model for the evacuation of urban rail transit stations. Li (2016) combined the cellular automata model with the social force model, and proposed a simulation model for evacuation of high-rise buildings. Zhou (2013) proposed a

simulation method for emergency behavior decision- making based on a decision-making network, which considered the influence of various uncertain factors in the decision-making. Dou et al. (2019) conducted a retrospective analysis of the emergency evacuation research in chemical industry clusters from the perspective of general research framework, and they proposed the idea of establishing an emergency evacuation simulation model based on the combination of cellular automata and artificial neural network.

From the existing research, the research on emergency behaviors in natural disasters (such as earthquakes and hurricanes), building fires, and crowded stampede events in large-scale events is relatively extensive (Wagner and Agrawal 2014; Poulos et al. 2018; Zhao 2016; Li 2016; Collins et al. 2017; Fahy 2013). At present, the research on emergency behaviors specific to the major toxic gas leakage and diffusion scenarios in chemical industry clusters is relatively weak. The existing research results are not enough to accurately describe the public emergency behaviors in such accident scenarios. The following aspects are urgently needed for in-depth study.

First, the effect of emergency information dissemination on public risk perception needs to be further improved. The dissemination of risk information for emergencies will increase the public's risk perception, which in turn will promote the dissemination of risk information. Existing research shows that public risk perception plays a vital role in emergency information dissemination. However, the current research outcomes on the impact of emergency information dissemination on public risk perception are few, and most remain at the level of qualitative research. In the all-media era, once a major toxic gas leak and diffusion occurs in a chemical industry cluster, the public will often face a large amount of risk information through diversified media. Moreover, the public has personalized information needs and behavioral characteristics, so the relationship between the spread of multi-source heterogeneous emergency information and the public risk perception needs to be further studied from the quantitative perspective.

Secondly, the difference in the emergence mechanism of public emergency behavior at different stages of the life cycle of such accidents has not been considered. The current empirical research on risk perception of emergencies mostly collects data by conducting static questionnaires on the situation after the incident occurs, while less consideration has been given to the description of the changing process of the public perception of risk when the incident occurs. The public risk perception often varies at different levels due to its cognitive changes in the evolution of emergencies, thereby affecting the public response behavior characteristics (Lindell 2008). Therefore, it is necessary to introduce the time factor into the study of public risk perception of major toxic gas leaks and diffusion in chemical industry clusters, as well as to analyze the emergence mechanism of public emergency behavior when the disaster evolutes.

1.2.2 Research on Public Emergency Behavior Guidance Strategy

What kind of refuge the public is guided to take is the first problem to be solved (Smith and Swacina 2017). After the toxic gas leak occurs, the first evacuation method currently adopted by many European countries is to take shelter-in-place, while in China, people are usually evacuated (The Administrative Center for China's Agenda 21 2006). However, when evacuating many people threatened by the potential risks from dangerous areas to safe areas within a short period of time after the accident occurs, a lot of manpower, financial resources, and material resources are required. This is a very severe test for the government's emergency rescue capabilities. Therefore, Zhao (2011) suggested to learn from foreign experience and guide the public to adopt a combination of both measures. Shimada et al. (2018) pointed out that that it is necessary to analyze a series of factors before making a comprehensive judgment to choose shelter-in-place or evacuation, or to combine the two approaches. Judging from the current domestic and foreign research on the decision-making of emergency evacuation methods, the existing studies are mainly based on some principled frameworks, and the decision-making optimization research on emergency response methods is rare. The national standard of China, *Measures for the Division of Emergency Planning Areas for Major Toxic Gas Leaks* (GB/T35622—2017), lists the factors to be considered in the selection of emergency response methods, but does not specify the specific technical methods. The American Industrial Hygiene Association proposed the principle of determining the emergency response method for the public based on whether the concentration of on-site chemicals exceeds its critical concentration. In addition, some scholars have given optimization methods for the selection of emergency response methods for the public. For example, Georgiadou et al. (2010) proposed a multi-objective optimizations method for the implementation of public protection measures concerning health consequences, social instability, and economic costs for major accidents such as hazardous chemical fires, explosions, and spills; Yin et al. (2010) proposed a decision-making method to determine whether to choose shelter-in-place or evacuation during toxic gas leaks by using the tabulation method and decision tree according to the evacuation time, toxic load, and other parameters. These existing research results provide a reference for the weighing of public emergency response methods in major toxic gas leaks and diffusions.

However, the emergency decision for accidents is relatively strong time-constrained and the method proposed in the relevant literature (Georgiadou et al. 2010; Yin et al. 2010) needs to calculate the cumulative "toxic load" concerning health consequences at first. It would not only take a lot of time but also acquire the initial leakage parameters explicitly, which is difficult to implement in toxic gas leaks and diffusions caused by chemical fires or explosions (Xi et al. 2016).

After determining the emergency response, leading the public to choose the route to reach the target area needs to be considered. The research on the assignment of emergency routes made by the domestic and international scholars is more in-depth, especially in the public emergency behaviors and guidance strategies for building fires

as well as natural disasters such as earthquakes, hurricanes, and tsunamis, achieving fruitful results. These studies focused more on macroscopic evacuation models, not paying enough attention to detailed individual behavior. Instead, they transformed some constraints of road networks into constraint formulas on the network flow for optimization (Comfort 1994; Borrmann et al. 2012). On one hand, emergency route assignment faces a classic traffic problem—the performance of evacuation network depends on the traffic load situation, and the evacuation velocity of individuals in a specific road will get slower with the increase of the number of evacuees. Thus, it belongs to a dynamic decision-making problem (Vermuyten et al. 2016). On the other hand, since considering many practical factors in emergency route assignment is necessary, which include time efficiency, road complexity, or the probability of traffic congestions, it is also a multi-objective optimization problem (Ikeda and Inoue 2016). Based on the above, the emergency route assignment model and the corresponding algorithm have been addressed by some scholars. For example, Ikeda and Inoue (Ikeda and Inoue 2016) studied the evacuation route selection in natural disasters while considering the objectives of evacuation distance, evacuation time, and the safety of evacuation routes, and they presented a multi-objective planning model for evacuation routes. Yuan and Wang (2009) proposed an emergency path selection model under time-varying conditions, and on such basis, they further put forward a multi-objective optimization model and algorithm aiming at minimizing the total path travel time and path complexity. Based on the existing studies, the traditional traffic load curve is widely employed for describing the generation and loading process of evacuation population flow, which need to meet some certain assumptions. And this modeling method already has a good application effect responding to natural disasters like earthquakes. However, the dissemination rules of emergency information and the risk perception characteristics of the public under major toxic gas leaks and diffusions that occurred in the chemical industry clusters are different from those of general disasters, which further affects the time for the public to enter the emergency transportation network, and makes the pedestrian flow loading curve show particularity. Therefore, it is not accurate to use the typical traffic load curve to describe the loading law of pedestrian flow in such accident scenarios. In addition, only a few scholars have considered the practical factor of health consequences in the existing research on emergency route assignment. For example, Xiao et al. (2001) addressed the concepts of traffic difficulty coefficient and hazard coefficient, and established the equivalent length model for evacuation route selection of toxic gas leaks. Liu and Shen (2018) set up an evacuation path planning model with the goal of minimizing the damage to people's health during the evacuation of toxic gas leaks. Different from natural disasters such as earthquakes and hurricanes, extreme phenomena (e.g. sediments, toxic clouds, thermal radiation, overpressure and debris) caused by major toxic gas leaks and diffusions may adversely impact the public health in the affected areas, which changes with time as well (Georgiadou et al. 2007). As a result, if the individual doesn't wear protective equipment and chooses an emergency route without considering health consequences, he/she may face relatively higher health risks in the process of emergency transfer.

The assignment and planning of emergency routes can aid the selection of guiding points for public emergency behaviors, such as path decision points and path convergence points (Zhao 2016). However, for each selected guidance point, the guidance mode to be selected is a problem to be considered in the formulation of emergency behavior guidance strategy, including the form, quantity, and location of guidance media (Hou et al. 2014; Boukas et al. 2015; Yang et al. 2016; Zhao 2016). Some scholars have made a preliminary study on the emergency guidance mode. For example, Boukas et al. (2015) proposed a cellular automata simulation model that uses mobile robot agent to guide crowd evacuation, which served to analyze the influence of robot guidance on evacuation efficiency. Hou et al. (2014) studied the impact of the number and position of guide-posts on evacuation dynamic in a room with limited visibility. Yang et al. (2016) expounded the necessity of evacuation guidance, considered individualistic behavior, herding behavior, and environmental influence, successfully established a guided evacuation dynamics model. The research shows that the guidance with appropriate initial position and number is more conducive to the evacuation of pedestrians in moderate initial density. Zhao (2016) presented a multi-agent evacuation guidance model and studied the optimization of evacuation guides and intelligent guidance signs in evacuation guidance in urban rail transit stations. Gao et al. (2016) studied the influence on evacuation process of guiding personnel to provide evacuation direction guidance in a fixed position for evacuated pedestrians through sound, action, warning lights, etc. By introducing wireless communication theory to calculate the reliability of guidance signal to quantify the guiding force, a new pedestrian evacuation cellular automata model was proposed. In terms of the emergency evacuation of railway passenger station buildings, Wu (2016) worked on the role of broadcast guidance information and other factors on the evacuation process, constructed an evacuation mode based on auditory perception to simulate the evacuation process to explore the factors affecting evacuation efficiency. From the existing research, current public emergency behavior guidance model has not been built into a complete system. There has been few studies targeting the topic, and most of them proposed to independently analyze the influence of emergency behavior guidance mode on evacuation efficiency by setting a single guidance medium in a local position (such as a guide, a guide robot, a guide broadcast, a guide sign and a guide post, etc.), and seldom focus on the optimization of emergency behavior guidance mode from a global perspective, considering various factors comprehensively such as the selection of guidance points, the form of guidance media, the number of guidance media, and the location of guidance media. Furthermore, the regional evacuation process of major toxic gas leaks involves not only the process people evacuate from the inside of the building to the exit but also the movement process from the exit to the resettlement site. The existing minority studies mainly focus on the analysis of the internal building environment, and less on the optimization of emergency behavior guidance mode in the process of people moving to emergency shelters or emergency evacuation network exits after escaping from buildings.

1.2.3 Research on Development Trends

According to the current research outcomes, the research on public emergency behavior and guidance in building fires as well as earthquakes, hurricanes and other natural disasters at home and abroad is relatively strong, but is still weak in the major toxic gas leaks and diffusions occurred in the chemical industry clusters. Although many scholars at home and abroad have done a series of research on disaster prevention and mitigation, risk assessment, emergency plan formulation, and other aspects of major accidents in chemical industry clusters and achieved certain results, due to the lack of understanding of the complexity of emergency response decision-making in major toxic gas leaks and diffusions in chemical industry clusters, the research work on public emergency behavior and guidance strategy optimization seriously lag behind engineering application, which also leads to the absence of sufficient theoretical basis for the design and evaluation of emergency plans and emergency drills for such scenarios.

The organization scope of public emergency response to major toxic gas leaks and diffusions in chemical industry clusters may include thousands of residents living in a large range of buildings and communities, such as the evacuation of more than 65,000 people in the blowout accident in Kaixian County, Chongqing in 2003 (Li et al. 2009), and another one evacuating over 150,000 crowds in the surrounding area in the explosion accident of liquid chlorine storage tank in Chongqing Tianyuan Chemical General Factory in 2004 (Deng and Jiang 2009). It is usually not feasible to study the emergence mechanism of emergency behavior in the process of massive public emergency response by the empirical method (Sun 2018). With the development of a new generation of high-tech like data mining, information management, artificial intelligence, and other technologies, smart city construction is identified as a hot research direction of urban construction. In the view of literature retrieval, taking advantage of the opportunity of smart city construction, building a dynamic model of public emergency behavior by applying a new generation of high-tech research such as data mining and artificial intelligence, and then studying the law of public emergency behavior and guiding strategies through simulation analysis, has been one of the frontier directions of theoretical research on public protection of major toxic gas leakage and diffusion scenarios in chemical industry clusters (Chen et al. 2016; Zhao 2016; Li 2017; Dou et al. 2019; Osman 2019). Moreover, the boundaries between modern disciplines tend to be more blurred, and the disciplines penetrate each other. Thus, one of the current development trends in the theoretical research of public protection is to study the decision-making mode of public protection suitable for emergency situations by utilizing the interdisciplinary integration method comprehensively.

Considering the above discussions and existing research results, the book will target major toxic gas leaks and diffusions in chemical industry clusters and study the emergency behavior law and guidance strategy. Through utilizing the technologies and methods of statistical analysis, modeling and simulation, multi-objective optimization and heuristic solution, and the multi-disciplinary theories of engineering

science, social science, psychology, behavior science, and management science, it aims to improve the implementation effect of public emergency protection measures, such as shelter-in-place and evacuation, as well as to perfect the theoretical system of public protection. In the following chapters, this book will be oriented to reduce accident casualties, with emergency decision-making as the core, and emergency management process development as the clue to gradually explain its research content. The first is the research on the current situation of hazardous chemical leakage accidents and emergency response. The second is the accident site risk assessment and the research on the model and method of evacuation route planning when the accident occurs. The last is an empirical case study of evacuation.

References

Borrmann, A., A. Kneidl, G. Köster, S. Ruzika, and M. Thiemann. 2012. Bidirectional coupling of macroscopic and microscopic pedestrian evacuation models. *Safety Science* 50 (8): 1695–1703.

Boukas, E., I. Kostavelis, A. Gasteratos, and G.C. Sirakoulis. 2015. Robot guided crowd evacuation. *IEEE Transactions on Automation Science & Engineering* 12 (2): 739–751.

Bryan, J.L. 1957. A study of the survivors reports on the public in the fire at the Arundel park hall, Brooklyn, Maryland on January 29th 1956. *University of Maryland*.

Chen, C., J. Ma, Y. Susilo, Y. Liu, and M. Wang. 2016. The promises of big data and small data for travel behavior (aka human mobility) analysis. *Transportation Research Part C: Emerging Technologies* 68: 285–299.

Collins, J., R. Ersing, and A. Polen. 2017. Evacuation decision-making during hurricane Matthew: An assessment of the effects of social connections. *Weather Climate and Society* 9 (4): 769–776.

Comfort, L.K. 1994. Self-organization in complex systems. *Journal of Public Administration Research and Theory*, 4(3): 393–410.

Deng, Y.F., and C.S. Jiang. 2009. Survey on the public evacuation behavior in the "4·16" accident at Tianyuan Chemical Factory of Chongqing. *Journal of Safety Science and Technology* 5 (3): 30–35 (in Chinese).

Dong, C.Z. 2006. Study of development strategy of Tianjin Lingang industrial district. *Tianjin University* (in Chinese).

Dou, Z., A. Mebarki, Y. Cheng, X.P. Zheng, J.C. Jiang, and Y. Wang. 2019. Review on the emergency evacuation in chemicals-concentrated areas. *Journal of Loss Prevention in the Process Industries* 60: 35–45.

Fahy, R.F. 2013. Overview of major studies on the evacuation of World Trade Center Buildings 1 and 2 on 9/11. *Fire Technology* 49 (3): 643–655.

Fisher, K.E. 2004. Information behavior of migrant hispanic farm workers and their families in the Pacific Northwest information grounds, information behavior, behavior, Washington, immigrants, information habits. *Information Research: An International Electronic Journal* 10 (1): 199–203.

Gao, F.Q., Y.Y. Yan, C. Xu, L.X. Lin, H. Ren, and J.Z. Pei. 2016. A new cellular automata model for pedestrian evacuation considering guiding effects. *Journal of Transportation Systems Engineering and Information Technology* 16 (6): 60–66 (in Chinese).

GB/T 35622—2017. 2017. Method on determination of emergency planning zone for major accident of toxic gas leaks. *Beijing: Standards Press of China* (in Chinese).

Georgiadou, P.S., I.A. Papazoglou, C.T. Kiranoudis, and N.C. Markatos. 2007. Modeling emergency evacuation for major hazard industrial sites. *Reliability Engineering and System Safety* 92 (10): 1388–1402.

Georgiadou, P.S., I.A. Papazoglou, C.T. Kiranoudis, and N.C. Markatos. 2010. Multi-objective evolutionary emergency response optimization for major accidents. *Journal of Hazardous Materials* 178 (1–3): 792–803.

He, G.Z., L. Zhang, Y.L. Lu, and A.P.J. Mol. 2011. Managing major chemical accidents in China: Towards effective risk information. *Journal of Hazardous Materials* 187 (1): 171–181.

Hou, L., J.G. Liu, X. Pan, and B.H. Wang. 2014. A Social force evacuation model with the leadership effect. *Physica A: Statistical Mechanics & Its Applications* 400 (2): 93–99.

Ikeda, Y., and M. Inoue. 2016. An evacuation route planning for safety route guidance system after natural disaster using multi-objective genetic algorithm. *Procedia Computer Science* 96: 1323–1331.

Killian, L.M. 1952. The Significance of multiple-group membership in disaster. *American Journal of Sociology* 1952: 309–314.

Klafft, M. 2013. Diffusion of emergency warnings via multi-channel communication systems an empirical analysis. IEEE. In 2013 IEEE e*leventh International Symposium on Autonomous Decentralized Systems* (ISADS).

Li, Q. 2017. Research on emergency scenario deduction method based on big data. *Chemical Safety & Environment* 2017: 13 (in Chinese).

Li, J.F., B. Zhang, Y. Wang, M. Liu. 2009. The unfolding of '12.23' Kaixian blowout accident in China. *Safety Science*, 47(8): 1107–1117.

Li, L.H. 2016. Study on individual and small groups behaviors in high-rise building evacuation. *Tsinghua University* (in Chinese).

Lindell, M.K., and R.W. Perry. 2004. *Communicating Environmental Risk in Multiethnic Communities Thousand Oaks*. London: Sage Publications.

Lindell, M.K., J.C. Lu, and C.S. Prater. 2005. Household decision making and evacuation in response to hurricane Lili. *Natural Hazards Review* 6 (4): 171–179.

Lindell, M. K. 2008. EMBLEM2: An empirically based large scale evacuation time estimate model. *Transportation Research Part A: Policy and Practice*, 42(1): 0–154.

Liu, H.L., and F. Shen. 2018. Evacuation route planning model based on toxic injury index. *China Safety Science Journal* 28 (1): 179–184 (in Chinese).

Liu, Y. 2014. Assessment of information influence based on information field and applicated on citation analysis. *Shanghai University* (in Chinese).

Mccaffrey, S., R. Wilson, and A. Konar. 2018. Should I stay or should I go now? Or should I wait and see? Influences on wildfire evacuation decisions: Should I stay or should I go now? *Risk Analysis* 38 (1): 1390–1404.

Mileti, D.S., J H. Sorensen. 1990. Communication of emergency public warnings. *Oak Ridge Laboratory* ORNL-6609, Washington, D.C.

Osman, A.M.S. 2019. A novel big data analytics framework for smart cities. *Future Generation Computer Systems* 91: 620–633.

Poulos, A., F. Tocornal, D.L.L.J. Carlos, J. Mitrani-R. 2018. Validation of an agent-based building evacuation model with a school drill. *Transportation Research Part C: Emerging Technologies*, 97: 82-95.

Rogers, G.O., and J.H. Sorensen. 1993. Diffusion of emergency warning: Comparing empirical and simulation results. *Risk Analysis* 8: 118–134.

Sahafizadeh, E., and L.B. Tork. 2018. The impact of group propagation on rumor spreading in mobile social networks. *Physica A: Statistical Mechanics and Its Applications* 506: 412–423.

Shannon, C.E. 1948. A mathematical theory of communication. *Mobile Computing and Communications Review* 5 (1): 3–55.

Shimada, Y., S. Nomura, A. Ozaki, A. Higuchi, A. Hori, Y. Sonoda, K. Yamamoto, I. Yoshida, and M. Tsubokura. 2018. Balancing the risk of the evacuation and sheltering-in-place options: A survival study following Japan's 2011 Fukushima nuclear incident. *British Medical Journal Open* 8 (7): 2044–6055.

Smith, D.A., and P.J. Swacina. 2017. The disaster evacuation or shelter-in-place decision: Who will decide? *Journal of the American Medical Directors Association* 18 (8): 646–647.

Sun, D. 2018. Research on typhoon disaster warning scheduling based on public risk perception. *Harbin Engineering University* (in Chinese).

The administrative center for China's agenda 21. 2006. *Guidelines on Emergency Response System for Chemical Industry Parks.* Chemical Industry Press (in Chinese).

Vermuyten, H., J. Beliën, and B.L. De. 2016. A review of optimization models for pedestrian evacuation and design problems. *Safety Science* 87: 167–178.

Wagner, N., and V. Agrawal. 2014. An agent-based simulation system for concert venue crowd evacuation modeling in the presence of a fire disaster. *Expert Systems with Applications* 41 (6): 2807–2815.

Wang, J.J., Z.G. Jiang, Y.F. Deng, and J.S. Chen. 2012. Modeling and influence factors of warning dissemination. *Journal of University of Science and Technology Beijing* 12: 97–101 (in Chinese).

Wang, S., W. Cheng, Y. Deng, and J. Hou. 2020. Enforced strategy for efficiently improving warning communications among evacuees. *Safety Science* 122: 104506.

Wu, Y. 2016. Emergency evacuation safety research for large railway stations based on auditory perception. *Harbin Institute of Technology* (in Chinese).

Xi, X.J. 2016. An evaluation method on effect of shelter in toxic gas accident. *Journal of Safety Science and Technology* 12 (1): 65–69 (in Chinese).

Xi, X.J., C.L. Shi, and D.J. Dai. 2016. Assessment method of personnel evacuation safety based on dynamic toxic load. *Journal of Safety Science and Technology* 12 (5): 170–173 (in Chinese).

Xiao, G.Q., L.M. Wen, B.Z. Chen, and H. Wang. 2001. Shortest evacuation route on toxic leaks. *Journal of Northeastern University* 22 (6): 674–677 (in Chinese).

Yang, X.X., H.R. Dong, X.M. Yao, X.B. Sun, Q.L. Wang, and M. Zhou. 2016. Necessity of guides in pedestrian emergency evacuation. *Physica A: Statistical Mechanics and Its Applications* 442: 397–408.

Yin, X., X.H. Pan, and Y.J. Wu. 2010. Decision making of personnel emergency protective actions for toxic gas leaks. *Journal of Nanjing University of Technology (Natural Science Edition)* 32 (1): 64–68 (in Chinese).

Yuan, Y., and D.W. Wang. 2009. Path selection model and algorithm for emergency logistics management. *Computers and Industrial Engineering* 56 (3): 1081–1094.

Zhao, Y.H. 2011. Research on personal protection and shelter manner in hazardous chemicals accidents. *China Safety Science Journal* 21 (9): 131–137 (in Chinese).

Zhao, W. 2016. Research on emergency evacuation guidance of urban rail transit station based on multi-agent. *Capital University of Economics and Business* (in Chinese).

Zhou, J.F. 2013. Study on an emergency response behavior decision-making simulation method for industrial accidents. *Industrial Safety and Environmental Protection* 39 (11): 32–35 (in Chinese).

Chapter 2
Hazardous Chemical Leakage Accidents and Emergency Evacuation Response from 2009 to 2018 in China

2.1 Introduction

In this chapter, we will make a statistical analysis on the leakage accidents of hazardous chemicals in recent years and study the emergency evacuation response, which can help clarify the characteristics of such accidents and understand the development tendency as well as challenges of emergency protection actions.

Since the second half of the twentieth century, hazardous chemical accidents (HCAs) have occurred all over the world that has increasingly become a major issue (Filiz and Pinar 2006). In China, the annual growth rate of the gross industrial product of the chemical industry has been far higher than that of the growth domestic product (GDP) since 2009 (China Statistical Yearbook 2019). Meanwhile, the speedy advance in China's chemical industry has not only increased the pressure of environmental governance, but also promoted the hazardous chemical accidents to gradually become an important threat to the safety of Chinese public life and property (Liu et al. 2005). Therefore, the safety of chemical industry has attracted more and more scholars' attention in recent years (Zhang and Zheng 2012; Shen et al. 2015; Dou et al. 2019).

So far, the space and time characteristics of HCAs, the types and causes of accidents, the types of chemicals involved, and the emergency response methods (Zhong et al. 2010; Tong et al. 2015; Heo et al. 2018; Wang et al. 2020) have been studied through statistical analysis. By analyzing 169 accidents in the French chemical industry, Dakkoune et al. (2018) drew a conclusion that human error was the leading cause of HCAs. Furthermore, the statistics of Zhang and Zheng (2012) showed that in China, about a fifth of HCAs will need the evacuations of nearby residents. For the control of HCAs occurrence and the consequences minimization, a variety of models have been proposed as risk assessment tools of hazardous chemical leakage

and the decision support system for emergency response decisions (Zografos and Androutsopoulos 2008; Qin et al. 2020; Zhou and Reniers 2021).

It is noteworthy that the most common situations in HCAs are found to be hazardous chemical leakage accidents (HCLAs), while transportation is the link most likely to cause such accidents (Yang et al. 2010). Due to some chemicals transport routes inevitably crossing heavily populated areas, the leakage of hazardous chemicals during transportation will pose a serious threat to public safety (Jardine et al. 2003). Furthermore, if emergency measures are not taken timely and effectively, the leakage of hazardous chemicals may induce secondary accidents (such as poisoning, explosion, and fire) and further worsen the situation. To address hazardous chemical leaks, Korean scholars worked to provide the safest evacuation route in the emergency evacuation plan using the deep neural network (Seo et al. 2021). In China, however, there still need more systematic studies in terms of the public evacuation induced by HCLAs.

Therefore, HCLAs between 2009 and 2018 occurred in China are collected and analyzed in this study to explore the features of HCLAs as well as the status of the emergency evacuation. Based on the statistical data, we first discuss HCLAs from time, space, and type and analyze five typical HCLAs in detail. Then, HCLAs are divided into four categories, including civilian residence, factory (industrial park), pipeline, and road transportation, and their respective characteristics are further analyzed. The evacuation induced by HCLAs has also been analyzed by classification to study the influencing factors of emergency evacuation using correlation analysis. Based on the statistical results, a comprehensive management framework including the safety management system of hazardous chemicals and the emergency protection actions in HCLAs is proposed. Finally, a conclusion has been drawn.

2.2 Methodology

2.2.1 Data Collection

Two data sources of China's HCLAs utilized in this study were the petrochemical accident statistics and data analytics platform (Accident.NRCC, http://accident.nrcc.com.cn:9090) and the Chinese chemical safety network (NRCC, http://service.nrcc.com.cn). Accident.NRCC was revised from the chemical accident information network in 2012, aiming at actively tracking the dynamics of chemical accidents at home and abroad and collecting accident resources systematically, comprehensively, and immediately. The present study has analyzed data from the HCLAs occurring in China during the period between January 1, 2009, and December 31, 2018, which refers to accidents caused or would have led to grave consequences for the leakage of hazardous chemicals. Among all of these accidents, we mainly got the information of the 2009–2012 cases from NRCC and used Accident.NRCC for the 2013–2018 cases. Besides, some news reports, as well as the local government sites, were used to supplement the case information.

The main information of HCLAs used in this chapter comprises time, location, types of chemicals involved, causes of accidents, casualties, and emergency actions. The research counted a total of 5207 hazardous chemical leakage accidents that occurred in China from 2009 to 2018, involving all provinces of the country (as the accident statistics system is still improving continuously, it might cause the loss of data in a small number of hazardous chemicals leakage cases). Therefore, the statistical results can help reveal the development trend and emergency response characteristics of hazardous chemical leakage accidents in China in recent years.

2.2.2 Methods

2.2.2.1 Statistical Methods of Hazardous Chemical Leakage Accidents

First of all, the valid information in the collected accident reports was extracted and then transformed into the data to build an Excel-format database. On this basis, the statistical results were analyzed in detail from time, space, occurrence site, accident causation, and consequences induced by HCLAs. The assessment indicators of HCLAs consist of accident frequency, accident rate, and mortality. The accidents frequency (F) refers to the number of HCLAs per unit time (e.g., per month or per year). The accident rate (AR) is calculated as the ratio of the amount of a certain type HCLAs to the total amount of hazardous chemical leaks that occurred in the current month (or year), which can be represented as follows:

$$AR_i = F_i/N_i \tag{2.1}$$

where i refers to the month (or year) in which the statistics occur; AR_i represents the accident rate of HCLAs in that month (or year); F_i is the frequency of HCLAs per month (or per year); and, N_i refers to the total number of HCLAs.

Mortality (M) refers to a parameter reflecting the death toll in HCLAs and can be calculated as follows:

$$M = n_d/F \tag{2.2}$$

where n_d is the death toll caused by HCLAs.

2.2.2.2 Classification of Evacuation Levels

Evacuation shall be implemented timely after the leakage of hazardous chemicals in areas that may be affected in the case that shelter-in-place cannot ensure personnel safety. So far, China has not yet set up a special statistical database in the field of evacuations. Therefore, the evacuation information discussed in this chapter was

obtained by searching the accident disposal part in the HCLAs database and supplemented with the relevant resources of official government websites and other news websites. The evacuation events selected in the retrieval process are in accord with the two following conditions.

(1) Evacuations that caused by the leakage of hazardous chemicals or its secondary disasters (such as poisoning, explosion, fire) from January 1, 2009, to December 31, 2018.
(2) Evacuations that involved at least 100 people or 50 households or the occupants over one independent building.

The difference of resources consumed by evacuation can be reflected in the evacuees' amount, the duration of the evacuation process, and the size of the evacuation area. In this sense, evacuation level (L) can be divided into five categories based on evacuation scope (S), evacuation duration (T), and evacuation number (P): I extra-small-scale evacuation; II small-scale evacuation; III medium-scale evacuation; IV large-scale evacuation; V extra-large-scale evacuation. The evacuation level can be defined as follows:

$$L = S + T + P \tag{2.3}$$

here, variable S represents the grade coefficient of the evacuation range, taking 1, 2, or 3 based on the size; variable T represents the grade coefficient of the evacuation duration, which can be taken as 1, 2, or 3 based on the length of time; similarly, variable P is the grade coefficient of the evacuated population, which can be taken as 1, 2, or 3 according to the number of evacuees. Table 2.1 shows the evaluation criteria of S, T, and P. To sum up, the evacuation level L can be graded according to the following criteria: when $L \geq 8$, the evacuation level is set to Level V (named extra-large-scale evacuation); when $L = 7$, the evacuation level is Level IV (named large-scale evacuation); when $L = 6$, the evacuation level is Level III (named medium-scale evacuation); when $L = 5$, the evacuation level is Level II (named small-scale evacuation); and when $L \leq 4$, the evacuation level is set to Level I (named extra-small-scale evacuation). Figure 2.1 is constructed as a three-dimensional coordinate to show the classification results of evacuation levels more clearly and intuitively.

2.3 Characteristics of Hazardous Chemical Leakage Accidents

2.3.1 Time Volatility of HCLAs

The time distribution of hazardous chemical leakage accidents in China from 2009 to 2018 is shown in Fig. 2.2. It can be seen from the statistical results that the change in the number of HCLAs mainly experienced three phases.

Table 2.1 Evacuation classification criteria

Grade	Number of evacuees (N)	Evacuation duration (t)	Range of evacuation (R)
1	$N < 1000$	$t < 60$ min	$R < 500$ m or just a few buildings
2	$1000 < N < 5000$	60 min $< t < 300$ min	500 m $< R < 2000$ m or a village (community, industrial park, school, etc.)
3	$N > 5000$	$t > 300$ min	$R > 2000$ m or more than one village (community, industrial park, etc.)
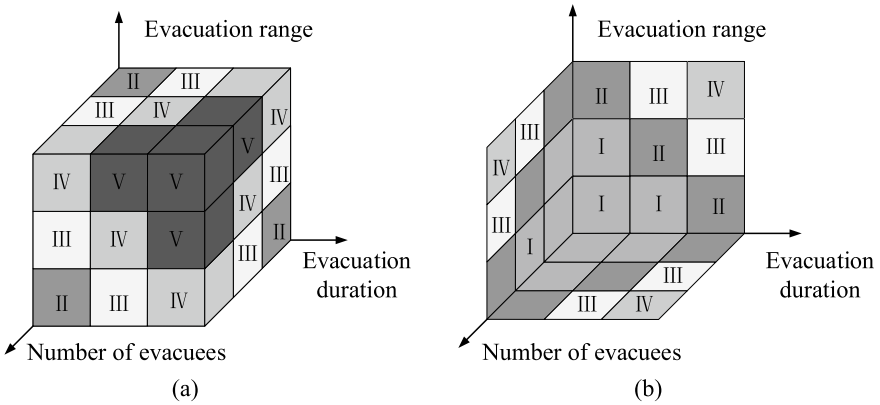
Fig. 2.1 Criteria for grading evacuation levels **a** evacuation level on top, front, and right sides; **b** evacuation level on bottom, back, and left sides
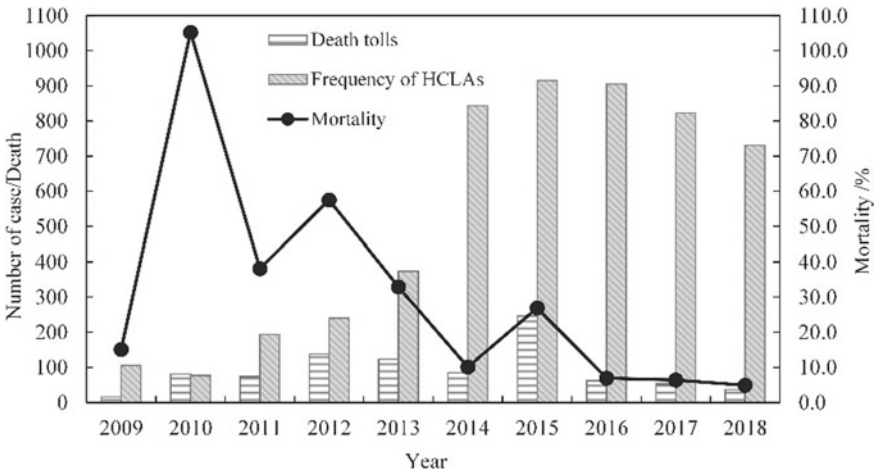
Fig. 2.2 Distribution of HCLAs by year

(1) From 2009 to 2010 is the first phase. The number of HCLAs witnessed a slight drop during that time, from 106 to 77. The reduction in the accident number was related to the increase of funds invested in emergency management to a certain extent. In 2010, China hosted the Guangdong Asian Games and the Shanghai World Expo. For the support of major activities, plenty of resources were invested by the Chinese government in the improvement of chemical industry level through a series of regulatory policies. However, two major accidents that killed more than 20 people in 2010 caused an increase in mortality of HCLAs at this phase.

(2) From 2010 to 2015 is the second phase, when the number of HCLAs increased more than ten times (from 77 to 914). Coinciding with China's implementation period of the "Twelfth Five-Year Plan" (2011–2015), the chemical industry has developed rapidly with the support of national policies. However, the regulatory capacity at that time could not match its development.

(3) After 2015, the number of accidents decreased year by year, which is the third stage. The effective reduction of HCLAs benefited from the revision of the work safety law of the People's Republic of China in 2014, making it more suitable for the current development of China's petrochemical industry.

In terms of the mortality rate of HCLAs, except 2015, the number of casualties has decreased year by year since 2012, rather than increasing with the increase of the number of accidents. The promulgation and implementation of the regulations on the safety management of hazardous chemicals in China in 2011 may be the turning point leading to the decline of mortality. After the promulgation of the regulations, the mortality first increased and then decreased year by year, which is in line with the safe Kuznets curve (Dumrongpokaphan and Kreinovich 2018); however, the mortality and the death toll of HCLAs in 2015 were much higher than those in other years. This can be mainly attributed to the occurrence of "8·12" explosion accident in Tianjin Binhai New Area, which killed 165 people. Consequently, the prevention of such extraordinarily serious HCLA will be a significant aspect of the risk reduction of hazardous chemicals.

Figure 2.3 displays the monthly frequency of HCLAs from 2009 to 2018. As Fig. 2.3 shows, clearly, April to October is the month with high frequency of HCLAs. In addition, the highest frequency of accidents occurred in July and August, with over 500 accidents per month. This could be explained by two reasons. On the one hand, from April to October is the peak season of trade in China. During this period, with higher chemical production and circulation intensity, the frequency of HCLAs increased correspondingly. On the other hand, hot and humid weather can have a serious impact on chemical reaction activities, and the hot season in China usually comes in July and lasts at least until August. Moreover, it is difficult for people to maintain their attention in such a season (Kang and Ryu 2019), so the possibility of HCLAs caused by human errors increases. Due to the Chinese Lunar New Year generally in January and February, these two months have the lowest accident frequency. Especially in February, the total number of HCLAs was less than 300. When employees return to their hometowns for the holiday, the majority of
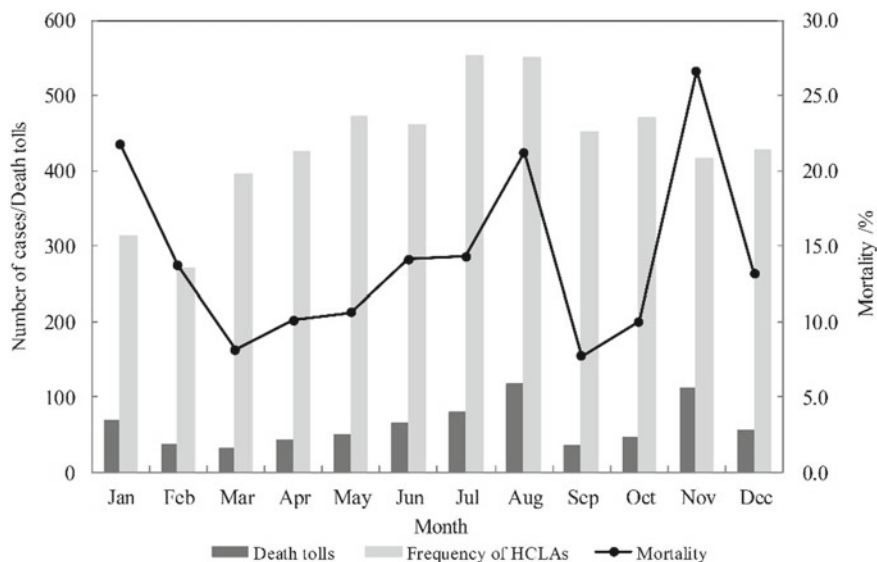
Fig. 2.3 Distribution of HCLAs by month

chemical enterprises will suspend production as well. Besides, the government will augment the supervision of all links of chemicals during the Spring Festival, which significantly reduces the occurrence of HCLAs.

The mortality of HCLAs reached the highest in November, followed by January, which is associated with China's climate. The secondary disasters caused by the hazardous chemical leakage are the main reason of death, such as poisoning, explosion, and fire. From November to January of the next year, most residents in Northern China use gas for heating their houses to survive the cold winter. Once people's improper operation causes gas leakage, they will be in danger of poisoning and death. November is when residents begin to use gas for heating every year, and problems such as pipeline aging and equipment failure are prone to be ignored at this time, which may induce more gas poisoning cases. In addition, the third-highest mortality of HCLAs is in August, when the humid and hot climate strengthens the chemical reactions to cause secondary disasters and heavy casualties easily.

2.3.2 Provincial Location Distribution of HCLAs

Combined with economic development and chemical industry level, we analyzed the occurrence and mortality of HCLAs in 34 provincial-level administrative regions during 2009–2018. Figure 2.4a compares the number of HCLA in each province with its annual GDP (at 2019 prices) and shows that the provinces with higher GDP happened more HCLAs. Similar to hazardous chemical accidents (Duan et al. 2011),

HCLAs disperse unequally in different regions. The top two provinces with the highest frequency of HCLAs are Jiangsu and Shandong Provinces (419 cases and 408 cases), followed by Zhejiang, Hubei, and Guangdong Provinces, with more than 300 cases. The petrochemical industry in these provinces is relatively developed, and its massive scale of employees increases the possibility of human error leading to HCLAs (Zhang and Zheng 2012). Consequently, China's emergency management should focus on chemical safety management in provinces where HCLAs frequently occurred, such as Jiangsu, Shandong, Zhejiang, and strive to minimize the occurrence of hazardous chemical leaks.

However, the mortality of HCLAs is not positively correlated with accidents amount in different provinces. Figure 2.4b demonstrates that the top seven provinces in terms of mortality are Taiwan, Tianjin, Shanghai, Hebei, Shaanxi, Qinghai, and Heilongjiang, while their annual GDPs are not in the forefront of the national level. For example, contrary to the high mortality, the annual GDP and the death toll of HCLAs in Qinghai and Heilongjiang are low. It could be reflected that the provinces with underdeveloped chemical industries rarely have HCLAs, but at the same time, they lack the ability to effectively mitigate the accident. Generally, it is difficult for provinces to take measures to control damage right after the hazardous chemical leakage. We can find that the case number, death tolls, and mortality of HCLAs are all high in Shaanxi. Therefore, the supervision of hazardous chemicals should be strengthened in provincial departments to improve their prevention and emergency response ability under the scenario of HCLA.

In combination with Figs. 2.4a, b, Taiwan, Tianjin, Shanghai, and Hebei rank among the top four in terms of mortality, while the number of HCLAs is not as high as that in other provinces. The survey results show that these provinces have all experienced the HCLAs causing mass deaths. In 2010, a coal gas leak at the Hebei Iron and Steel Company killed 21 people. In 2013, the leakage of liquid ammonia in the cold storage of the Shanghai Industrial Park resulted in 15 deaths. In 2014, there were 30 victims dead in the leakage accident of an underground propylene pipeline in Taiwan. And a year later, a huge explosion involving a variety of hazardous chemicals occurred in Tianjin Binhai New Area, killing 165 people.

Shandong has the second-highest death toll of HCLA in China except Tianjin. In 2013, an oil pipeline leakage accident occurred in Qingdao, which significantly increased the death toll in Shandong Province. In this accident, the leaked crude oil was accidentally detonated, killing 62 people.

During the statistical period, there have been many major accidents and extraordinarily serious accidents in China, which reflect that the emergency response capability of most regions still needs to be improved. Therefore, to prevent or eliminate accidents, the dual-prevention working mechanism for risk grading management, hidden trouble investigation is adopted in the chemical industry in China. The adoption of technologies such as dynamic monitoring of hazardous chemicals and early warning of abnormal situations can help the government intervene before emergencies occur. Personal protection and emergency rescue are the final measures to cut down the risk of HCLAs. Improving the government's emergency rescue capability and the public's self-rescue and mutual rescue capability play roles in avoiding the
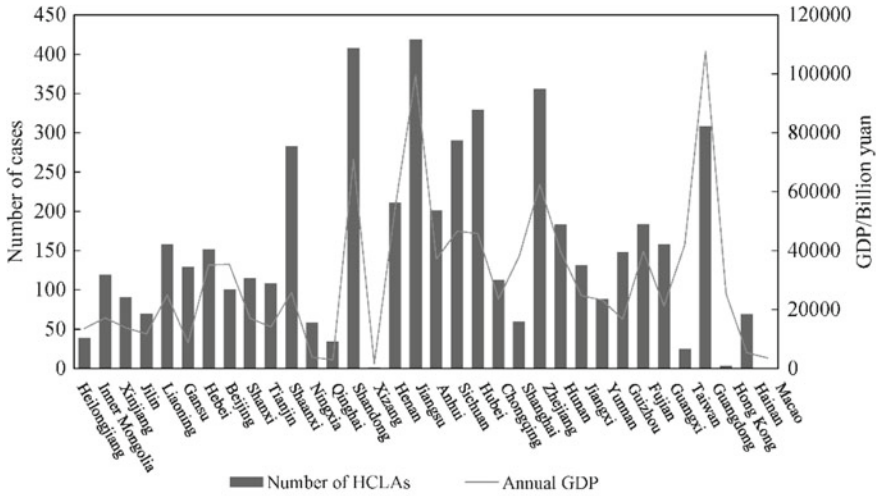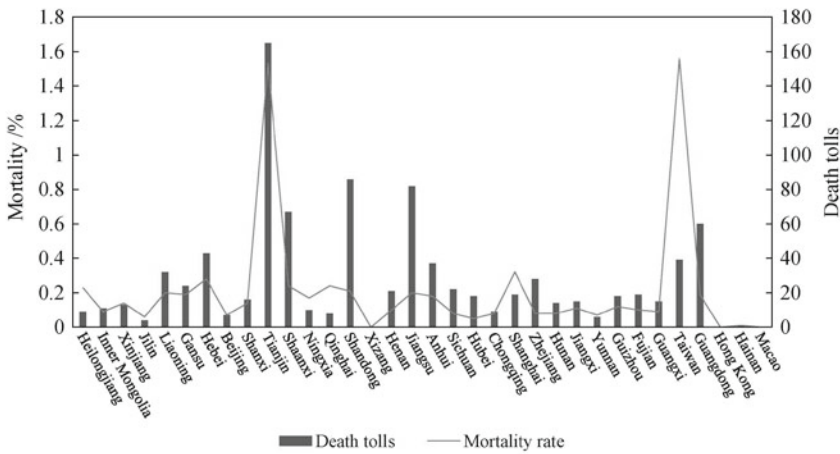
Fig. 2.4 Provincial distribution of HCLAs and annual GDP in China during 2009–2018 (Beijing, Chongqing, Shanghai, and Tianjin are municipalities) **a** number of HCLAs and annual GDP in each province; **b** death toll and mortality

expansion of the impact of such accidents and protecting the safety of people's lives and property.

Figure 2.5 shows further statistics on provinces with high incidence or high mortality of HCLAs by year. China's chemical industry entered a period of rapid development in 2010, so we can observe the increasing number of HCLAs in most province in the same period. At the initial stage of development, the regulatory mechanism and policies for chemicals in China were far from perfect, leading to an increase in the number of accidents year by year. Therefore, after 2015, China
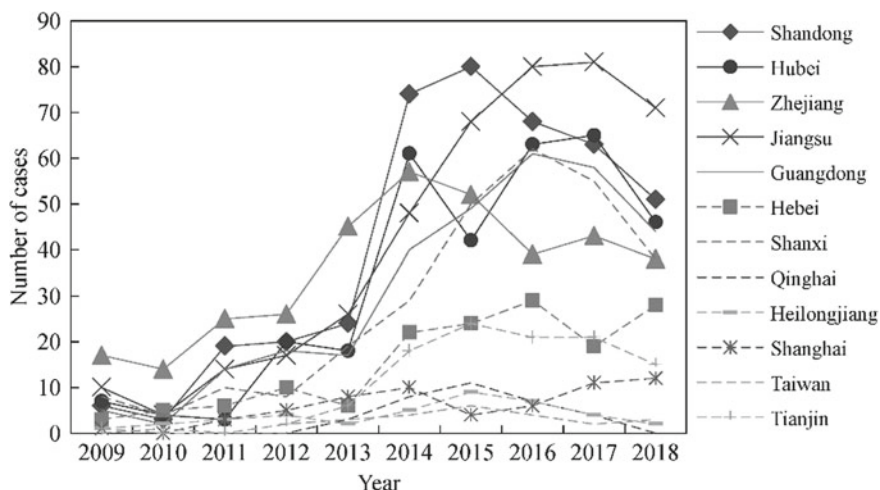
Fig. 2.5 Provincial HCLA occurrences by year

began to tighten up the supervision of hazardous chemicals and achieved the result of a decline in the number of HCLA in most provinces. However, the incidences of HCLAs in Shanghai and Hebei were still rising, indicating that the local government needs more measures to improve the management of hazardous chemicals and reduce the frequency of HCLAs.

2.3.3 Categories of HCLAs

Drawing on the type of places where hazardous chemicals leak, we divided hazardous chemical leakage accidents into the following six categories: HCLAs in road transportation, HCLAs in pipeline transportation, HCLAs in factories (industrial parks), HCLAs in gas stations, HCLAs in civilian residences, and HCLAs in other sites (such as hotels, hospitals). Six types of HCLAs from 2009 to 2018 have been counted and shown in Fig. 2.6. The majority of HCLAs occur in road transportation and pipeline transportation, accounting for 72.9% of the total accidents, indicating that transportation route is the most likely location for chemical leakage. Therefore, chemical transportation safety should be the focus of chemical safety managers. With the adoption of high-tech supervision technology and mechanized technology, the incidence of HCLAs in the usage, storage, production, and other links of chemicals (Kockmann et al. 2017) has decreased significantly. However, as of 2018, more than 60% of hazardous chemicals are still transported by road (Lu 2018), during which poor environmental conditions or the driver's driving error may lead to the leakage of hazardous chemicals. As the second-largest mode of transportation, the pipelines used to transport chemicals are often suspended in the air or buried underground, which are vulnerable to the influence of the external environment, causing hazardous

chemical leaks. The difference between leaks causes reveals that for different types of HCLA, managers need to take targeted regulatory measures to prevent the leakage of hazardous chemicals in effect.

The number of deaths and the mortality rate of six categories of HCLAs were counted and shown in Fig. 2.7. HCLAs in factories (industrial parks) have the highest mortality, mainly because factories (industrial parks) usually have a large number of various hazardous chemicals. As the disposal of chemical leakage in factories (industrial parks) is very complex, improper handling will cause serious consequences. As we analyzed in the monthly mortality distribution, the hazardous chemicals leaked from civilian residences are often gas or natural gas, resulting in high mortality. There are limited responses from the public to hazardous chemicals in an emergency. Secondary disasters, the principal source of casualties, are easily caused by improper operation of personnel. It is worth noting that the death toll of HCLAs in road transportation is high, yet the mortality is not high. Because in this category of HCLA, traffic accidents are often the direct cause of death rather than leakage.

As shown in Fig. 2.8, we conducted a statistical analysis on the quantity distribution of six types of HCLAs from 2009 to 2018. There was a decrease in all categories of HCLAs in 2014 or 2015, which confirms the positive role of the revised work safety law of the People's Republic of China implemented in 2014 in reducing accidents.

In China, the HCLAs in road transportation are much more than those in pipeline transportation, which seems different from the research results in Europe or the United States (Boot 2013). The research of Boot (2013) points out that pipeline transportation has a higher "individual risk" than road transportation in Europe or America. The difference between the above two conclusions can be explained from two aspects. ① In China, road transportation is the main way to transport hazardous chemicals, which is influenced by vehicles, drivers, and environment. Problems in any of the three aspects may lead to the occurrence of HCLAs (Lu 2018). ② As shown in Fig. 2.7, there is higher mortality of HCLAs in pipeline transport than in road transport in China. The occurrence of HCLAs alone is insufficient to estimate the "individual risk" in road transportation. That is to say, the two conclusions do not conflict.
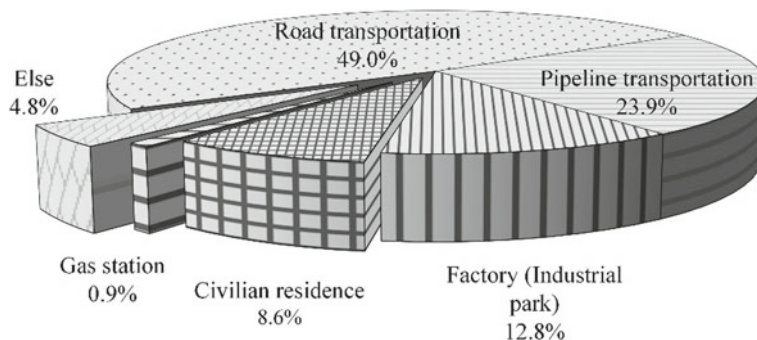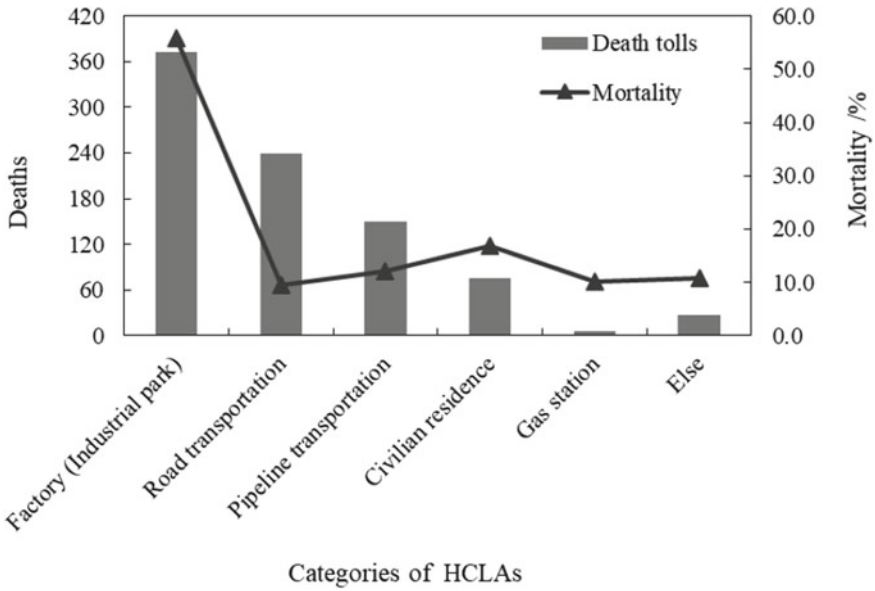

Fig. 2.6 Categories of HCLAs

Fig. 2.7 Death tolls and mortality of six categories of HCLAs
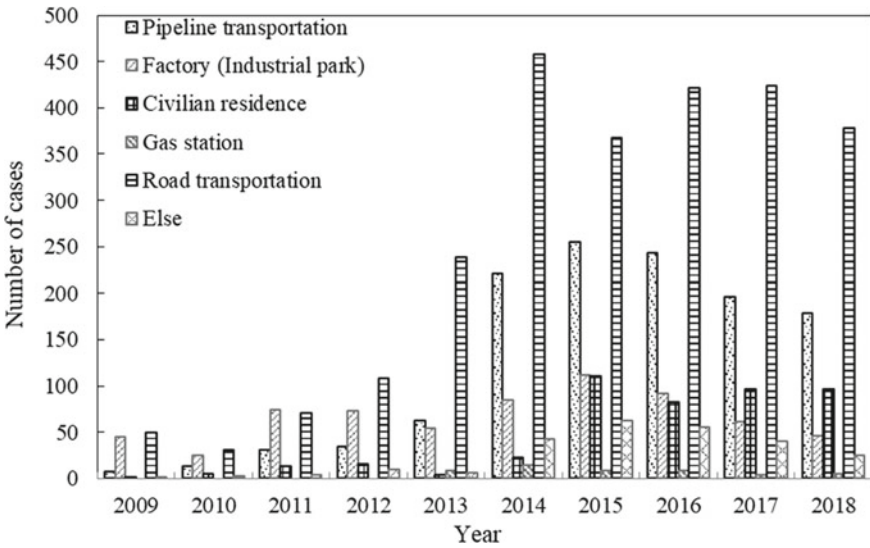
Fig. 2.8 Trends of various categories of HCLAs from 2009 to 2018

2.3.4   Typical HCLA Analysis

To draw up measures to mitigate the risks of HCLAs, we picked up five typical cases (Table 2.2) that caused heavy casualties and grievous social impact for further analysis. From the types of typical accidents listed in Table 2.2, HCLAs with multiple deaths often occurred in pipeline transportation and factories (industrial parks). For pipeline transportation, pipelines carrying hazardous chemicals may pass through densely populated areas, where an accident that occurs will pose a threat to a large number of people. For factories or industrial parks that store a large number of hazardous chemicals, the domino effect may greatly increase the scope of disaster impact. As mentioned many times before, the deaths in HCLAs mainly occur in secondary accidents. Therefore, to eliminate further accidents risk after the leakage of hazardous chemicals, emergency responders should take control measures as soon as possible before disaster escalation. The safety managers of hazardous chemicals can conduct warning and mitigation measures to prevent secondary disasters, such as gas detection devices, automatic shutdown systems, and evacuation alarms.

Table 2.2 shows the main causes of multiple deaths in typical accidents, which can be summarized into the following three factors; ① Unreasonable construction plan or site selection of chemical facilities; ② Failure accident mitigation strategy after leakage of hazardous chemicals; ③ Insufficient emergency preparedness, unscientific emergency rescue, and irrational emergency protective actions of the public. From 2009 to 2018, the HCLA that brought the largest casualties in China was the "8·12" explosion accident in the Tianjin Binhai New Area—it is also one of the world's worst chemical accidents in recent decade.

The "8·12" extraordinarily major fire and explosion accident is a production safety responsibility accident, and the final approved direct economic loss of it was as high as 6.866 billion yuan. Significantly, the victims in this accident include not only 55 surrounding workers and residents but also 110 police officers and firefighters involved in the disposal process. We arranged the accident timeline (see Fig. 2.9) and the accident evolution process (see Fig. 2.10). The initial cause of the accident is that the nitrocotton decomposed on its own to cause spontaneous combustion and leaked from a container. Then, the spreading fire triggered two strong explosions due to the domino effect.

Combined with the accident investigation report, the main causes of the "8·12" explosion accident in the Tianjin Binhai New Area are as follows: ① Ruihai Company illegally constructed and operated a dangerous goods yard; ② Ruihai Company stored excessive dangerous chemicals such as ammonium nitrate in violation of regulations; ③ Ruihai Company has brutal loading and unloading operations, resulting in broken packaging and leakage of dangerous chemicals; ④ Government departments lacked an effective emergency response to determine the quantities and kinds of hazardous chemicals on-site and to evacuate staff and nearby residents in time.

Based on the above analysis, we conclude that the mortality of HCLA mainly depends on the scale of hazardous chemicals stored, personnel density in the affected area, and the emergency response efficiency of enterprises and governments. Therefore, chemical places, which store a lot of hazardous chemicals or surrounding dense

Table 2.2 Five typical HCLAs

Year	Description of HCLA	Type of hazardous chemical	Category of HCLA	Secondary accident type	Main cause of multiple deaths	Death toll
2010	"1·4" coal gas leakage accident in Hebei Industrial Park	Coal gas	Factories (industrial parks)	Poisoning	Lack of gas detection equipment to detect the leakage on time	21
2013	"8·31" liquid ammonia leakage accident in Shanghai	Liquid ammonia	Factories (industrial parks)	Poisoning	Unreasonable layout of workshop and liquid ammonia pipeline, which resulted in the failure of employees to evacuate after the accident	15
2013	"11·22" Qingdao oil pipeline explosion accident in Shandong	Crude oil	Pipeline transportation	Explosion	Residents in the surrounding area were not immediately evacuated after the oil spill; during the emergency disposal, the repair equipment produced an open fire, resulting in the explosion of crude oil	62
2014	"7·31" propylene explosion accident in Taiwan	Propylene	Pipeline transportation	Explosion	Lack of leakage alarm device and failure to accurately determine the leakage position of propylene, resulting in wrong judgment of accident; residents in the nearby area were not evacuated immediately	30

Table 2.2   (continued)

Year	Description of HCLA	Type of hazardous chemical	Category of HCLA	Secondary accident type	Main cause of multiple deaths	Death toll
2015	"8·12" explosion accident in Tianjin Binhai New Area	More than 100 types of hazardous chemicals, such as ammonium nitrate, potassium nitrate, and sodium cyanide	Factory (industrial parks)	Explosion, fire	Storage of a large number of dangerous chemicals in violation of regulations, the types and quantities of hazardous chemicals were not recorded in advance, insufficient measures for emergency preparedness, staff and residents in the surrounding area were not evacuated immediately	165
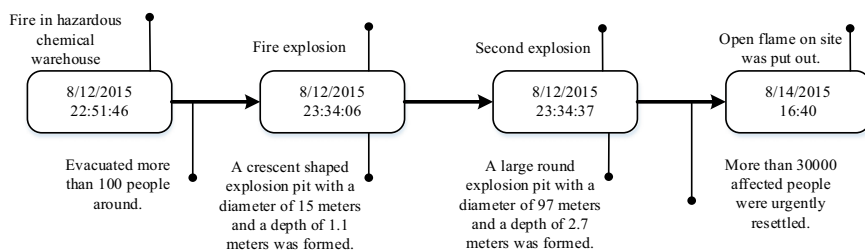
Fig. 2.9   Timeline of the "8·12" explosion accident in the Tianjin Binhai New Area

populations, should adopt inherent safety designs to avoid accidents fundamentally. For accident risks control, chemical enterprises can improve their emergency response capability by establishing a dynamic risk assessment system, and industrial parks can develop a cluster safety management system. For disaster escalation avoidance, it is necessary to make mitigation strategies (e.g., gas detections–automatic shutdown–alarms) in the initial stage of the accident. In addition, the government should improve the construction of the emergency information management system and public emergency shelter guidance system, serving as guiding the public to take correct protective actions in time (such as respiratory protection, local refuge, and evacuation).
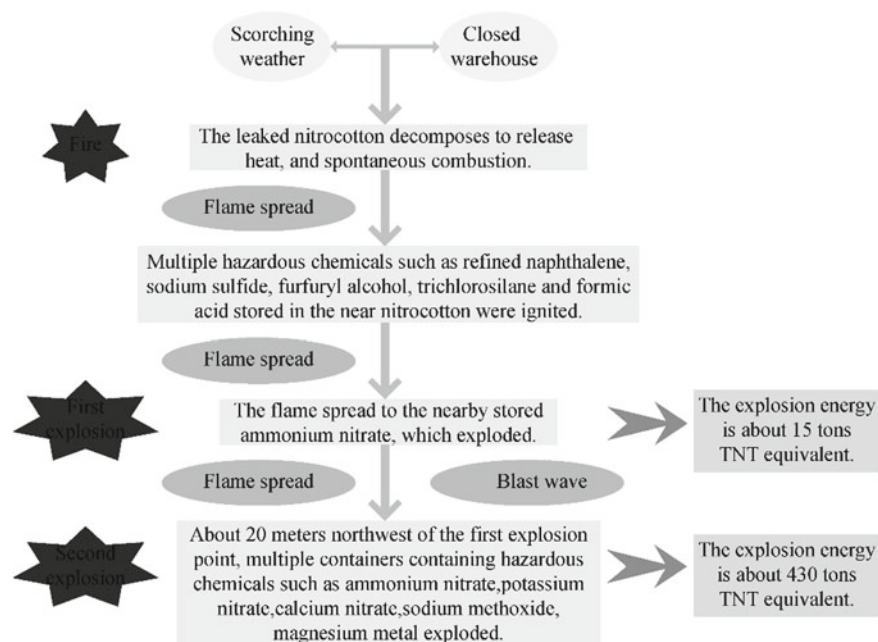
Fig. 2.10 Evolution process of the "8·12" explosion accident in the Tianjin Binhai New Area

2.4 Analysis of Various Categories of HCLAs

2.4.1 HCLAs in Road Transportation

The HCLAs in road transportation are the most frequent. We analyzed the change trends in the frequency and accident rate of HCLAs in road transportation and showed the results in Fig. 2.11. The occurrence number of HCLAs in road transportation grew exponentially from 2010 to 2014 and declined slowly after that. Meanwhile, the accident rate fluctuated around 50% all along. There is still a discussible issue in terms of available measures to reduce the occurrence of HCLAs in road transportation.

To deeply explore the causes of HCLAs in road transportation, we counted and analyzed the frequency and mortality of accidents during each period of the day and compared them with the human arousal level in Fig. 2.12. The frequency of HCLAs has two peaks at 8:00–9:00 a.m. and 2:00–3:00 p.m., respectively. Throughout the day, human arousal levels continued to decline from 8 p.m. until 5 a.m. the next day (Du et al. 2020). Since there is no restriction on the driving time for drivers to transport chemicals, they have to keep their mental tension on a high level when driving at night. As the human arousal level rises between 6:00 a.m. and 10:00 a.m., the drivers get relaxed and are prone to make mistakes. From 2:00 p.m. to 3:00 p.m., people are more likely to produce fatigue and drowsiness under the influence of hormones,
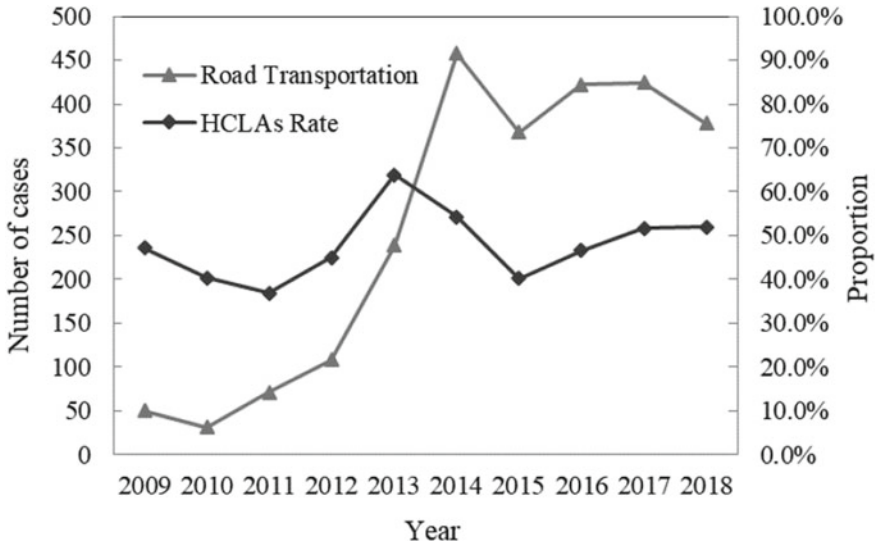
Fig. 2.11 Change trends of HCLAs in road transportation

implying that driving during this period is prone to cause traffic accidents. The higher mortality of HCLAs in road transportation was from 0:00 a.m. to 5:00 a.m., during which the decline of human arousal level leads to the weaker drivers' capability to address emergencies. If the driver is unable to adopt effective emergency measures immediately after the accident, the accident situation may get out of control and cause heavy casualties. Therefore, the transportation of hazardous chemicals should be carried out outside 0:00 to 5:00 a.m. as far as possible to reduce the mortality of HCLAs in road transportation. Some provinces have implemented compulsory rest time for dangerous chemical vehicles driving at night.

2.4.2 HCLAs in Pipeline Transportation

Figure 2.13 represents the frequency and accident rate of HCLAs in pipeline transportation, both of them have shown an upward trend since 2009 and decreased after 2015. The accident rate fluctuated slightly and remained between 20 and 30% from 2014 to 2018, requiring more effective supervision measures to reduce HCLAs in pipeline transportation based on their characteristics.

Figure 2.14 shows the classification and statistics of the causes of pipeline leakage accidents during 2015–2018. The principal reason of pipeline leakage is improper construction (78.6%). If the ground construction neglects the pipeline layout and detailed inspection in advance, there will be a risk of damaging buried pipeline and
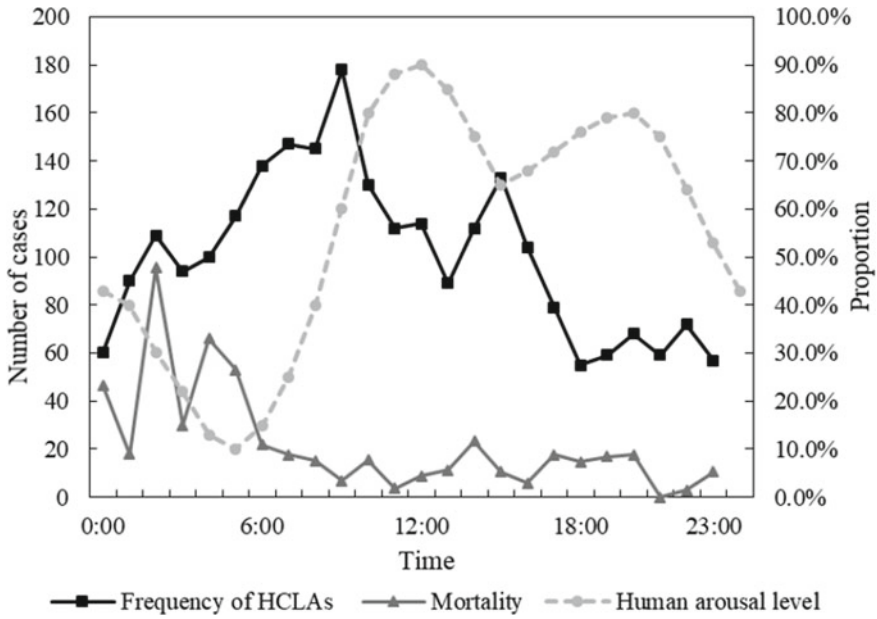
Fig. 2.12 Frequency and mortality of HCLAs in different periods of road transportation
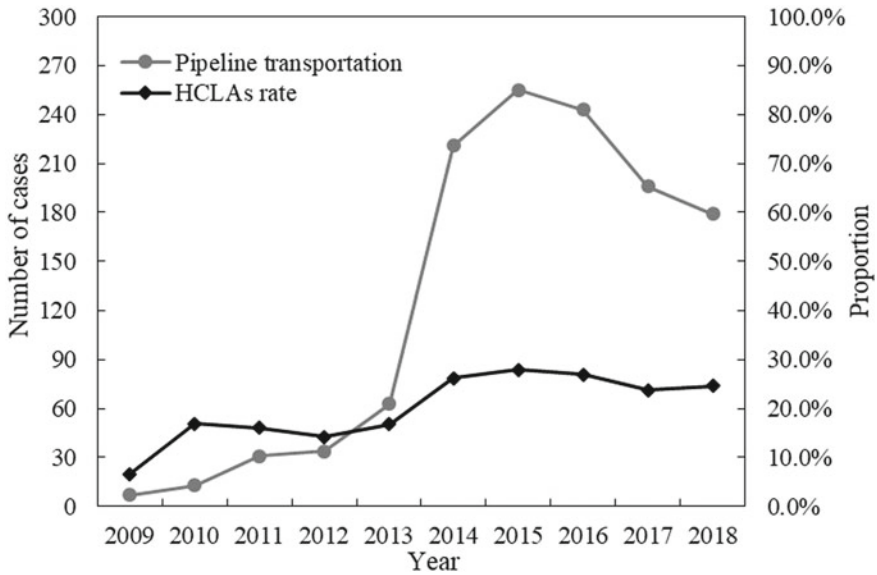
Fig. 2.13 Frequency and accident rate of HCLAs in pipeline transportation

7.4%

4.1%

3.4%

2.7%

1.8%

1.3%

0.7%

3.8%

78.6%

☐ Improper construction　　☒ Vehicle impact
☐ Aging/Corrosion　　☐ Geological
☐ Falling objects　　☒ Connection defect
☒ Bioerosion　　☐ Else
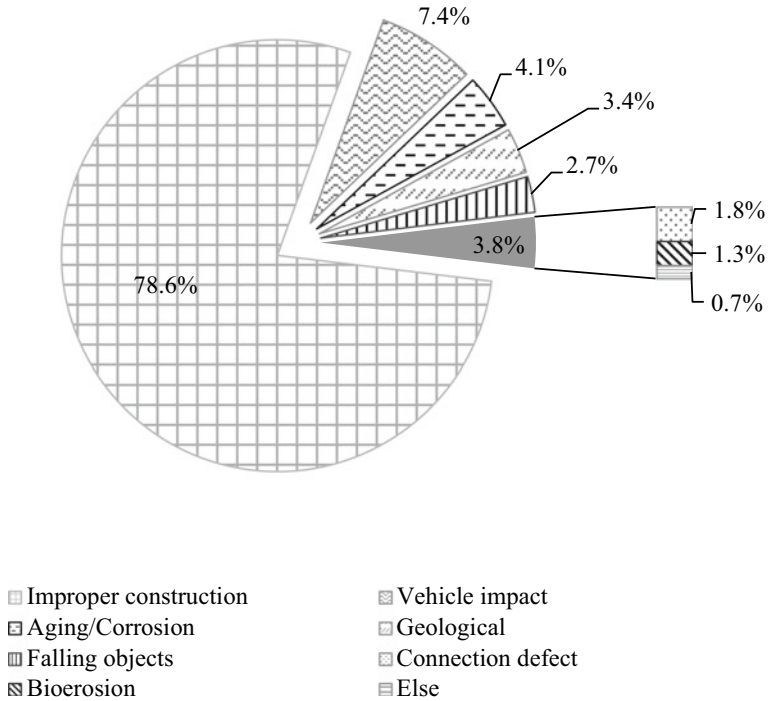
Fig. 2.14 Reasons for HCLAs in pipeline transportation

causing HCLAs during the construction process. Another significant cause of underground pipeline leakage is geological damage (e.g., the ground collapses). Falling objects and vehicle impact mainly impact the ground pipeline, which requires that protective facilities must be set on the exposed pipelines to enhance the ability of the pipelines to withstand the impact of external energy. Solving the problems of pipeline corrosion, aging, and connection defects is also the focus of pipeline leakage prevention and control. Enterprises and government management departments should attach importance to daily maintenance and management of pipelines, timely detection and replacement of faulty pipelines, and pipeline laying technology.

2.4.3 HCLAs in Factories (Industrial Parks)

The chemical safety of factories (industrial parks) is one of the significant components of public safety. In Fig. 2.15a, we counted the frequency and accident rate of HCLAs in factories (industrial parks), displaying that the number of accidents decreased by more than half from 2015 to 2018. Besides, the accident rate of HCLAs in factories (industrial parks) continued to decline since 2009 and stabilized at about 10% after

2015. However, according to the statistics of death tolls and mortality of HCLAs in factories (industrial parks) in Fig. 2.15b, the mortality did not decrease significantly like the frequency of accidents. Thus, in addition to accident prevention, early disaster control also plays a vital role in accident risk reduction. Once the mitigation measures fail, the enormous number of hazardous chemicals stored in the factories (industrial parks) will cause accident escalation and mass mortality. Before the situation gets out of control, the government must apply emergency rescue and organize protective actions to guarantee public safety to the greatest extent.
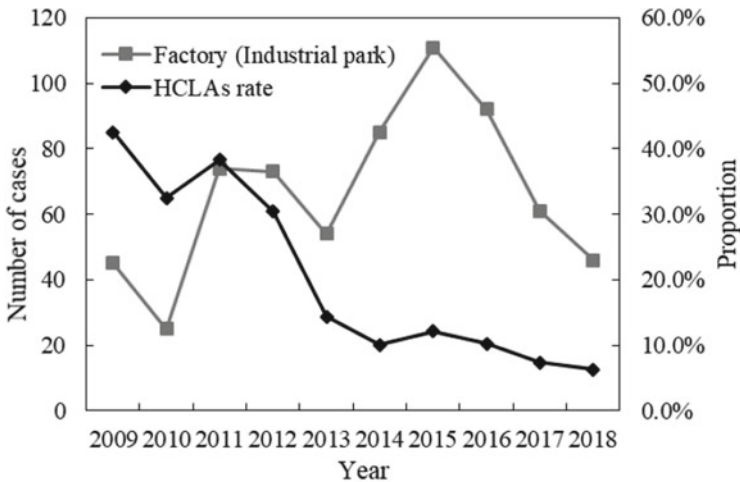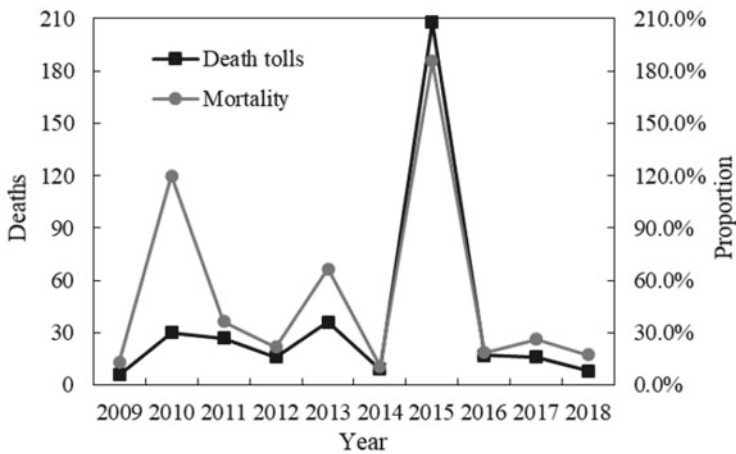
Fig. 2.15 HCLAs in the factories (industrial parks) **a** frequency and accident rate; **b** death tolls and mortality

2.4.4   HCLAs in Civilian Residence

Comparing the first three categories, the frequency of HCLAs in civilian residences is lower. Figure 2.16a presents the changing trend in occurrence number and accident rate of HCLAs in civilian residences during 2009–2018. As shown in Fig. 2.16a, a surge of HCLAs in civilian residences appeared since 2013. From 2015 to 2018, the number of accidents remained at a high level, with an annual average of nearly 100 accidents per years. During the same period, the accident rate of HCLAs in civilian residences fluctuated around 10%. Furthermore, we investigated the type of hazardous chemicals involved in the leak, including coal gas, liquefied petroleum gas, natural gas, and others. As shown in Fig. 2.16b, leaks of the first three fuel gas take up almost all HCLAs in civil residences, and only about 1% of accidents are the leakage of other hazardous chemicals. Among different fuel gas, the mortality of coal gas leakage accidents is the highest, reaching 20.9%, which even exceeds the mortality of HCLAs in pipeline transportation (12.1%) and road transportation (9.4%), becoming the accident with the highest death rate after HCLAs in factories (industrial parks). As a colorless and odorless gas, coal gas is difficult to be perceived by humans in the early stage of leakage. If the public does not have the relevant knowledge of gas characteristics, their rash disposal will lead to poisoning or explosion. That is a great source of the high mortality in coal gas leakage accidents, which can be eliminated by installing a gas detection system in the room to give an alarm. At the same time, the government should strictly regulate the use of gas, accelerate the standardization construction, and popularize the emergency measures for gas leakage to the public.

2.5   Evacuation Caused by HCLAs

To protect the public from secondary disasters of HCLAs, the emergency command needs to evacuate the people in the affected areas to safety in time in case of the failure of local shelters. In this section, we investigated the evacuation actions caused by HCLAs in China from 2009 to 2018 to analyze their central features and influence factors.

2.5.1   Evacuation Situations Triggered by HCLAs

In this study, a total of 157 evacuation events with statistical information is available and shown in Fig. 2.17 by provincial distribution and the types of HCLAs involved. Most evacuation events occurred in Sichuan, Guangdong, Zhejiang, Guizhou, Hubei, and Henan, with more than 10 incidences in each province. Contrary to the categories proportion of HCLAs, the evacuation caused by HCLAs in pipeline transportation (34.4%) is more than that in road transportation (27.4%). As the accident type with

(a)

(b)
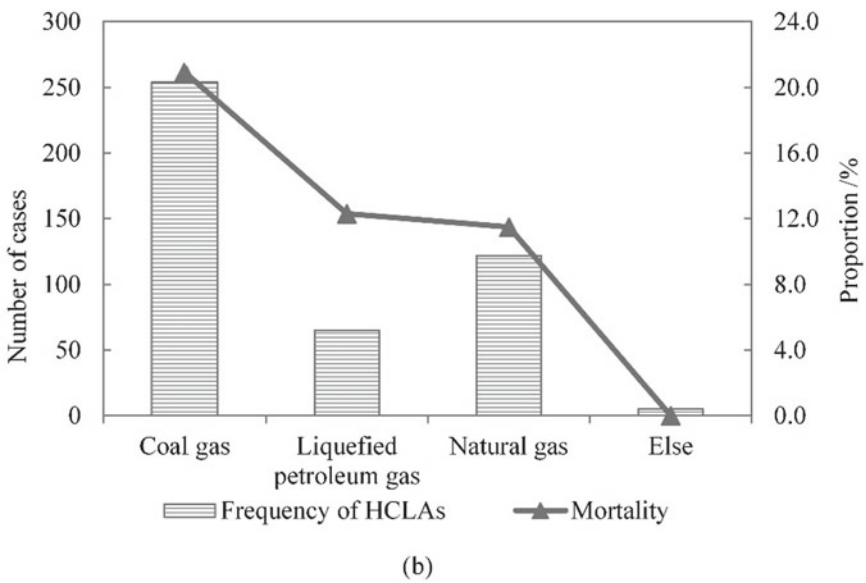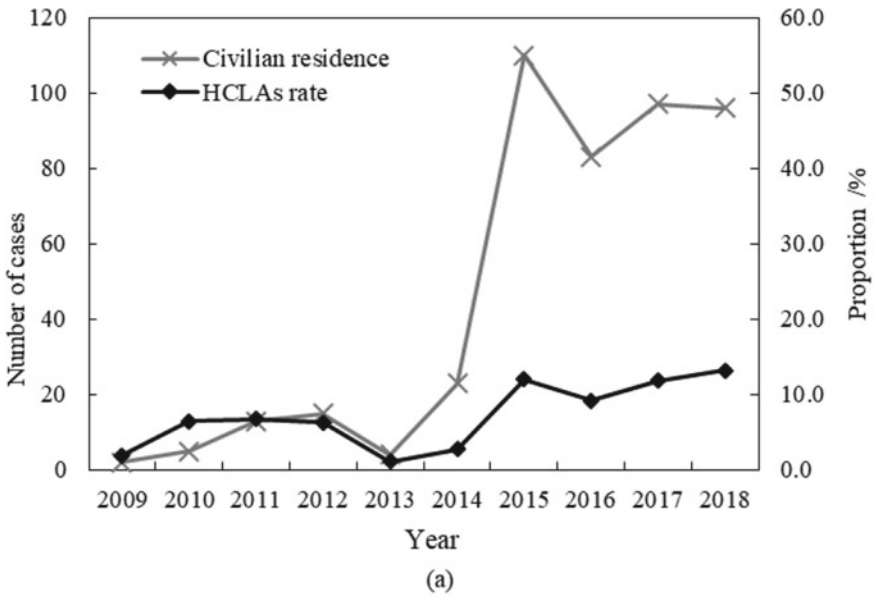
Fig. 2.16 Statistics of HCLAs in civilian residences **a** frequency and accident rate, **b** fuel gas type and mortality of HCLAs

the highest mortality, HCLAs in factories (industrial parks) caused 24.8% of all evacuation events, far exceeding the cases HCLAs in civilian residences and gas stations triggered.

In evacuations, the objects to be evacuated include a variety of groups with different identities. According to the characteristics of evacuation target groups, we divide the evacuation events in this study into urban residential area evacuation, rural evacuation, corporate evacuation, campus evacuation, and special evacuation (such as the evacuation in prisons, kindergartens, hospitals), showing their proportions in

(a)

(b)
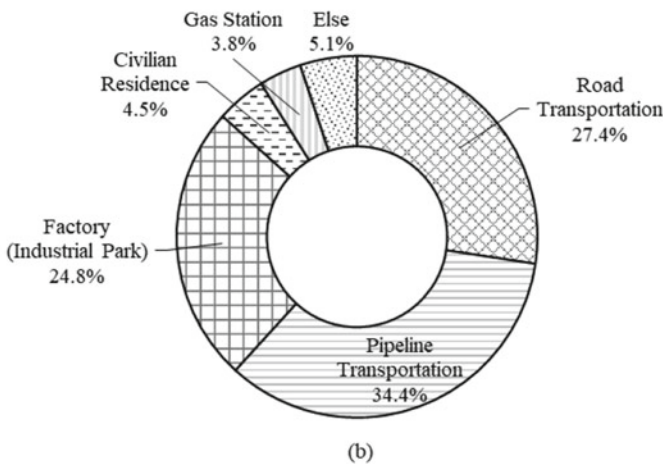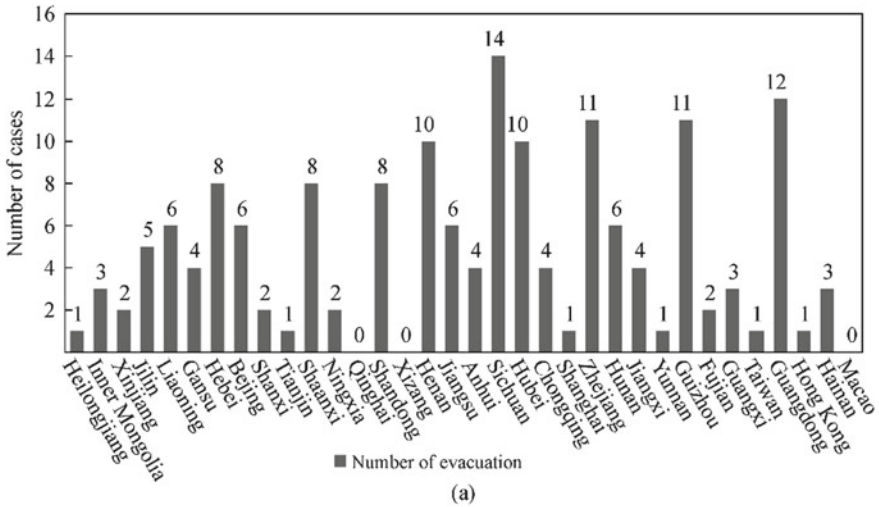
Fig. 2.17 Evacuation caused by HCLAs **a** provincial distribution, **b** distribution of categories of HCLAs involved

Fig. 2.18. The frequency of rural evacuation (61.8%) is much higher than that of other types of evacuation, and most of the evacuees in rural areas are local villagers. In the remaining 40% of incidents, the evacuation of urban residential areas accounts for half, and campus evacuation, enterprise evacuation, and special evacuation all fewer than 10%.

The statistics also describe the characteristics of 157 evacuation events in terms of the starting time of the evacuation. By dividing a day into four time periods, Fig. 2.19 shows the distribution of evacuation events starting in the forenoon (6:00–12:00), afternoon (12:00–18:00), evening (18:00–24:00), and before dawn (0:00–6:00). In the statistical results, there are more evacuation events during the day (in the forenoon and afternoon) than at night (in the evening and before dawn), which can be attributed to the weak evacuation capability of people and the delayed diffusion of evacuation alarms during the night (Sun and Sun 2020). Therefore, formulating evacuation plans should consider whether the evacuation occurs during the day or at night.

Fig. 2.18 Evacuation categories based on the objects
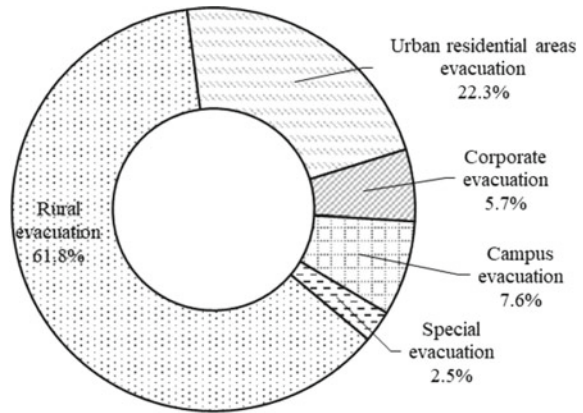
Fig. 2.19 Start time of evacuation events caused by HCLAs
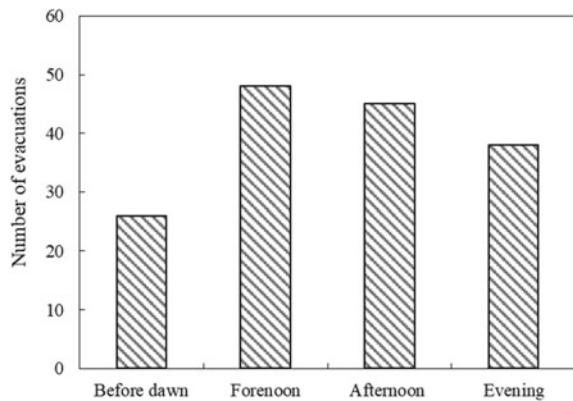
Fig. 2.20 Proportion of hazardous chemicals causing evacuation events
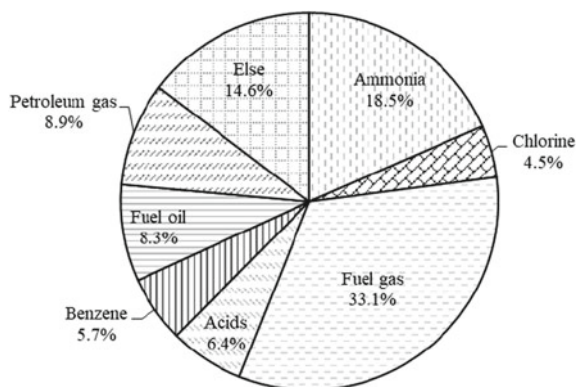
Among the hazardous chemicals involved in the leakage accident in this study, there are eight categories causing evacuation: acids (nitric acid, salt acid, and sulfuric acid), fuel oil (diesel, gasoline), benzene, chlorine, ammonia, petroleum gas, fuel gas, and else. In Fig. 2.20, the evacuation events are distinguished and counted based on the types of hazardous chemicals causing the evacuation. Nearly a third of the evacuation cases occurred in fuel gas leakage accidents, followed by the leakage of ammonia (18.5%) and else (14.6%). Meanwhile, the leakage of the remaining five hazardous chemicals caused less evacuation events.

2.5.2 Evacuation Process and Level Analysis

As a crucial part of chemical accident damage assessment, evacuation analysis includes three indicators in this study: evacuees' number, evacuation duration, and evacuation scope. The number of evacuees in 157 evacuations caused by HCLAs is graded by two thresholds of 1000 and 5000: 61 evacuation cases with less than 1000 people; 4 evacuation cases with more than 5000 people. The evacuation events with evacuees between 1000 and 5000 occurred most frequently, accounting for 58.6% of the total evacuation events. In 2012, more than 27000 people were evacuated due to phosphine leakage in Hedong grain depot, Liaoning, which is the HCLA with the most evacuees involved in this study.

The size of the evacuation range depends on the specific situation of the accident, which can be quantified through the local administrative division and the estimated impact radius of the leakage accident. A total of 147 evacuation incidents caused by HCLAs collected in this study contains information related to evacuation scope. According to the classification criteria in Table 2.1, the distribution of the three evacuation ranges is as follows: 65 evacuation events occurred in a single building or within a radius of 500 m; 20 evacuation incidents involved multiple villages (community, industrial park, etc.) or the crowd within a radius of more than 2000 m; and

Fig. 2.21 Statistic of
evacuation duration of
evacuation events caused by
HCLAs

Above 300 min
6.1%

60 min - 300min
24.5%

Within 60 min
69.4%
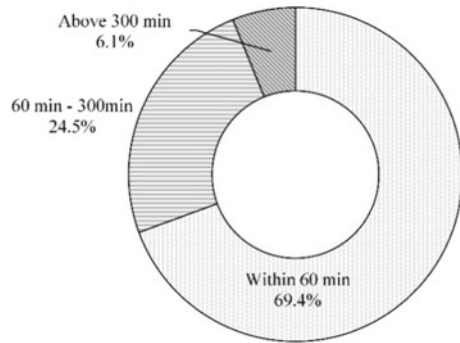
62 evacuations occurred between the first two scales, which takes up the equivalent proportion of evacuations on a small scale.

In this study, the evacuation duration starts from the occurrence of the HCLA until all relevant evacuees leave the dangerous zone. In various evacuation events, the large gap in the evacuation scope and evacuees causes the evacuation duration can differ by more than several hours. Therefore, this study selects 60 min and 300 min as the grade threshold to divide the duration process of 147 evacuation cases with relevant time information. In Fig. 2.21, the statistical results show that nearly 70% of evacuations can be finished within 60 min.

To comprehensively study the characteristics of regional evacuation in China's HCLA, we substitute the number of evacuees, evacuation duration, and evacuation range of evacuation events into Table 2.1 to obtain the corresponding grade coefficient and calculate the evacuation level through Eq. (2.3). Among the counted HCLAs in this chapter, only 147 cases have the evacuation information required by all evaluation indicators, and their evacuation levels are counted in Fig. 2.22. Combined with Figs. 2.1 and 2.22, extra-small-scale evacuation accounts for over half of the total 147 evacuation events, and the higher the level of evacuation events, the lower the frequency. Generally, the actual situation is consistent with the statistical results, demonstrating the rationality of the evacuation classification method applied in this study.

2.5.3 Analysis of Factors Affecting Evacuation Levels

To identify the influencing factors of evacuation level, we conducted a Spearman rank correlation analysis on the evacuation level and specific situation listed in Table 2.3 (accident location, category of leaked hazardous chemicals, category of evacuation object, evacuation start time). As a method to determine the correlation between variables, Spearman rank correlation analysis calculates the correlation coefficient of rank and then looks up the table to verify whether the bilateral significance P is less than 0.05 (Astivia and Zumbo 2017). If the p-value is less than 0.05, there is a

Fig. 2.22 Statistics of evacuation levels of evacuation events caused by HCLAs
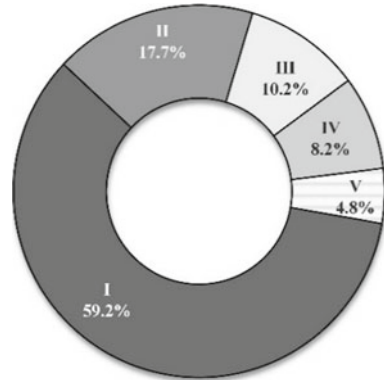
Table 2.3 Test results of correlation between evacuation situation and evacuation level

Evacuation situation	Correlation coefficient (rs)	P-value	Relevance
Location of the accident	− 0.331	0.000	Relevant
Category of leakage hazardous chemicals	0.286	0.000	Relevant
Category of evacuation object	− 0.101	0.222	Uncorrelated
Start time of evacuation	− 0.102	0.218	Uncorrelated

correlation between variables. The results show that the type of hazardous chemicals leaked in HCLAs and accident locations has an effect on the level of evacuation events.

Figure 2.23 shows the distribution of evacuation levels in HCLAs at different locations. Only HCLAs in pipeline transportations and road transportations have caused evacuation events of all levels, among which nearly one-fifth of evacuations are extra-large-scale and large-scale evacuations. However, there was no extra-large-scale evacuation in HCLAs in factories (industrial parks) with the highest mortality (see Fig. 2.7). In addition, the evacuation events triggered by HCLAs in gas stations and civilian residences are no more than Level II, and extra-small-scale evacuation accounts for more than 80%.

The level distribution of evacuations caused by the leakage of specific hazardous chemicals is in Fig. 2.24. In the evacuation caused by fuel gas, chlorine, and ammonia leaks, extra-small-scale evacuation accounts for the vast majority. More than 90% of the evacuation events caused by fuel oil leakage are small-scale evacuations and extra-small-scale evacuations, which indicate the low possibility of large-scale evacuation caused by such hazardous chemicals. At the same time, extra-large-scale evacuations, most occurring in the acid leakage, account for a certain proportion of the evacuations of chlorine, gas, petroleum gas, and other hazardous chemical leakage accidents. It is
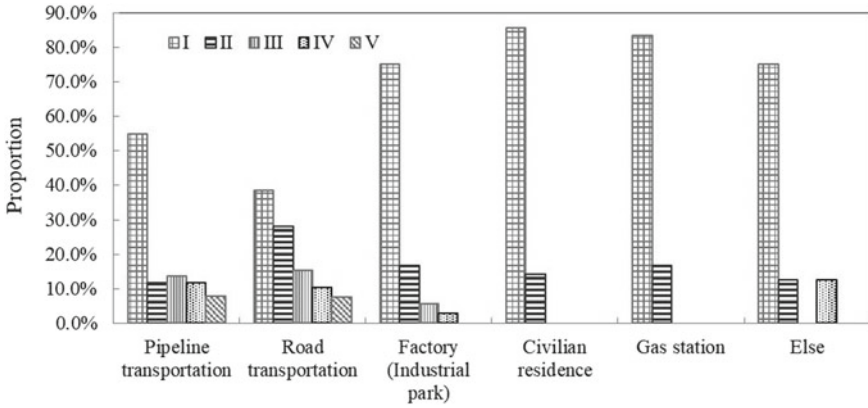
Fig. 2.23 Evacuation level in HCLAs at different locations

worth noting that chlorine leaks induced either extra-small-scale evacuations or large-scale and extra-large-scale evacuations, reflecting the extreme risk of this hazardous chemical.
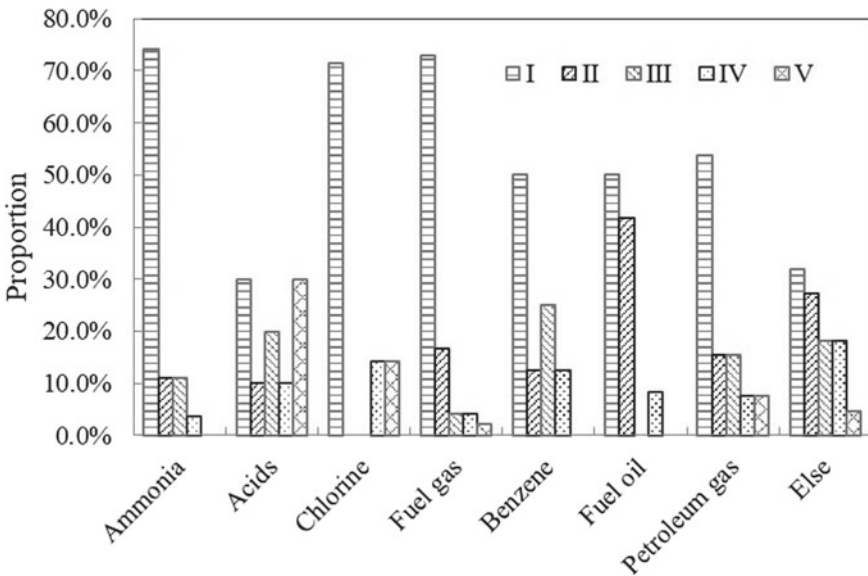
Fig. 2.24 Evacuation level in leakages of different hazardous chemicals

2.6 Framework of Integrated Management of Hazardous Chemicals

2.6.1 Management of HCLA

2.6.1.1 Management Status of HCLA

In the United States, the information disclosure system requires enterprises to provide accurate reports on the management of hazardous chemicals to the regulatory authorities. Governments at all levels cooperate with regulatory agencies, such as medical and fire services, to timely assess the risk of HCLA and improve the emergency level and linkage law enforcement ability. Furthermore, to comprehensively and systematically analyze the cause of chemical accidents, the US Congress has set up an independent chemical safety and hazard investigation committee that can timely disclose the progress of accident investigation to the whole society to eliminate public misunderstanding (Fyffe et al. 2016; Tinney et al. 2016). In Japan, where the access system for hazardous chemicals is also strict, the government has set up a professional team responsible for chemicals supervision (Hashimoto et al. 2017). Japanese enterprises pay attention to cultivating safety awareness and encouraging employees to participate in safety management (Hsu et al. 2008). To identify and handle hazardous chemicals, the European Union created the Classification and Labelling Inventory (C&LI) database that contains substances information received from the notification and registration of manufacturers and importers (Oltmanns et al. 2014). In 2007, a policy on the "Registration, Evaluation, Authorization, and Restriction of Chemicals" (REACH) was implemented to create a unified chemical management system within the European Union. As a regulation for the preventive management of chemicals, REACH limits the market access, use, and manufacture of hazardous chemicals. To manage the safe transportation of hazardous chemicals under a globally unified framework, the United Nations Committee of Experts on the Transport of Dangerous Goods issued the "Recommendations on the Transport of Dangerous Goods Model Regulations" and constantly revised it during implementation.

The safety management of hazardous chemicals in China is still in the development stage compared to developed countries. More than ten departments, such as safety supervision, transportation, and environmental protection, are in charge of the supervision and management of hazardous chemicals safety. The Regulations of Safety Management on Hazard Chemicals newly revised in 2011 further clarified the responsibilities of relevant departments. In 2016, China proposed that the chemical sector implements the dual-preventive mechanism for risk grading control and hidden danger investigation and management, focused on curbing major accidents and moving forward risk control. In 2019, to improve the safety management level of chemical parks and hazardous chemical enterprises, the Ministry of Emergency Management formulated "Guidelines for Hazardous Chemical Enterprise Safety Risk Investigation and Governance" and "Guidelines for Chemical Park Safety Risk Investigation and Governance (Trial)".

Even though the international safety management system for hazardous chemicals has steadily improved, the risk of chemical accidents persists as long as particular industries employ large quantities of hazardous substances. The development of the dangerous waste exemption system lacks more research and practice, and chemical enterprises need more mature hazardous waste disposal technologies. In addition, the potential hazards of release accidents such as equipment aging and maintenance failure still threaten the safety of hazardous chemicals. As a result of these reasons, while industrialized countries have succeeded in reducing the casualties caused by the vast majority of chemical accidents, they keep facing the catastrophic risk caused by chemical hazards.

2.6.1.2 Challenges in Management

In the statistics of this chapter, there were over 5200 hazardous chemical leakage accidents in China during 2009–2018. Even though the number of such accidents shows a downward trend in recent years, the occasional occurrence of extraordinarily serious HCLAs has inflicted massive loss of life and property. In China, the safety management of hazardous chemicals is still in the face of several challenges as follows:

(1) Imperfect legal system governing hazardous chemical management. For now, the "Law on Work Safety" served as the basic law to supervise and manage hazardous chemicals in China, which is too general to possess sufficient enforcement standards and operability. Specific laws, regulations, and rules for production safety in the chemical industry, including the "Hazardous Chemical Safety Law", have been gradually formed around the "Law on Work Safety". However, to solve special safety problems in other fields, specific legislation such as the "Fire Control Law" and "Road Traffic Safety Law" also puts forward requirements for the safety management of hazardous chemicals. Therefore, it is inevitable to have overlapping and cross-cutting problems in the division of responsibilities for hazardous chemicals management, and the standards are difficult to unify (Tang et al. 2015).

(2) Weak government regulation (Zhang and Zheng 2012). The government institutional reform in 2018 integrated the relevant responsibilities of 13 disaster-related departments and established the national emergency management department. In addition to the comprehensive supervision and management of safe production such as hazardous chemicals, the responsibility scope of the emergency management department also includes the prevention and emergency rescue of fire, natural disasters, and others. As a result of this situation, there is a lack of emergency management personnel at the grass-roots level who are familiar with hazardous chemical supervision and have professional skills, causing the safety management functions to weaken. Furthermore, emergency management, transportation, public security, railway, civil aviation, ecological

environment, and other departments respectively undertake the safety supervision responsibilities related to the production, storage, use, operation, transportation, disposal, and other links of hazardous chemicals. This condition leads to the unclear implementation of responsibilities in all links and the imperfect law enforcement system.

(3) Improper selection of pipeline laying locations and factory (industrial park) sites. The regional population structure of developing countries, such as China, has changed considerably as national urbanization has progressed. Some plant site selection and pipeline laying in terms of hazardous chemicals without long-term planning may be close to or pass through densely populated areas in the process of local development, resulting in a high evacuation rate of HCLA in China.

(4) Insufficient management level of hazardous chemical enterprises. By 2019, there were nearly 300,000 production and operation units of hazardous chemical and over 850 chemical industrial parks in China. However, the current enterprise safety management system cannot adapt to the rapid development of the chemical industry, which makes it awkward to implement the main responsibility of safety production. As the majority of China's chemical enterprises, small- and medium-sized chemical enterprises have frequent safety problems due to insufficient safety investment and weak safety awareness of employees. In addition, the chemical process is very complex and involves a variety of hazardous materials, requiring employees to have professional skills. Therefore, the lack of professionals is also one of the reasons for the insufficient level of hazardous chemical management.

(5) Immature emergency management of HCLA. As the chief basis for guiding the implementation of emergency protection measures, the emergency plan covers limited accident scenarios. After an unconventional HCLA, the emergency plan is ineffective for the complex and changeable situation. Moreover, roads and civilian residences are also at risk of HCLA. Due to the lack of public awareness and attention to hazardous chemicals, it is impossible to carry out an effective emergency response to the leakage of hazardous chemicals.

(6) The aging of equipment and facilities. The failure rate of the equipment at different stages of its life is shown as the bathtub curve. Due to the fatigue, aging, and wear, the failure rate of equipment increases rapidly with the extension of time, which is easy to cause HCLA.

2.6.1.3   Future Tasks

According to the statistical characteristics analysis of HCLAs in China from 2009 to 2018, drawing on superior management experience in terms of hazardous chemicals, this chapter puts forward LGCETE guidelines to strengthen hazardous chemicals safety management. As shown in Fig. 2.25, LGCETE guidelines cut down the risk of hazardous chemicals from legal regulation, government supervision, corporate

responsibility, emergency management, technical improvement, and environmental protection.

(1) Legal regulation

Hazardous chemical management is predicated on perfect legal regulation. Referring to the successful management cases of developed countries and the lessons learned from major historical accidents, the management of hazardous chemicals in developing countries requires a comprehensive framework of legislation and unified management standards on hazardous chemicals (Russell et al. 1998; Zhao et al. 2013). In China, for example, the improvement of the safety laws and regulations system of hazardous chemical safety shall take the "Law on Work Safety" and "Law on Hazardous Chemical Safety" as the main body of the legislative framework and supplement by local and departmental regulations.

(2) Government supervision

Government supervision is a powerful guarantee for the implementation of hazardous chemicals management. To begin with, the government should perform a complete inquiry into hazardous chemicals within its jurisdiction and strengthen the information monitoring system for the entire life cycle of hazardous chemicals. With the help of information collecting, the regulatory authorities should establish a risk-based regulatory model to implement policies accurately and realize the dynamic risk management of hazardous chemicals (Aneziris et al. 2017). While expanding the scope of supervision and inspection, the key areas such as dangerous waste should become the supervision focus. Secondly, aiming at improving the overall level, the construction of a safety supervision team of hazardous chemicals should strengthen
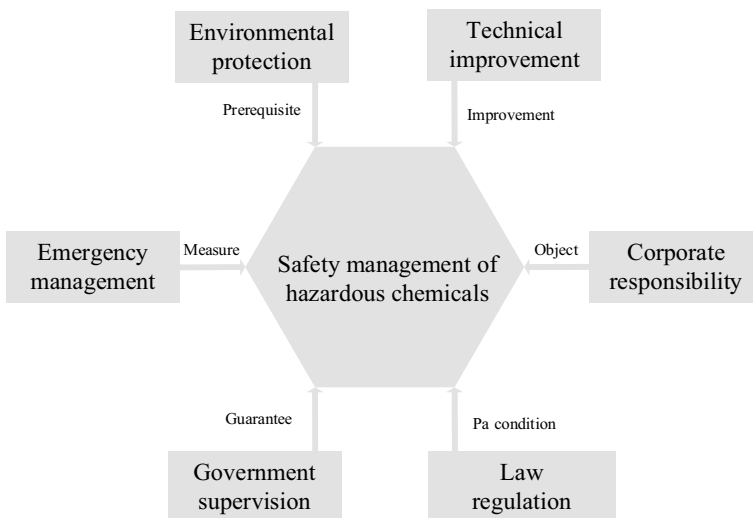
Fig. 2.25 LGCETE guidelines for safety management of hazardous chemicals

the capability of grass-roots teams and develop professional teams. Furthermore, actively organizing various forms of publicity and education activities is also one of the tasks of the regulatory authorities to enhance people's attention and awareness of the safety of hazardous chemicals. For example, some local governments have produced videos and posters to promote the prevention and treatment of domestic gas leakage. It is available in the future to create a cloud publicity platform based on internet technology, which teaches the public online about characteristics and safe disposal methods of hazardous chemicals to boost their accident prevention and response capacities (Smolders et al. 2014; Nakai et al. 2017).

(3) Corporate responsibility

The corporation is fully responsible for the safety management of hazardous chemicals in its unit, and strengthening the main responsibility of the corporation plays a vital role in reducing accident risk (Aneziris et al. 2017). First of all, for enterprises, a perfect safety management system of hazardous chemicals can promote the strict implementation and continuous improvement of various management measures. Cluster management should be implemented among chemical enterprises in the same industrial chain or adjacent location to build a unified safety management system and strengthen communication and cooperation on risks. Within the enterprise, the responsibilities of relevant departments and employees should be clarified in safety management and an accident accountability system should be established to strengthen execution (Zhang et al. 2020). Another crucial duty of the enterprise is to enhance the professional quality and access conditions of employees with the help of the training and evaluation system (Li et al. 2020). Furthermore, the dynamic risk assessment system in the enterprise can function as a self-inspection tool to eliminate the potential hazards in time. In the production process, enterprises should attach importance to equipment maintenance and install a real-time monitoring system to timely replace the aging equipment (Kockmann et al. 2017). At last, the construction of an enterprise safety culture should be promoted along with a correct safety concept and the high safety awareness of all employees.

(4) Emergency management

Emergency management systems in some developing countries such as China are still in the early stage of construction. Hence, numerous difficulties still exist in preventing and mitigating the risk of hazardous chemical accidents. Firstly, under the concept of being people-oriented, the emergency management department should form a scientific emergency plan system. The emergency rescue base and team need a reasonable planning layout based on the hazardous chemical distribution map and regional development (Dou et al. 2019). Disaster mitigation is a priority to avoid secondary catastrophes throughout the emergency response phase (Smolders et al. 2014). Secondly, to improve emergency management ability should promote cooperation with the third-party professional rescue team based on a professional emergency team, sufficient capital investment, and high-quality talents. At last, an intelligent emergency management system is the development prospect of emergency management to realize resource sharing based on internet technology, helping emergency

decision-makers quickly select emergency plans suitable for the dynamic scenario. High and new technology like UAVs and fire robots can perform emergency rescue tasks that human beings cannot complete; social software, news media, and other tools can disseminate early warning information (Dou et al. 2019).

(5)   Technical improvement

With the application of new technologies in the chemical industry, the safety level of hazardous chemicals has been significantly improved (Chikhalikar and Jog 2018). The implementation of automation transformation in the factory contributes to reducing the accident risk caused by human error. Vehicles transporting hazardous chemicals need to keep stable during transportation to prevent road accidents (Liu et al. 2005). The system information management of hazardous chemicals pipeline transportation relies on the information platform provided by the urban pipe network database to provide a blueprint for urban planning and construction (Dou et al. 2019). Gas detection and alarm devices can be widely used in residential buildings for fewer gas leakage accidents.

(6)   Environmental protection

Environmental pollution is one of the principal threats facing the globe today. Both accidental leakage of hazardous chemicals and intentional discharge of hazardous wastes are significant sources of pollution (Cao et al. 2018). The notion of sustainable development points out that the precondition for the safety management of hazardous chemicals is environmental protection. The capability of a country to control environmental risks depends on the management level of hazardous chemicals and the response efficiency in dealing with environmental pollution events (Chan et al. 2015). As a result, legislation needs to clarify the critical role of environmental protection in the safety management of hazardous chemicals (Vogel and Roberts 2011). To meet national standards, enterprises should increase their investment in environmental protection resources, strengthen environmental monitoring (Chiang and Roy 2012), and improve the response mechanism for environmental emergencies. In particular, hazardous waste discharge should be closely regulated. Green chemical processes and transforming the dangerous waste into resources are possible measures to mitigate the environmental threat posed by hazardous waste.

2.6.2   Emergency Protection Action in HCLA

2.6.2.1   Status and Challenges

Guiding the public to carry out emergency protection immediately after the occurrence of HCLA is the crux to minimize casualties and property losses (Georgiadou et al. 2010). In many European countries, the recommended emergency protection approach is to direct people to take shelter on the spot; however, in China, the most common decision is to evacuate the surrounding population. The United

States, Canada, and other countries joined to formulate the Emergency Response Manual to determine the selection criteria for emergency protection actions in specific hazardous chemical accidents. In China, the "Method on Determination of Emergency Planning Zone for Major Accident of Toxic Gas Leakage (GB/T 35622–2017)" provides a reference for the specific implementation of public emergency protection. Researches choose emergency protection actions based on massive calculations and explicit initial parameters of leakage, which are hard to operate in reality. Furthermore, some scholars have studied the public risk perception and decision-making behavior in emergencies from the perspective of sociology and psychology (Mccaffrey et al. 2018). However, the accidents studied in existing research are mainly natural disasters like building fires, hurricanes, or earthquakes instead of hazardous chemical leakage, leading to research results that are not entirely appropriate for public emergency response in HCLAs.

In HCLA, the issue of public emergency protection actions exists many challenges as follows:

(1) Due to its toxicity, explosion, or flammability, the leakage of hazardous chemicals is prone to induce secondary disasters as the accident evolves. Once the leakage spreads in factories (industrial parks) storing massive hazardous chemicals, a domino effect could result in more significant disasters. This situation highlights the importance of the optimal decision on emergency protection action and guidance strategy for the public in the accidental leakage of hazardous chemicals.

(2) With the evolution of the accident, the scope of public emergency response may enlarge, which requires decision-makers to adjust the notification scope and content of warnings dynamically (Gai et al. 2017). Today, the rapid development of communication technology provides diversified channels for emergency notification and enriches guidance strategies (Bao et al. 2020). However, the ubiquity of modern media technologies, including network communication and mobile phones, also creates a platform for the propagation of disaster rumors, which may hamper rescue operations.

(3) The current relevant requirements and standards lack clear terms and technical routes for emergency protection actions. The types of hazardous chemicals, the location of the accident, and the objects to be evacuated all have an impact on the effectiveness of emergency response actions (Hou et al. 2020). If the evacuation is blindly selected after the leakage of hazardous chemicals, a collapse of evacuation traffic may occur and cause additional casualties (Wang et al. 2013).

(4) Many researchers have achieved significant advances in assessing accident risk, formulating emergency plans, and preventing disasters in terms of hazardous chemicals (Pittinger et al. 2003; Dakkoune et al. 2018), but poor focus on emergency response decision-making problems in HCLA. As a result, the formulation and evaluation of emergency plans and drills in hazardous chemical management still lack a sufficient theoretical basis.

2.6.2.2 Development Trend of Emergency Protection Action in HCLA

In an emergency, warning information improves the risk perception in public as the impetus for emergency protection actions. Due to the dynamic nature of warning dissemination, it is more suitable to predict the risk perception level of the public in a time-based emergency information dissemination model. On this foundation, the model simulation can analyze the public behavioral tendency in the scenarios of HCLA.

Based on the development of information technology, smart city has become a new frontier of urban construction research. The dynamic model of public emergency response can be developed utilizing data mining, complex networks, and other technologies, thanks to the opportunities in smart city building. In addition, artificial intelligence can be applied to verify decision-making models of emergency protection behavior, which uphold the theory of public emergency protection behavior in HCLA (Dou et al. 2019).

When determining evacuation procedures, guiding the public to the destination in the shortest time is the crux of ensuring safety. First, based on the features of hazardous chemical leaks, the risk assessment of public evacuation actions should be undertaken from the perspectives of health implications and social impact. Integrated with the regional features of the accident location, the minimization of the evacuation time can be implemented by optimizing many aspects such as vehicles, evacuation routes, media guidance, and others. Establishing an intelligent guidance system for public emergency shelters can enhance evacuation efficiency and lessen the risk to rescue workers. For example, intelligent guidance robots can serve as evacuation guides and crowd monitoring.

The public emergency protection theory involves management, behavioral science, psychology, social science, engineering, and other multi-disciplinary concepts. As a result, optimizing the public emergency behavior guidance strategy should adopt multi-objective optimization and heuristic solutions. Meanwhile, it is necessary to improve the implementation of the public emergency protection actions in HCLA and attach importance to the theoretical system construction of public protection.

2.7 Conclusions

This chapter introduces the characteristics of hazardous chemical leakage accidents (HCLAs) in China and the emergency evacuation response caused by them. Drawing on accident data acquired from the China Chemical Information Net, we extract relevant information from the 5207 HCLAs and 157 evacuation events caused by some HCLAs in China from 2009 to 2018. Since 2015, the frequency of HCLAs in China has been declining. However, massive casualties have happened on occasion, and the frequency of HCLA is inconsistent across China's east and west. From 2016

to 2018, the HCLAs mortality remained within 10%. From April to October, the frequency of HCLAs is higher, especially in July and August.

HCLAs are most common in road and pipeline transportations, while the highest mortality occurs in factories (industrial parks) and civil residences. In road transportation, HCLAs are more likely to occur between 6:00–10:00 a.m. and 3:00 p.m., and the period with high mortality is 0:00–5:00 a.m. Improper pipeline construction is the leading cause of pipeline transportation accidents. Our future research direction is to unify the risk assessment criteria and make a comparative analysis of "individual risk" and "social risk" under different transportation channels. The rate of HCLAs in factories (industrial parks) is reducing continuously, and the mortality is decreasing from the overall trend. The HCLAs in civilian residences are most caused by fuel gas, among which the mortality of coal gas leakage is the highest, reaching 20.9%.

Most of the evacuations caused by HCLAs occur in rural areas, which mainly involve extra-small-scale evacuation. Nearly 70% of evacuations can be finished within 60 min. The locations of the HCLA and categories of hazardous chemicals leaked have a substantial impact on the evacuation level.

Saving lives is the first priority. Many governments now place a premium on the proper management of hazardous chemicals. However, certain developing countries, such as China, continue to face challenges in this area, such as inadequate rules, gaps in government oversight, a high number of firms, and a low degree of safety management. In addition, in the case of hazardous chemical leaks, the study on public emergency protection actions and guidance strategy is insufficient to satisfy the needs of public safety. To this end, the six dimensions of LGCETE guidelines proposed in this chapter point to the future tasks of hazardous chemical safety management that give prominence to the development trend of emergency protection actions. The research results can function as a guide to improving hazardous chemical safety management in China and a reference for the growth of hazardous chemical industry in other nations. In addition to evacuation, shelter-in-place is also an important public protection action in major chemical accidents. In the following chapter, we will study how to balance these two protection actions.

References

Aneziris, O.N., Z. Nivolianitou, M. Konstandinidou, G. Mavridis, and E. Plot. 2017. A total safety management framework in case of a major hazards plant producing pesticides. *Safety Science* 100: 183–194.

Astivia, O.L.O., and B.D. Zumbo. 2017. Population models and simulation methods: The case of the spearman rank correlation. *British Journal of Mathematical & Statistical Psychology* 70 (3): 347–367.

Boot, H. 2013. The use of risk criteria in comparing transportation alternatives. *Chemical Engineering Transactions* 31: 199–204.

Cao, G.Z., L. Yang, L.X. Liu, Z.W. Ma, J.N. Wang, and J. Bi. 2018. Environmental incidents in China: Lessons from 2006 to 2015. *Science of the Total Environment* 633: 1165–1172.

Chan, E.Y., Z. Wang, C.K. Mark, and L.S. Da. 2015. Industrial accidents in China: Risk reduction and response. *The Lancet* 386: 1421.

Chiang, T.A., and R. Roy. 2012. An intelligent benchmark-based design for environment system for derivative electronic product development. *Computers in Industry* 63 (9): 913–929.

Chikhalikar, A.S., and S.H. Jog. 2018. A review of methodologies for safety and hazard management in chemical industries. *ChemBioEng Reviews* 5 (6): 372–390.

China statistical yearbook 2019 *China Statistics Press Beijing PRC* (in Chinese)

Dakkoune, A., L. Vernières-Hassimi, L. Sébastien, D. Lefebvre, and L. Estel. 2018. Risk analysis of French chemical industry. *Safety Science* 105: 77–85.

Dou, Z., A. Mebarki, Y. Cheng, X. Zheng, J. Jiang, Y. Wang, Y. Li, and J. Li. 2019. Review on the emergency evacuation in chemicals-concentrated areas. *Journal of Loss Prevention in the Process Industries* 26: 35–45.

Du, N., F. Zhou, E. Pulver, D. Tilbury, L.J. Robert, A. Pradhan, and X.J. Yang. 2020. Examining the effects of emotional valence and arousal on takeover performance in conditionally automated driving. *Transportation Research Part c: Emerging Technologies* 112: 78–87.

Duan, W.L., G.H. Chen, Q. Ye, and Q.G. Chen. 2011. The situation of hazardous chemical accidents in China between 2000 and 2006. *Journal of Hazardous Materials* 186 (2–3): 1489–1494.

Dumrongpokaphan, T., and V. Kreinovich. 2018. Kuznets Curve: A simple dynamical system-based explanation. International Conference of the Thailand Econometrics Society. *Springer, Cham* 753: 177–181.

Filiz, H., and E. Pinar. 2006. Toxic Industrial Chemicals (TICs) — chemical warfare without chemical weapons. *FABAD Journal of Pharmaceutical Sciences.* 31 (4): 220–228.

Fyffe, L., S. Krahn, J. Clarke, D. Kosson, and J. Hutton. 2016. A preliminary analysis of key issues in chemical industry accident reports. *Safety Science* 82: 368–373.

Gai, W.M., Y.F. Deng, Z.A. Jiang, J. Li, and Y. Du. 2017. Multi-objective evacuation routing optimization for toxic cloud releases. *Reliability Engineering & System Safety* 159: 58–68.

Georgiadou, P.S., I.A. Papazoglou, C.T. Kiranoudis, and N.C. Markatos. 2010. Multi-objective evolutionary emergency response optimization for major accidents. *Journal of Hazardous Materials* 178 (1–3): 792–803.

Hashimoto, H., K. Yamada, H. Hori, S. Kumagai, M. Murata, T. Nagoya, H. Nakahara, and N. Mochida. 2017. Guidelines for personal exposure monitoring of chemicals: Part II. *Journal of Occupational Health* 59 (6): 471–476.

Heo, S., M. Kim, H. Yu, W.K. Lee, J.R. Sohn, S.Y. Jung, K.W. Moon, and S.H. Byeon. 2018. Chemical accident hazard assessment by spatial analysis of chemical factories and accident records in South Korea. *International Journal of Disaster Risk Reduction* 27: 37–47.

Hou, J., W.M. Gai, W.Y. Cheng, and Y.F. Deng. 2020. Prediction model of traffic loading rate for large-scale evacuations in unconventional emergencies: A real case survey. *Process Safety and Environmental Protection* 144: 166–176.

Hsu, S.H., C.C. Lee, M.C. Wu, and K. Takano. 2008. A cross-cultural study of organizational factors on safety: Japanese VS Taiwanese oil refinery plants. *Accident Analysis and Prevention* 40 (1): 24–34.

Jardine, C., S. Hrudey, J. Shortreed, L. Craig, D. Krewski, and C. Furgal. 2003. Risk management frameworks for human health and environmental risks. *Journal of Toxicology and Environmental Health-Part B-Critical Reviews* 6 (6): 569–718.

Kang, K., and H. Ryu. 2019. Predicting types of occupational accidents at construction sites in Korea using random forest model. *Safety Science* 120: 226–236.

Kockmann, N., P. Thenée, C. Fleischer-Trebes, G. Laudadio, and T. Noel. 2017. Safety assessment in development and operation of modular continuous-flow processes. *Reaction Chemi- Stry & Engineering* 2 (3): 258–280.

Li, X.W., T.Z. Liu, and Y.K. Liu. 2020. Cause analysis of unsafe behaviors in hazardous chemical accidents: Combined with HFACs and Bayesian Network. *International Journal of Public Health* 17 (1): 11.

Liu, T.M., M.H. Zhong, and J.J. Xing. 2005. Industrial accidents: Challenges for China's economic and social development. *Safety Science* 43 (8): 503–522.

Lu, Y.D. 2018. Research on real-time risk warning method for hazardous materials transportation by road. Doctoral Dissertation, China University of Geosciences Beijing.

Mccaffrey, S., R. Wilson, and A. Konar. 2018. Should I stay or should I go now? Or should I wait and see? Influences on wildfire evacuation decisions. *Risk Analysis* 38 (7): 1390–1404.

Nakai, A., Y. Kajihara, K. Nishimoto, and K. Suzuki. 2017. Information-sharing system supporting onsite work for chemical plants. *Journal of Loss Prevention in the Process Industries* 50: 15–22.

Oltmanns, J., D. Bunke, W. Jenseit, and C. Heidorn. 2014. The impact of REACH on classification for human health hazards. *Regulatory Toxicology and Pharmacology* 70 (2): 474–481.

Pittinger, C.A., T.H. Brennan, D.A. Badger, P.J.B. Hakkinen, and M.C. Fehrenbacher. 2003. Aligning chemical assessment tools across the hazard-risk continuum. *Risk Analysis* 23 (3): 529–535.

Qin, G., P. Zhang, X. Hou, S. Wu, and Y. Wang. 2020. Risk assessment for oil leakage under the common threat of multiple natural hazards. *Environmental Science and Pollution Research.* 27: 16507–16520.

Russell, R.M., S.C. Maidment, and I. Brooke. 1998. An introduction to a UK scheme to help small firms control health risks from chemicals. *Annals of Occupational Hygiene* 42 (6): 367–376.

Seo, S.K., Y.G. Yoon, J. Lee, J. Na, and C.J. Lee. 2021. Deep Neural Network-based Optimization Framework for Safety Evacuation Route during Toxic Gas Leak Incidents. *Reliability Engineering and System Safety.* 218 (2022): 108102.

Shen, Y., Q. Wang, W. Yan, and J. Sun. 2015. An evacuation model coupling with toxic effect for chemical industrial park. *Journal of Loss Prevention in the Process Industries* 33: 258–265.

Smolders, R., A. Colles, C. Cornelis, M. Van Holderbeke, H. Chovanova, D. Wildemeersch, M. Mampaey, and K. Van Campenhout. 2014. Key aspects of a flemish system to safeguard public health interests in case of chemical release incidents. *Toxicology Letters* 231 (3): 315–323.

Sun, Y., and J. Sun. 2020. Self-assessment of tsunami evacuation logistics: Importance of time and earthquake experience. *Transportation Research Part d: Transport and Environment.* 87: 102512.

Tang, Z., Q. Huang, and Y. Yang. 2015. China: Overhaul rules for hazardous chemicals. *Nature* 525 (757): 455.

Tinney, V.A., S.C. Anenberg, M. Kaszniak, and B. Robinson. 2016. Eighteen years of recommendations to prevent industrial chemical incidents: Results and lessons learned of the US Chemical Safety Board. *Public Health* 139: 183–188.

Tong, S.J., Z.Z. Wu, R.J. Wang, Y.Q. Duo, and G.X. Yi. 2015. Statistical analysis and countermeasures on larger and above grades accidents of dangerous chemical enterprises from 2001 to 2013. *Journal of Safety Science and Technology* 11 (3): 129–134.

Vogel, S.A., and J.A. Roberts. 2011. Why the toxic substances control act needs an overhaul, and how to strengthen oversight of chemicals in the interim. *Health Affairs* 30 (5): 898.

Wang, J.W., H.F. Wang, W.J. Zhang, W.H. Ip, and K. Furuta. 2013. Evacuation planning based on the contraflow technique with consideration of evacuation priorities and traffic setup time. *IEEE Transactions on Intelligent Transportation Systems* 14 (1): 480–485.

Wang, B., D. Li, and C. Wu. 2020. Characteristics of hazardous chemical accidents during hot season in China from 1989 to 2019: A statistical investigation. *Safety Science.* 129: 104788.

Yang, J., F. Li, J. Zhou, L. Zhang, L. Huang, and J. Bi. 2010. A survey on hazardous materials accidents during road transport in China from 2000 to 2008. *Journal of Hazardous Materials* 184 (1–3): 647–653.

Zhang, H.D., and X.P. Zheng. 2012. Characteristics of hazardous chemical accidents in China: A statistical investigation. *Journal of Loss Prevention in the Process Industries* 25 (4): 686–693.

Zhang, Y.Y., C. Sun, W. Shan, J.Q. Cai, L.L. Jing, and W. Shao. 2020. Systems approach for the safety and security of hazardous chemicals. *Maritime Policy Management* 47 (4): 500–522.

Zhao, J., R. Joas, J. Abel, T. Marques, and J. Suikkanen. 2013. Process safety challenges for smes in China. *Journal of Loss Prevention in the Process Industries* 26 (5): 880–886.

Zhong, M., C. Shi, T. Fu, L. He, and J. Shi. 2010. Study in performance analysis of China urban emergency response system based on Petri net. *Safety Science* 48: 755–762.

Zhou, J., and G. Reniers. 2021. Petri net simulation of multi-department emergency response to avert domino effects in chemical industry accidents. *Process Safety and Environmental Protection* 146: 916–926.

Zografos, K.G., and K.N. Androutsopoulos. 2008. A decision support system for integrated hazardous materials routing and emergency response decisions. *Transportation Research Part c: Emerging Technologies* 16 (6): 684–703.

Chapter 3
Shelter-In-Place Risk Assessment for High-Pressure Natural Gas Wells with Hydrogen Sulfide

3.1 Introduction

In the previous chapter, we conducted a systematic statistical analysis of historical accident data. When a hazardous chemical accident occurs, should the public in the threatened area choose to evacuate or take refuge in place to minimize the risks that the accident brings to themselves? In this chapter, we will study the application of risk assessment methods in public protection decision-making and emergency management.

Because the nature gas is the most important source of clean energy, in recent years, with the government's increasing attention to environmental protection, China's demand for natural gas is increasingly growing. At present, many high-sulfur gas fields in China have entered the large-scale development stage, but due to the lack of targeted risk control and measures for safety, many accidents have occurred one after another in the stage of drilling and completion, such as hydrogen sulfide poisoning and out-of-control blowout. These accidental could cause huge economic losses, personal injuries, and environmental pollution (Xu and Fan 2014).

In general, most sulfur-containing high-pressure gas wells are built in mountainous and hilly areas, especially in China, where the altitude of gas wells is usually 300–600 m (Xu and Fan 2014). High pressure, high sulfur content, and complex geological conditions are easily to cause accidents. For example, on December 23, 2003, in Kaixian County, Chongqing, a well blowout accident occurred in Luojia 16 H well. The accident affected more than 93,000 people, caused 65,000 people evacuated, and killed 243 people; on March 25, 2006, a blowout accident occurred in Luojia 2 well in Kaixian County, Chongqing, more than 10,000 people were evacuated; in Deyang Xinchang Gas Field, Sichuan Province, an accident occurred in well

926–2 on May 19, 2009, in which blowout led to an evacuation of more than 1000 households.

For the blowout accident of hydrogen sulfide high-pressure natural gas well, the common public protection measures include evacuation, shelter-in-place, and respiratory protection (Georgiadou et al. 2010; Gai et al. 2018; Gai and Deng 2019). However, it is difficult to provide personal protection for each individual when the accident affects the large numbers of the public. Therefore, once accidents occur, evacuate the affected public in time is the fundamental way to protect the public (Yin et al. 2010; Yang et al. 2013; Zhang et al. 2017; Gai et al. 2017). In many cases, due to the long-term preparation and implementation process, the public may also be exposed to toxic clouds during evacuation (Rogers et al. 1990). Therefore, sheltering-in-place in their homes or specific places of refuge may be more reliable and effective. If the emergency shelters cannot let all the public shelter-in-place, local residences can also be considered, but it is necessary to determine whether the shelter meets the requirements of safety (James and Calvin 2005).

Shelter-in-place is a strategy to reduce human exposure to toxic gas in a leakage accident. If people shelter in buildings instead of outdoors, their exposure to radiation may be reduced (James and Calvin 2005). Wilson (1988) assessed the variability of the effectiveness of indoor shelter and found that the variability of buildings led to the difference in house air leakage rates between Canada and the United States, which was about twice the average. Rogers et al. (1990) published *Evaluating Protective Actions for Chemical Agent Emergencies*, which is an extensive report that involved an evaluation of the shelter-in-place strategy. James and Calvin (2005) provided a method assessing the effectiveness of expedients in place to prevent airborne hazards, as outlined in America. However, the evaluation of the effectiveness of sheltering-in-place cannot provide a direct reference for emergency preparedness or decision-making of emergency responses.

At present, the quantitative risk assessment (QRA) for major hazards has attracted considerable attention, and the aim of QRA is limiting potential risks to a given range. Although QRA-related research started late in China, great progress of accident probability and consequence analysis has been obtained. (Xu and Fan 2014). For example, based on the accident probability analysis of fault tree simulation and the accident consequence analysis of high-pressure sour gas wells in drilling and completion stages, the evaluation framework of individual risk calculation was proposed (Xu and Fan 2014). The simulation of H_2S gas diffusion process in blowout accidents is also analyzed (Wu et al. 2009). However, when analyzing the consequences of the accident, most of them focus on the individual exposure risk in a certain place and do not consider the impact of individual emergency protection behavior on individual risk, so they are unable to provide an effective recommendations from the point of the public's emergency protection, in order to analyze how the public prepare for refuge in advance under normal circumstances, or whether to choose shelter-in-place as protection action in case of emergency. Combined with accident probability analysis, accident consequence analysis, and the impact of different individual emergency response actions on individual risks, it is a scientific and effective solution to evaluate the safety level of alternative emergency protection measures.

Through the accident probability analysis, the accident consequence analysis based on the calculation of gas concentration inside and outside the buildings for sheltering-in-place, and probability analysis of the corresponding emergency response action during refuge, this paper focuses on an assessment method of individual risk calculation after emergency protection measures, sheltering-in-place, for blowout accident. And a case study in China is performed and analyzed.

3.2   Risk Assessment of Sheltering-In-Place

Individual risk is often defined as the probability that an average unprotected person, permanently present at a certain location, is killed due to an accident resulting from a hazardous activity (Jonkman et al. 2003). Obviously, the above definition of individual risk is not applicable to the individual risk calculation after adopting emergency protective measures. In order to evaluate the effectiveness of sheltering-in-place as an emergency response to a hydrogen sulfide high-pressure natural gas well blowout accident, this chapter proposes the concept of in situ hedging, which is defined as the probability of death of a person ordered to shelter-in-place in a building due to accidents caused by hazardous activities.

Studies have shown that after the emergency protection order is issued, a certain proportion of people are in a wait-and-see state and do not take designated emergency protective actions (Mccaffrey et al. 2018). Therefore, the shelter-in-place risk can be estimated by integrating the following two indicators: The first is the health consequences of an individual taking an emergency action on a shelter-in-place emergency order issued by the emergency decision-maker P_i, and the second is the probability f_i of the corresponding emergency response action.

The shelter-in-place risk can be estimated as follows:

$$\text{SR} = \sum_i^m f_i \cdot p_i \tag{3.1}$$

where i represents the ith emergency response action of the individuals, $i = 1, 2, \ldots, m$.

3.2.1   Probability Calculation of Individual's Emergency Response Action

The probability i associated with an individual emergency response action can be calculated as follows:

$$f_i = F \cdot r_i \tag{3.2}$$

where F is the accident probability. When $F = 1$ means the accident has occurred, and F can be estimated by fault tree analysis and statistical analysis if the accident has not occurred (Xu and Fan 2014). r_i is the probability that people will take certain response actions after issuing emergency orders of sheltering-in-place, such as negative (in situ) and positive (sheltering-in-place in a building). Such probability can be obtained by investigating the public's emergency response in accidents.

3.2.2 Health Consequences Analysis

3.2.2.1 Accident Scenario Simulation

Once a blowout accident occurs in high-pressure natural gas wells containing hydrogen sulfide, a large amount of toxic gas (mainly is hydrogen sulfide) is diffused in the atmosphere along the horizontal and vertical directions, and its diffusivity is mainly affected by factors such as release rate, wind (speed and direction), atmospheric stability, and topography (Papazoglou et al. 1992).

The prediction of toxic gas diffusion based on different gas diffusion models can provide a basis for health consequence estimation and emergency response zone determination. CFD model can be used to simulate the diffusion of heavy gas, which is the most accurate technique for simulating the airborne transport of pollutants (Pontiggia et al. 2010; Epstein et al. 2011; Li et al. 2015). Therefore, in this chapter, in order to achieve a compromise between the accuracy and performance, the CFD model was used in toxic gas diffusion prediction.

3.2.2.2 Estimation of Toxic Gas Concentration

The outdoor toxic gas concentration in affected areas can be calculated according to the gas diffusion model mentioned in Sect. 3.2.1. Based on this, the indoor gas concentration can be calculated by the following equation (Chan 2006):

$$\frac{\mathrm{d}c_{\mathrm{in}}(t)}{\mathrm{d}t} = e(c_{\mathrm{out}}(t) - c_{\mathrm{in}}(t)) \tag{3.3}$$

where $c_{\mathrm{in}}(t)$ is the concentration of indoor toxic gas at time t; $c_{\mathrm{out}}(t)$ is the concentration of outdoor toxic gas at time t; and e is a constant, the air exchange rate of the building, which can be measured by the air exchange rate test (James and Calvin 2005).

3.2.2.3 Estimation of Death Probability

In the case of blowout of high-pressure gas well containing hydrogen sulfide, the appropriate model corresponding to each point in the area can be used as a function of time to calculate the spatial and temporal distributions of extreme conditions (Georgiadou et al. 2007; Zhou and Liu 2012). Therefore, according to the profile, the probability of individual death $P_r(x, y)$ at a specific leakage location (x, y) during the time interval Δt can be obtained according to the probability function (Crowl and Louvar 2001):

$$P_r = k_1 + k_2 \ln(D_t) \tag{3.4}$$

where D_t is the lethal dose. And for those who have taken sheltering-in-place, D_t can be calculated according to the following formula:

$$D_t = \int_{\Delta t} c_{in}(t)^n dt \tag{3.5}$$

For those who are staying in place outside, D_t can be estimated as follows:

$$D_t = \int_{\Delta t} c_{out}(t)^n dt \tag{3.6}$$

More specifically, Eq. (3.7) used to convert a given "probit" value to the percentage affected in the spreadsheet calculation (Zhou and Liu 2012) is:

$$P = 50\left[1 + \frac{V-5}{|V-5|}\text{erf}\left(\frac{|V-5|}{\sqrt{2}}\right)\right] \tag{3.7}$$

3.2.3 Determination of Acceptable Risk Level

To reduce the risk, a widely accepted standard is set for individual risk according to the As Low As Reasonably Achievable (ALARA) guideline (also known as the As Low As Reasonably Achievable (ALARP) Guidelines) (Aven and Vinnem 2005; Zhou and Liu 2012; Xu and Fan 2014). Under the ALARA criterion, risks can be divided into three areas: intolerable area, widely acceptable area, and the area in between, which is called "acceptable" area or "ALARP" area. For emergency decision-makers, based on the results of the shelter-in-place risk assessment, they can further determine whether additional risk mitigation measures should be used in peacetime emergency management, or which public protection actions should be selected in an emergency.
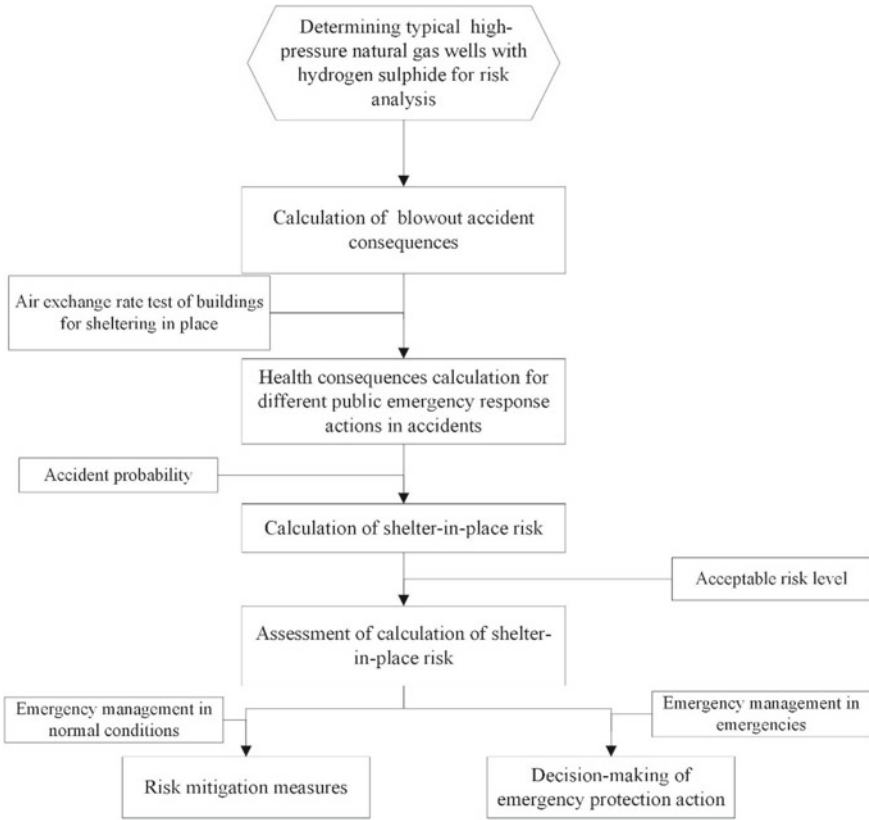
Fig. 3.1 Flowchart of shelter-in-place risk analysis and assessment for high-pressure sour gas wells

Figure 3.1 shows the risk assessment process of shelter-in-place for high-pressure sour gas wells.

3.3   Case Study

A well named XX is located in Xuanhan County, Sichuan Province, China. The elevation of the well site is 559 m, and the three sides are mainly reclaimed. There are few forests and primitive landforms. The southeast side is mainly shallow hills and hills, with an elevation drop of 100 m. The maximum open flow rate of the XX well is 438.5×10^4 m³/d, containing 14.71% hydrogen sulfide (volume content).

3.3.1 Preliminaries

3.3.1.1 Estimation of Accident Consequences

The wind speed is 1 m/s, according to local conditions. The CFD model was used for simulation calculation. According to the maximum unobstructed flow in the cluster well, the estimated leakage is 438.5×10^4 m^3/d. At the same time, 8 wind directions were calculated, to obtain the most remote diffusion distance (the farthest point of the diffusion). According to the above leakage parameters, the diffusing amount of H$_2$S was calculated with 8 wind directions, corresponding to the longest distance of each concentration.

Figure 3.2 shows the calculation results. It can be evidently seen that the diffusion distance of hydrogen sulfide gas was closely related to the prevailing wind direction. In the downwind direction, the dispersion distance was much shorter. For example, it can be seen from Fig. 3.2a that 7.5 min after the leakage, 100 ppm concentration of hydrogen sulfide diffuses to 535 m, 300 ppm to 470 m, and 1000 ppm to 385 m. In addition, the east side of well XX had the farthest hydrogen sulfide diffusion distance.

Table 3.1 shows the longest dispersion distance of H$_2$S release at 1000 ppm in each direction at various times. The table shows that the longest dispersion distance of the 1000 ppm H$_2$S release was approximately 1000 m.

3.3.1.2 Air Exchange Rate Test of the Local Residences

Because there are only a limited number of shelters near the XX well, once a blowout accident occurs, a large number of the public will be affected, and it becomes difficult to effectively shelter-in-place. The residences can provide shelter-in-place if the residences provide adequate protection. However, to assess the effectiveness of shelter-in-place use of residential buildings, it is necessary to test the air exchange rate of the residences. The value of air exchange rate e is only related to the porosity of the building structure under a certain external wind speed and temperature. For buildings used for sheltering in the air exchange rate test, $c_{out} = 0$. According to Eq. (3.3), the air exchange rate e can be calculated by integrating Eq. (3.7) (James and Calvin 2005),

$$e = \frac{\ln c_{in}^{t_1} - \ln c_{in}^{t_2}}{t_2 - t_1} \tag{3.8}$$

where $c_{in}^{t_1}$ and $c_{in}^{t_2}$ are the volume fractions inside the sheltering building at time t_1 and time t_2, respectively, and both can be measured via the test.

In conclusion, a local house (used as a temporary shelter) was tested for gas tightness against H$_2$S leakage caused by a well spray accident. SF$_6$ gas with a purity of 99.99% was selected as the infrared trace gas, and the quantitative infrared SF$_6$ detector was used in the experiment. Here, the most representative houses in the area
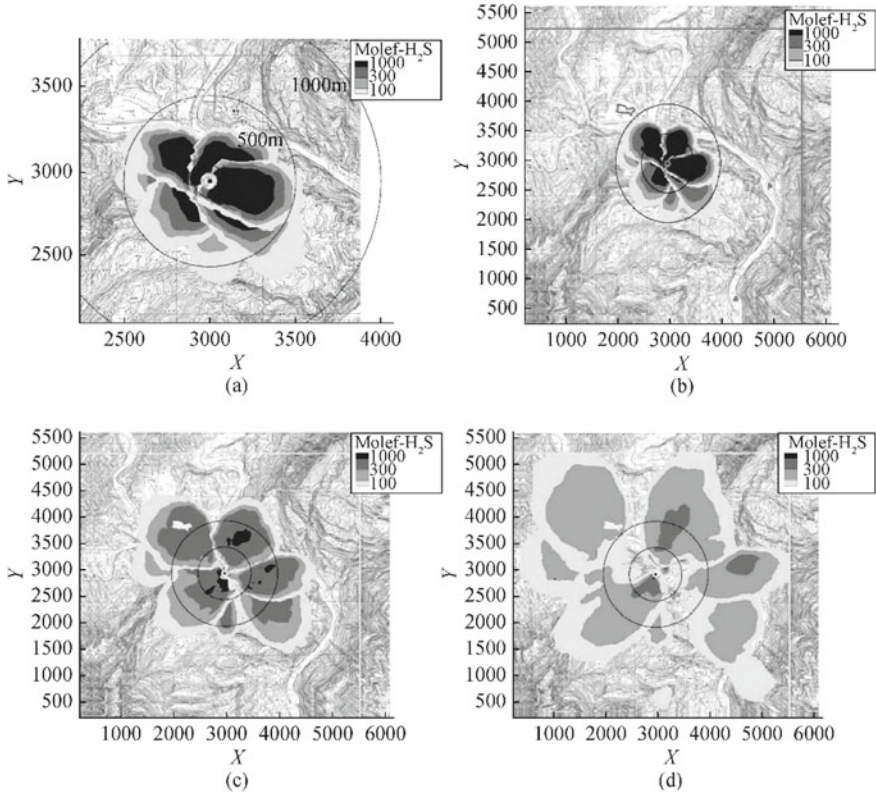
Fig. 3.2 Dispersion of H_2S in different periods after the accident **a** 7.5 min; **b** 15 min; **c** 30 min; **d** 45 min

Table 3.1 Maximum diffusion distance of 1000 ppm hydrogen sulfide release at different times after the accident

Time/min	Dispersion distance of H_2S of 1000 ppm/m
7.5	385
15	747
30	970
45	116

were selected for the air exchange rate test. For each experimental building, involved different kinds and ages, the main bedroom with doors and windows was selected as the measurement object.

The tests found that the brick-tile buildings were not suitable for use as emergency shelters, as they had the highest air exchange rate at 16.616%/min. In addition, the air exchange rate is not only related to the opening or closing of doors and windows, but also closely related to their status. The air exchange rate of them would be lower if intact or sealed.
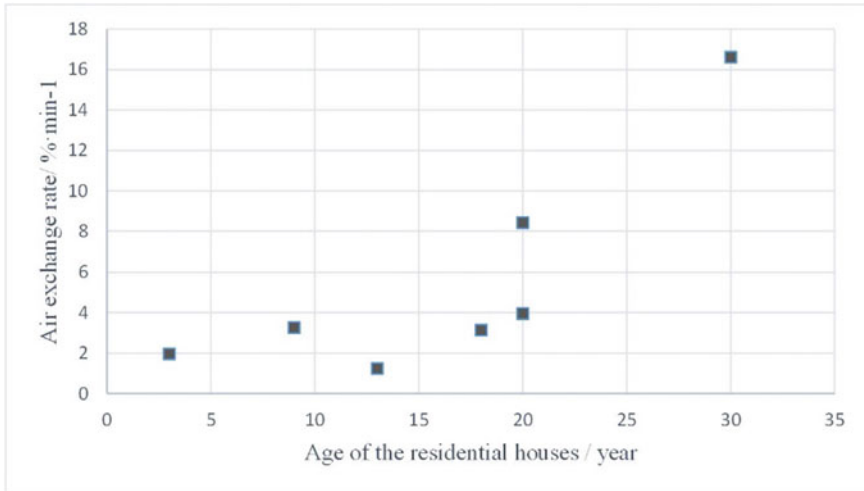
Fig. 3.3 Relationship between air exchange rate and the age of the house

The test results of air exchange rate of local residences of different ages in the study area are shown in Fig. 3.3. We can see that the 30−year−old house has the largest air exchange rate. For houses in good condition, the air exchange rate under 20 years can be less than 4%/min, and the air exchange rate under 3−13 years should be less than 2%/min. Therefore, the air exchange rate can be controlled below 2%/min if protective measures are properly formulated.

3.3.1.3   Health Consequence Analysis of Staying Indoors and Outdoors

According to the test results of the 4.3.1 simulation calculation, it can be found out that the hydrogen sulfide release of 1000 ppm diffuses farthest with the westerly wind. Therefore, assuming the wind direction is west wind, the risk analysis will be carried out on the sheltering of the local residential buildings in the downwind direction about 300, 500, and 1000 m away from the XX well. If the air exchange rate of these houses is 2%/min, the distributions of hydrogen sulfide concentration outside and inside the residential house are shown in Fig. 3.4.

From Fig. 3.4, after the outdoor hydrogen sulfide dissipates, the hydrogen sulfide concentration in the house is still very large. From Fig. 3.4c, we can see that the concentration outside the residential area reaches 250 ppm at 1000 m, which may be harmful to the humans, but the concentration inside the house does not exceed 50 ppm, which would not be harmful to humans.

The cumulative mortality probability was calculated from the concentration distributions and Eqs. (3.3) and (3.4), as shown in Fig. 3.5. In Fig. 3.5a, the probability of mortality exceeds 80% within 40 min of the accident. This suggests that in the event of such an accident, a house within 300 m of the gas leak is not suitable for shelter.

Fig. 3.4 Distribution of
hydrogen sulfide
concentrations outside and
inside the residential houses
at about 300, 500, and
1000 m from the well **a**
300 m; **b** 500 m; **c** 1000 m
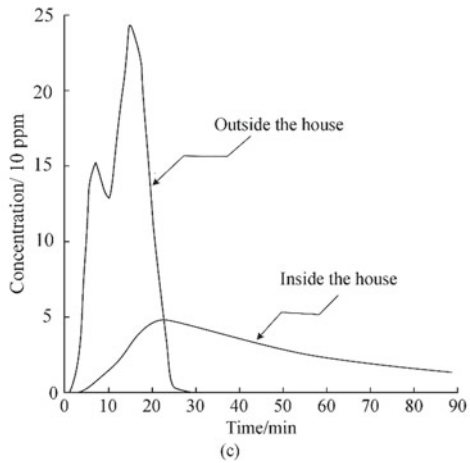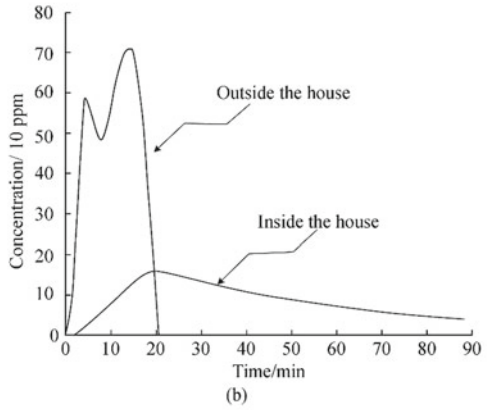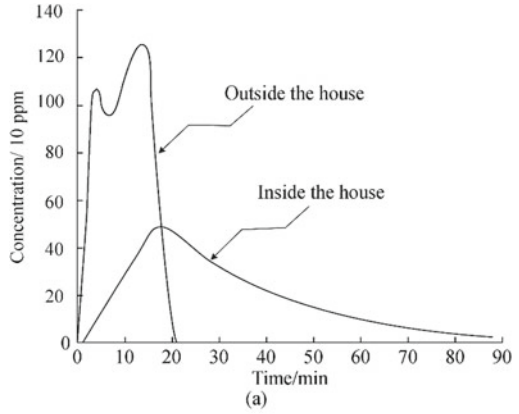
In addition, for residents near 300 m, the probability of mortality will rise rapidly from nearly 0–20% within 20 min after the accident.

According to Fig. 3.5b, when such an accident occurs, if the occupants located within 500 m from the gas leak shelter in their residential houses, the maximum probability of death would not exceed 6×10^{-6}. The death probability would become 0 if they take shelter in a house located 1000 away from the leakage, as shown in Fig. 3.5c.

3.3.2 Results of Shelter-In-Place Risk Assessment

Assuming that residences with an air exchange rate of 2%/min are used for sheltering-in-place, according to Eqs. (3.4), (3.5), and (3.6), by analyzing the indoor and outdoor toxic gas concentrations of 300, 500 and 1000 m, the health consequences of those who shelter-in-place or not take emergency protection measures are calculated. The results are shown in Table 3.2.

3.3.2.1 Results for Emergency Management Under Normal Conditions

Referring to the blowout accident probability in scanpower database, in the emergency management of high-pressure natural gas wells containing hydrogen sulfide under normal circumstances, the blowout accident probability is 8.71×10^{-4}. Assuming that the emergency response probability of the public is between 0 and 100%, combined with the data of health consequences and accident probability mentioned above, the risk of sheltering in the local residences at 300, 500, and 1000 m in downwind direction of the XX well can be calculated (Fig. 3.6).

The distances corresponding to the individual evacuation risks are assumed here to be 10^{-5}/a and 10^{-6}/a, which are chosen as the boundaries between the risk areas which are defined by ALARP. According to Fig. 3.6, under normal conditions, for high-pressure natural gas wells, the shelter-in-place risk assessment of emergency management is as follows:

(1) For the individuals who are about 300 m away from the XX well in the down-wind direction, even if emergency response is 100% carried out, the risk of shelter-in-place is still higher than 10^{-5}/a, which is unacceptable. Therefore, if people in this area do not have enough time for safe evacuation, it is suggested to formulate risk mitigation measures in daily emergency management, such as to establish more efficient emergency shelters and increase the reserve of emergency resources, such as respiratory protective equipment, rescue vehicles.

(2) For the individuals who are about 500 m away from the XX well in the downwind direction, if the probability of the public's emergency response is less than 99.3%, the risk of shelter-in-place would become unacceptable, which exceeds 10^{-5}/a. Therefore, if the population in this area does not have enough time for

Fig. 3.5 Cumulative
mortality probability of H_2S
in the houses at 300, 500,
and 1000 m away from the
accident site **a** 300 m; **b**
500 m; **c** 1000 m
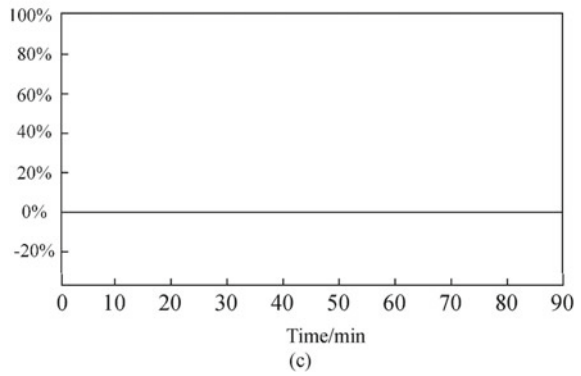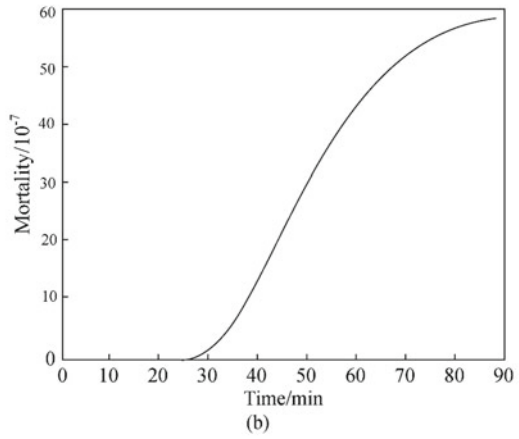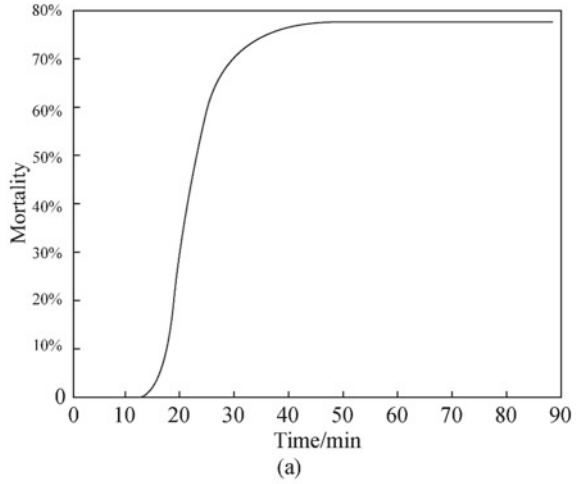
Table 3.2 Individual risk: Health consequences of people performing different emergency protective actions

Distance to the wellhead/m	300	500	1000
Outside-the-house death probability	1	0.98	8.3×10^{-5}
Death probability inside the house	0.085	6×10^{-6}	0
Individual risk outside the house	8.71×10^{-4}	8.54×10^{-4}	7.23×10^{-8}
Individual risk inside the house	7.4×10^{-5}	5.23×10^{-9}	0
Time required for reaching the death rate of 5% outside of the house/min	2	6	∞
Time required for reaching the death rate of 5% inside the house/min	40	∞	∞
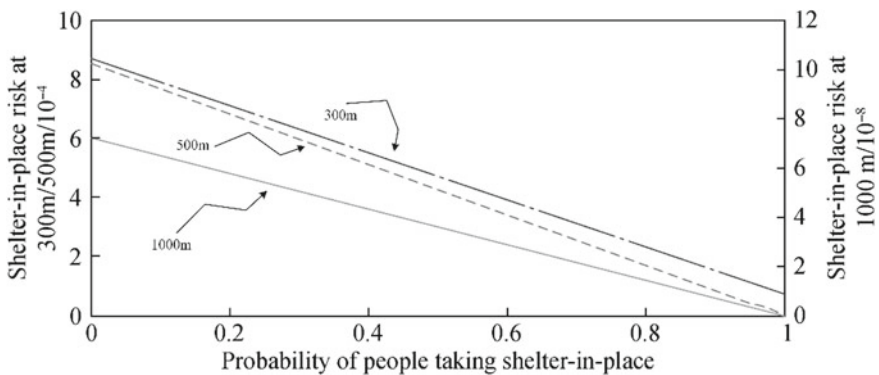
Fig. 3.6 Results of the risk evaluation of shelter-in-place for emergency management under normal situations

safe evacuation, it is recommended to formulate risk mitigation measures in daily emergency management, such as increasing emergency drills and training for the population in the area to improve self-rescue and mutual rescue capabilities.

(3) For the individuals who are more 1000 m away from the XX well in the downwind direction, the shelter-in-place risk is below 10^{-6}/a, which is negligible. In this case, for buildings with air exchange rate not higher than 0.02, risk mitigation measures can be ignored temporarily. For the cases that air exchange rate higher than 0.02, if emergency managers does not have enough time to safely evacuate the people, it is necessary to formulate risk mitigation measures for them, such as enhancing the air tightness of the houses in the area or providing more respiratory protection equipment.

However, as can be seen from Table 3.2, if the traditional individual risk calculation method is followed, the risk for sheltering-in-place can be neglected for the crowd in the downwind direction at a distance of not less than 500 m from XX well, due to the fact that the corresponding individual risk in the house is less than 10^{-6}/a.

Clearly, because the calculation of individual risk does not consider the fact that some individuals disobeyed the emergency order to shelter-in-place, this probably underestimates the risk of individuals who sheltered in place approximately at a distance of 500 m downwind from the XX well.

3.3.2.2   Results for Emergency Management in Emergencies

If the probability of an accident is 1, i.e., an accident has happened, the evaluation result of the shelter-in-place risk can also be used as a guide for emergency decision-making. The risk of shelter-in-place can also be derived using the above method for the corresponding scenario, as shown in Fig. 3.7. Emergency decision-makers can give an acceptable level of risk. It is assumed that the distances that correspond to the risks of evacuation for individual 0.05 and 10^{-4} are selected by the emergency decision-makers as the borders between risk areas. According to Fig. 3.7, the risk of sheltering-in-place is assessed as follows:

(1) For individuals located approximately 300 m downwind from the XX well, the risk of sheltering-in-place continues to be unacceptable in spite of a 100% probability of public emergency response. Consequently, additional public protection measures, such as evacuation or more rescue vehicles, should be considered to assist the public in evacuation.

(2) For individuals located approximately 500 m downwind from the XX well, the risk of sheltering-in-place is unacceptable if the public's emergency response probability is under 95%. Consequently, if the public cannot be guaranteed to have excellent emergency response efficiency, additional public protection measures, such as evacuation or more rescue vehicles, should be considered to assist the public in evacuation.
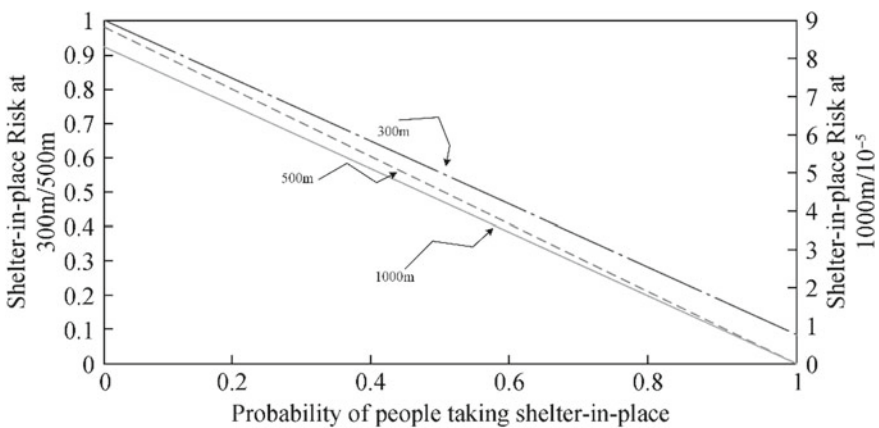
Fig. 3.7   Results of the risk evaluation of shelter-in-place for emergency management in emergencies

(3) For individuals less than 1000 m downwind from the XX well, the risk of sheltering-in-place is less than 10^{-4} and can be neglected. In other words, if the air exchange rate of residences is lower than 0.02 in the area, the public can shelter inside the residence.

However, as can be seen from Table 3.2, if the traditional approach based on the human vulnerability model is followed, the risk of sheltering-in-place can be negligible at a downwind distance of not less than 500 m from XX well, as the corresponding probability of death in the house is less than 10^{-4}. Clearly, because the calculation of individual risk based on human vulnerability model does not consider the fact that some individuals disobeyed the emergency order to shelter-in-place, this probably underestimates the risk of individuals who sheltered in place approximately at a distance of 500 m downwind from the XX well.

3.4 Conclusions

In the case of gas leakage, it is extremely important to scientifically and rationally choose public protection strategies. There are two common public protection strategies: evacuation and shelter-in-place. Quantitative risk assessment can help decision-makers choose public protection strategies.

This chapter puts forward a risk assessment method for emergency measures such as shelter-in-place for a hydrogen sulfide high-pressure natural gas well blowout accident. In this method, the probability of public emergency response is considered in addition to the health consequences and accident probability under different protective measures. The evaluation outcomes that are grounded in the above methods can not only offer suggestions for risk mitigation measures for emergency management under normal circumstances, but also assist decision-makers in making public protection decisions in emergency conditions.

The results of the risk assessment in the case study indicate that the further away from the XX well, the lower the risk of sheltering-in-place if the air exchange rate of the residence is 2%/min. Sheltering in residential houses at a distance of not less than 1000 m from XX well is safe. Even if the air exchange rate is sufficiently low, the risk of sheltering-in-place would still be too high for the residents, who are approximately 300 m from well XX, to bear. For residential houses about 500 m from XX wells, this can result in a higher risk of sheltering-in-place if the residents' emergency response is inefficient, in spite of a sufficiently low air exchange rate.

This chapter highlights an application of risk evaluation approaches to public protection planning and emergency management. The analysis of the case shows the process of shelter-in-place risk assessment presented in this chapter, which hypothesizes an acceptable level for the risk of sheltering-in-place. However, the formulation of the acceptable level for shelter-in-place risk should take into account the cost of risk mitigation, the results of risk evaluation, and the risk appetites of decision-makers. However, many practical factors, such as the cost of risk mitigation, the results of

risk evaluation, and the risk appetites of decision-makers, should be considered when formulating acceptable standards for shelter-in-place risks. This will be discussed further in our future study.

In the next chapter, we will introduce how to evaluate the dynamic risk of the public in the process of evacuation and choose a scientific and correct route to minimize the evacuation risk.

References

Aven, T., and J.E. Vinnem. 2005. On the use of risk acceptance criteria in the offshore oil and gas industry. *Reliability Engineering & System Safety* 90 (1): 15–24.

Chan, W.R. 2006. *Assessing the Effectiveness of Shelter-in-Place as an Emergency Response to Large-Scale Outdoor Chemical Releases.* California: Lawrence Berkeley National Laboratory University of California.

Crowl, D.A., and J.F. Louvar. 2001. Chemical process safety: Fundamentals with applications. *Pearson Education* 15: 35–62.

Epstein, J.M., R. Pankajakshan, and R.A. Hammond. 2011. No combining computational luid dynamics and agent-based modeling: A new approach to evacuation planning. *PLoS ONE* 6 (5): e20139.

Gai, W.M., and Y.F. Deng. 2019. Survey-based analysis on the diffusion of evacuation advisory warnings during regional evacuations for accidents that release toxic vapors: A case study. *Journal of Loss Prevention in the Process Industries* 57: 174–185.

Gai, W.M., Y.F. Deng, Z.A. Jiang, J. Li, and Y. Du. 2017. Multi-objective evacuation routing optimization for toxic cloud releases. *Reliability Engineering & System Safety* 159: 58–68.

Gai, W.M., Y. Du, and Y.F. Deng. 2018. Evacuation risk assessment of regional evacuation for major accidents and its application in emergency planning: A case study. *Safety Science* 106: 203–218.

Georgiadou, P.S., I.A. Papazoglou, C.T. Kiranoudis, and N.C. Markatos. 2007. Modeling emergency evacuation for major hazard industrial sites. *Reliability Engineering & System Safety* 92 (10): 1388–1402.

Georgiadou, P.S., I.A. Papazoglou, C.T. Kiranoudis, and N.C. Markatos. 2010. Multi-objective evolutionary emergency response optimization for major accidents. *Journal of Hazar- Dous Materials.* 178 (1–3): 792–803.

James, J.J., and W. Calvin. 2005. Effectiveness of expedient sheltering in place in a residence. *Journal of Hazardous Materials* 119 (1–3): 31–40.

Jonkman, S.N., P.H.A.J.M. van Gelder, and J.K. Vrijling. 2003. An overview of quantitative risk measures for loss of life and economic damage. *Journal of Hazardous Materials* 99 (1): 1–30.

Li, Y., D.S. Chen, S.Y. Cheng, T.T. Xu, Q. Huang, X.R. Guo, X. Ma, N. Yang, and X.X. Liu. 2015. An improved model for heavy gas dispersion using time-varying wind data: Mathematical basis, physical assumptions, and case studies. *Journal of Loss Prevention in the Process Industrie* 36: 20–29.

Mccaffrey, S., R. Wilson, and A. Konar. 2018. Should I stay or should I go now? Or should I wait and see? Influences on wildfire evacuation decisions: Should I stay or should I go now? *Risk Analysis* 38 (1): 1390–1404.

Papazoglou, I.A., Z. Nivolianitou, O. Aneziris, and M. Christou. 1992. Probabilistic safety analysis in chemical installations. *Journal of Loss Prevention in the Process Industries* 15: 181–191.

Pontiggia, M., M. Derudi, M. Alba, M. Scaioni, and R. Rota. 2010. Hazardous gas releases in urban areas: Assessment of consequences through CFD modelling. *Journal of Hazardous Materials* 176: 589–596.

Rogers, G.O., A.P. Watson, J.H. Sorensen, R.D. Sharp and S.A. Carnes. 1990. *Evaluating protective actions for chemical agent emergencies.* ORNL-6615. Oak Ridge National Laboratory, Oak Ridge, TN.

Wilson, D.J. 1988. Variation of indoor shelter effectiveness caused by air leakage variability of houses in Canada and the USA. In *USEPA/FEMA Conference on Sheltering In Place During Chemical Emergencies, Nov.*

Wu, Q.S., X.M. Qian, and Z.F. Guo. 2009. Probability of receptor lethality in blowout of sour gas wells. *Petrol Explor Develop* 36 (5): 641–645 (in Chinese).

Xu, J.H., and Y. Fan. 2014. An individual risk assessment framework for high-pressure natural gas wells with hydrogen sulphide, applied to a case study in China. *Safety Science* 68 (10): 14–23.

Yang, S, Q Fang, Y Zhang, H Wu and L Ma. 2013. An integrated quantitative hazard analysis method for natural gas jet release from underground gas storage caverns in salt rock. I: Models and validation. *Journal of Loss Prevention in the Process Industries*, 26(1): 74–81.

Yin, X., X. Pan, and Y. Wu. 2010. Decision making of personnel emergency protective actions for toxic gas leakage accident. *Journal of Nanjing University Technology* 32 (01): 64–68 (in Chinese).

Zhang, N., X.Y. Ni, H. Huang, and M. Duarte. 2017. Risk-based personal emergency response plan under hazardous gas leakage: Optimal information dissemination and regional evacuation in metropolises. *Physica a: Statistical Mechanics and Its Application* 473: 237–250.

Zhou, Y.F., and M. Liu. 2012. Risk assessment of major hazards and its application in urban planning: A case study. *Risk Analysis* 32: 566–577.

Chapter 4
Dynamic Emergency Route Planning for Major Chemical Accidents: Models and Application

4.1 Introduction

We covered the shelter-in-place risk assessment approach in the previous chapter, but when deciding to evacuate, evacuation is a dynamic process: How to evaluate its risk? Simultaneously, choosing an evacuation route is a crucial aspect of emergency decision-making. It is critical to understand how to select a safe and feasible path in order to reduce casualties. In this chapter, we will mainly study the solution and evaluation methods of dynamic multi-objective evacuation route selection.

In recent years, the rapid growth of the world economy has led to a significant increase in the range of manufacturing parks using flammable, explosive, poisonous, and dangerous materials (Hosseinnia et al. 2018; Zhou and Liu 2012; Reniers and Soudan 2010). Poor production organization, malfunctioning equipment, improper environmental factors, or human mistakes are the primary causes of any possible dangers. These main dangers inside an area might cause incidents like poisonous proliferation, explosions, fires, or leaks. In such situations, the public is advised to either execute emergency evacuees or shelter in position. However if existing shelters could give appropriate protection to the afflicted people, the second choice is recommended (Sorensen et al. 2004). Nevertheless, the quantity of shelters provided for each impacted area is usually restricted, as well as the infrastructures are sometimes unfit to provide enough protection. As a result, evacuation is frequently used to safeguard the people. In any circumstance, people will always have to migrate from the impacted regions to selected safety regions, which should be carefully determined. Researching evacuation route design is important and valuable from a practical standpoint, especially whenever the people in regions impacted by significant chemical catastrophes have to be safeguarded immediately. Furthermore, significant chemical

accidents, unlike traditional natural catastrophe, may have negative health consequences for the people living in the impacted area as a result of being exposed to the severe circumstances that followed (poisonous clouds, heat radiation, overpressure, fallout, and fragmentation are only a few examples) (Georgiadou et al. 2007). The essential to selecting the best emergency response strategy is accurate assessment of these adverse effects. Some research in such subjects has already been conducted, including several excellent simulation models. Several of these research explain the spatially and temporally distribution of poisonous gas dispersion concentrations following hazardous chemical leak (Jeong and Baik 2018; Kim et al. 2019) or assess the incidence of hazardous elements such as fire shock wave and explosions when dangerous chemical incidents occur (Khakzad 2018; Ding et al. 2020).

Emergency route planning seems to be a shortest path issue in which the goal is to identify the shortest path between two nodes in the graph with the minimum sum of weights of the constituent edges (a graph made up of nodes and pathways) (Shimbel 1953; Yadav and Biswas 2010). In present studies on emergency evacuation management, various methods and techniques depending on the network concept are available to address the challenge of path selection in emergency response, notably in disaster scenarios (Xiao et al. 2001; Georgiadou et al. 2007; Yi and ÖZdamar 2007; Stepanov and Smith 2009; Yuan and Wang 2009; Georgiadou et al. 2010; Shi et al. 2012; Zhang et al. 2013; Gai et al. 2015). The accuracy of the solutions is assessed using a variety of objective functions (Vermuyten et al. 2016). The majority of them prioritize time, and just a handful assesses the health risks posed by hazardous chemicals to evacuees (Gai et al. 2017). Yoo and Choi (2019) proposed an evacuation strategy that was selective enough to take into account the outdoor and indoor concentrations of surrounding buildings, as well as the period when the maximum permitted concentration might occur. Zhang et al. (2017) developed a mixed-integer programming model with the goal of reducing the concentration of dangerous substances in areas where people are exposed during the emergency evacuation. When a person is not wearing respiratory protection and the emergency evacuation route is selected solely to reduce transfer time, the individual's health may be jeopardized during the emergency evacuation. Another problem worth mentioning would be that the ideal path travel time computed could be unsatisfactory if just health implications are taken into account. Furthermore, depending on the time restriction utilized, the performance of protective equipment, such as breathing equipment, might vary dramatically.

These activities are often next to one another due to the integration and connectivity seen between activities of enterprises within the zone (Hosseinnia et al. 2018). A domino effect is produced if a catastrophic chemical accident happens in these kind of chemical clusters (Khakzad 2018; Ding et al. 2020). In these situations, emergency route design has been endowed new difficulties and demands. For instance, in Tianyuan Chemical Plant, Chongqing, China, on April 16, 2004, a liquid chlorine storage tank erupted. Two emergency evacuation choices were taken on the spot: One would be to evacuate all people within a 150 m warning area around the accident site, and the other was taken out 4.5 h after that order was given. The goal was to evacuate additional workers within a one-kilometer radius of the scene of the

accident because the site leadership was worried about possible further accidents (In this accident, about 13,000 kg of liquid chlorine might explode and spill) (Deng and Jiang 2009). The second emergency evacuation in the preceding example demonstrated that while picking the emergency path, decision-makers must consider not just reducing the population's health implications, but also ensuring that impacted people depart safely before secondary catastrophes develop.

When choosing an emergency route, several practical issues should be considered. A rising group of scholars had already recently begun looking into the impact of increased accident frequency on evacuation times (Zhang et al. 2013). Yuan (2009) developed a model that explains the impact of catastrophe expansion on evacuating pace. Several scholars looked at the evacuation decision-making process. Smith et al. (2017) employ a cognitively modeling technique to model decisions and use decision trees to assess path selection method that is based upon education curriculum and learning simulations. In the meantime, they assessed the role of human engagement and creativity in the evacuation judgment process and the effect of external and cognitive factors (Danial et al. 2019b). In addition, those evacuees with social ties are more likely to create a group (Hu et al. 2014). Many academics have exploited behavioral traits of individuals in groups to model collective phenomenon (such as competing, waiting, and herd tendencies) (Sharma 2009). Hong et al. (2018) recreate the people judgment process using the herd behavior concept.

Emergency facilities, individual features, and emergency alerts, and on the other hand, were not taken into account in their selection procedures. Warning signs for major accidents are typically insufficient and are mostly only delivered that after precipitating circumstances have happened (Gai and Deng 2019). As Gai and Deng (2019) point out, various communication warning methods might result in disparities in the time individuals might receive the warning. Additionally, variances in some parameters, such as the pace of different persons, protection conditions, and suitable safety destinations, cause emergency risk kinds (such as health and time risks) as well as degrees to fluctuate dramatically throughout each emergency movement. Therefore, they have different needs in emergency path planning solutions (Georgiadou et al. 2010;). As a result, if such practical aspects really are not incorporated as made by the decision models, delivering appropriate targeted emergency advise for the people in the impacted areas might be tough, if not unattainable.

Norazahar et al. (2015) studied the event tree assessment of the risks and repercussions in relation to risk appraisal of evacuating activities. Numerous scholars have undertaken quantitative study using environment, behavior of a person, organizational, and accidents data (Norafneeza et al. 2018). From the point of view of the population, evacuees would invariably encounter risks from catastrophes or secondary catastrophes on their way from the point of departure to the point of arrival; such condition is also linked to the emergency evacuation route selected. Evacuee risks should be assessed during evacuation processes, which will aid in the development of a much more rational emergency management strategy for local residents.

In summary, this model needs account for elements including the progression of accidents, emergency facilities, personal traits, and alert notifications. According

upon that crisis situation, decision-makers must determine the optimization goal(s), which could include health repercussions and time cost. The suggested model is being used to quantify the emergency response risk for significant chemical catastrophes. This research is an effort to solve several of the above-mentioned issues.

The research makes five contributions.

(1) It is investigated how to design an emergency route in a multi-disaster scenarios caused by significant chemical mishaps. We take into account not only the health effects of the original catastrophe on the individuals in the impacted region, but also the time constraints on the evacuation induced by potential subsequent disasters.

(2) A multi-indicator urgent evacuation risk evaluation technique pertaining to time risk and health risk is being presented. It could really give a much more detailed as well as accurate risk evaluation than the traditional single-dimensional technique.

(3) The dynamic multi-objective path optimization issue is solved using a revised Dijkstra algorithm. It avoids the classic Dijkstra algorithm's flaw of producing a local optimum. By comparing the suggested technology's conclusions with those of the standard algorithm, the effectiveness of the novel approach is proved.

(4) A detailed sensitivity analysis is also carried by using a case study. It primarily investigates the effects of time of departure and evacuee velocity on the best route, as well as contributing to the discovery of danger locations and essential people.

(5) There is a strategic plan of serious accidents which can be put into effect. The presented approach offers recommendations for a community safety strategy for significant chemical catastrophes and taking into account the time of concerning alerts, disaster scenarios, demographic composition, the level of velocity, individual protective conditions, as well as other practical details.

The remainder of this chapter is given. The description of the issue and its modeling are introduced in Sect. 4.2. The solutions approach is described in Sect. 4.3. Case studies from that of an emergency evacuation case are used in Sect. 4.4 to explain the provided concepts as well as methodology. Section 4.5 summarizes the findings and suggests some next study directions.

4.2   Modeling of Dynamic Emergency Route Planning for Major Chemical Accidents

4.2.1   Formulation of Emergency Network

To simplify the study of evacuation route optimization in large chemical catastrophes, we split every emergency response region into numerous sub. The emergency evacuation path destination node, like v_d, can be chosen based on the specified protective

actions from of the source node where such a specific impacted people is, like v_s. The node v_d represents the emergency response area's exit. If a shelter-in-place operation is necessary, the closest shelter facilities would be designated as v_d. The arc (v_j, v_i) represents the capacity to connect nodes v_i and v_j.

We use a directed graph $G(V, A)$ to define our emergency network, where $V = V_d \cup V_s$, with $V_d = \{v_d| d = 1, 2,…, n_d\}$ and $V_s = \{v_s| s = 1, 2,…, n_s\}$ are a group of destination nodes (response region exits or shelter exits) and a group of source nodes (population centers); the set of arcs is $A = \{(v_j, v_i)|v_j, v_i \in V\}$.

Let (x_i, y_i) be the locations of nodes v_i in the urgent system, as well as $c_{ij}(x, y, t)$ be the amount of the negative impact (dangerous substance concentrations, overpressure, and thermal radiation are only a few examples) on arc (v_j, v_i) at point (x, y) and at time t with $(x, y) \in (v_j, v_i)$:

(1) (x, y): a location on the arc (v_j, v_i)'s coordinates.
(2) d_{ij}: the estimated dosage while moving over arc (v_j, v_i), which would be computed by the following formula (Zhou and Liu 2012):

$$d_{ij} = \int_{t_i}^{t_j} f\{c(x, y, t)\}\mathrm{d}t \qquad (4.1)$$

where t_j and t_i represent the time when people reach node v_j as well as node v_i along the arc (v_j, v_i), accordingly.
(3) N_p: the variety of separate populations' kinds (three kinds, for instance: young, old, as well as adults with kids.)
(4) $s_{ij,p}(t)$: during catastrophe circumstances at time t, the population's movement velocity of type p ($p = 1, 2,…, N_p$) on every arc (v_j, v_i) of the network.
(5) s_{ij}^n: given usual circumstances, the movement velocity of uninjured normal young adults on the arc (v_j, v_i).
(6) t_s^w: after the emergency manager issued an alert message, the time when the personnel in the danger area received the message.

Individuals' travel speeds may be influenced by their own circumstances under normal circumstances. For example, older people, young children, and people with disabilities may have a much slower pace than healthy, normal young adults. The pace of the older people, young children as well as people with disabilities may have much slower than normal adults (Menz et al. 2004). When normal young individuals assist members of the family, including by helping the elderly as well as carrying young children, their movement pace could be reduced.

Accordingly, assume the event happens at time 0 as well as consider $s_{ij,p}^n$ as the movement pace of population type p ($p = 1, 2,…, N_p$) on arc (v_j, v_i) in normal circumstances. The following formula could be used to estimate this:

$$s_{ij,p}^n = \xi \cdot s_{ij}^n \qquad (4.2)$$

where ξ is the speed influencing coefficient, showing how much movement velocity is influenced by constrained mobility as well as aiding others. In disastrous situations, the movement velocity on every arc of the system $s_{ij,p}(t)$ may decrease as space as well as time pass, as shown in the formula below (Georgiadou et al. 2010; Zhang et al. 2013).

$$s_{ij,p}(t) = s_{ij,p}^n \cdot \alpha_{ij} \cdot e^{-\beta_{ij}t} \tag{4.3}$$

where α_{ij} and β_{ij} are the parameters that control the $s_{ij,p}(t)$ movement velocity function's decline $s_{ij,p}(t)$. $\alpha_{ij} \in (0, 1]$ and $\beta_{ij} \in [0, +\infty)$.

4.2.2 Objective Functions Considering the Impact of Secondary Disasters

We will focus on the three models in this section, which we will refer to as Models I, II, and III. The first two are single-objective optimization problems with a certain degree of similarity as well as simply differs of the objective function utilized, while the latter addresses the issue as just a bi-objective issue with the second model's objective inserted as a restriction.

Model I

If there is no threat of secondary disasters, the first consideration while choosing an emergency evacuation route is safety; during emergency evacuation response, there is also an objective of limiting health repercussions. Following a significant chemical disaster, the less poisonous material evacuees are exposed to during the transfer, the less severe the impact on their health (Georgiadou et al. 2007).

Let $W = \{(v_s, v_{R_1}, ..., v_{R_K}, v_d)|v_s \in V_s; v_d \in V_d; v_{R_k} \in V - \{v_s\} - \{v_d\}; 1 \leq R_k \leq n \ \forall k = 2, ..., K\}$ represent the path of K intermediate nodes that could comprise both destination and source nodes.

In addition to the above symbols, the following symbols are used:

(1) t_{ji}: the amount of time it takes to move around an arc(v_j, v_i).
(2) l_{ji}: the length of arc (v_j, v_i).
(3) d_i: the dosage received at node v_i.
(4) χ_{ij} is the choice variable. When arc (v_j, v_i) is not included in the fixed path, it is set to 0; otherwise, it is set to 1.

The dynamic emergency route selection (DERS) (model I) formula of severe significant chemical incidents is depicted in Eqs. (4.4)–(4.14) as follows:

$$\min f_1 = \text{Minimize} \left\{ \sum_{i=s}^{d} \sum_{j=s}^{d} \chi_{ij} d_{ij} \right\} \tag{4.4}$$

subject to

$$\int_{t_i}^{t_j} si_{j,p}(t)\mathrm{d}t = l_{ij} \quad \forall i, j = 1, 2, ..., n; \ p = 1, ..., N_{\mathrm{p}} \tag{4.5}$$

$$l_{ij} = \sqrt{\left(x_j - x_i\right)^2 + \left(y_j - y_i\right)^2} \quad \forall i, j = 1, 2, ..., n \tag{4.6}$$

$$t_{ij} = t_j - t_i \quad \forall i, j = 1, 2, ..., n \tag{4.7}$$

$$t_s = t_s^w \tag{4.8}$$

$$s_{ij,p}(t) = s_{ij,p}^{\mathrm{n}} \cdot \alpha_{ij} \cdot \mathrm{e}^{-\beta_{ij}t} \quad \forall i, j = 1, 2, ..., n; \ p = 1, ..., N_{\mathrm{p}} \tag{4.9}$$

$$d_{ij} = \int_{t_i}^{t_j} f\{c(x, y, t)\}\mathrm{d}t \quad \forall i, j = 1, 2, ..., n \tag{4.10}$$

$$d_s = \int_0^{t_s} f\{c(x, y, t)\}\mathrm{d}t \tag{4.11}$$

$$\sum_{\substack{j=s \\ j \neq i}}^{d} \chi_{ij} - \sum_{\substack{j=s \\ j \neq i}}^{d} \chi_{ij} = \begin{cases} 1 & i = s \\ -1 & i = d \\ 0 & \text{otherwise} \end{cases} \tag{4.12}$$

$$\sum_{\substack{j=s \\ j \neq i}}^{d} \chi_{ij} \begin{cases} \leq 1 \ i \neq d \\ = 0 \ i = d \end{cases} \tag{4.13}$$

$$\chi_{ij} \in \{0, 1\} \quad \forall i, j = 1, 2, ..., n \ \text{ and } \ t_i \geq 0 \ \ \forall i = 1, ..., n \tag{4.14}$$

where Eq. (4.4) denotes the model's goal, which is to minimize the estimated dosage along a path. Equations (4.5), (4.6) and (4.7), as well as (4.8) are the total movement time across a path recursion equation which show that arc (v_j, v_i) is traveled through with the speed $s_{ij,p}(t)$ during time period t_{ij}. When catastrophes and people kinds rise, the declining formula of arc (v_j, v_i) movement velocity is in Eq. (4.9). The predicted dosage of arc (v_i, v_j) along a path is calculated using Eqs. (4.10) as well as (4.11). By limiting the value of χ_{ij}, constraint (4.12) assures a viable path from the source node v_s to the destination node v_d. A path with looping is not permitted due to the viability of the emergency evacuation strategy as well as the urgency of urgent response time. As a result, constraint (4.13) assures that paths are free of loops. The binary choice

factors as well as continuum nonzero factors are referred to as constraints (4.14). There are n^2 continuum nonzero variables in this model, as well as ten constraints as well as binary variables.

Model II

When a person is wearing safety equipment with limited protection time, the person has to arrive the safety locations as quickly as feasible before the safety equipment fails. As a result, DERS (model II) for severe chemical major accidents with no additional disaster risk is comparable with Model I, with the exception that the goal function stated by Eq. (4.15) is utilized instead. The following formula is a description of the model:

$$\min f_2 = \text{Minimize} \left\{ \sum_{i=s}^{d} \sum_{j=s}^{d} \chi_{ij} t_{ij} \right\} \tag{4.15}$$

subject to Eqs. (4.5, 4.6, 4.7, 4.8, 4.9, 4.10, 4.11, 4.12, 4.13 and 4.14).

Namely Model II differs from Model I by using the evacuation time t_{ij} rather than the dosage d_{ij} between nodes v_i and v_j as the objective function.

Model III

Both goals are analyzed concurrently in this model, with Model I's goal retaining the main objective function as well as the second model's goal added to the model as a constraint. The latter would be used to specify the objective that must be met depending on the urgent response's capabilities. The parameters that were employed in the two previous models have not altered. For instance, if there would be a risk of additional catastrophes following the original catastrophe, inside the processes of urgent evacuation path design, it is necessary to address not only health issues, but also the influence of the incidence and progression of secondary catastrophes on the urgent evacuation response time. This issue comes under the jurisdiction of multi-objective optimization, and the formula of DERS (Model III) with severe major incidents with additional catastrophe threats is illustrated as follows:

$$\min f_1 = \text{Minimize} \left\{ \sum_{i=s}^{d} \sum_{j=s}^{d} \chi_{ij} d_{ij} \right\} \tag{4.16}$$

$$f_2 = \sum_{i=s}^{d} \sum_{j=s}^{d} \chi_{ij} t_{ij} \leq L_t \tag{4.17}$$

subject to Eqs. (4.5)–(4.14), where L_t denotes the available urgent reaction time as defined by the incidence and progression of secondary catastrophes.

4.2.3 Application in Emergency Response Risk Assessment

A scenario in which persons or assets may experience negative effects is generally referred to as a risk (Yoo and Choi 2019). Dangerous chemical catastrophes are made worse by the fact that significant chemical catastrophes may have negative health consequences for the people living in the affected region as a result of being exposed to the severe phenomena that follow (overpressure, poisonous clouds, fragmentation, fallout, as well as heat radiation are only a few examples). The risk involved with the aforementioned health sequences is referred to as health risk in this section and that might be computed using the probit function as given (OGP 2010):

$$Y = A + B \ln d \tag{4.18}$$

A and *B* are constants. *Y* stands for the probit parameter. *Y* may be used to calculate lethality.

People might potentially be exposed to risks as a result of time delays. As instance, owing to the possibility of additional catastrophes, the people should move from the afflicted region to a safe location inside a specified amount of time as well as the urgent protective gears people are using have a limited effective protection period. In this section, the term "time risk" represents a set of various negative outcomes brought due to time delays. On the basis of journey time as well as health effect, the risk of urgent response to significant catastrophes might well be calculated, according to the emergency route planning results

$$\mathrm{RE}_h\left(v_s, P, t_s^{w}\right) = \sum_{p \in P} \sigma_{s,p} \cdot \left[A + B \cdot \ln f_1\left(W^*\right)\right] \tag{4.19}$$

$$\mathrm{RE}_t\left(v_s, P, t_s^{w}\right) = \sum_{p \in P} \sigma_{s,p} \cdot f_2\left(W^*\right) \tag{4.20}$$

$P = \{p | p = 1, 2, \ldots, N_p\}$ denotes the populations kind set at the source node v_s.

$\mathrm{RE}_h\left(v_s, P, t_s^{w}\right)$ and $\mathrm{RE}_t\left(v_s, P, t_s^{w}\right)$ represent the average health implications as well as temporal risk of obtaining an advance warning time t_s^{w} inside the event of a catastrophic disaster for all human populations P at source node v_s, respectively. W^* denotes the best urgent path discovered via Models I, II, III and $\sigma_{s,p}$ denotes the fraction of people of type p that is impacted in the population overall at node v_s.

Let L_T and L_{HC} be the threshold values of the high-risk and low-risk area, respectively. Let L_{HC} as well as L_T be the low-risk and high-risk area's respective threshold values. Health repercussions as well as time risks could be used to estimate these values. According to Fig. 4.1, the urgent risk of the people at v_s is classified into four grades in this research.

Fig. 4.1 Multi-indicator emergency risk assessment method for major chemical accidents
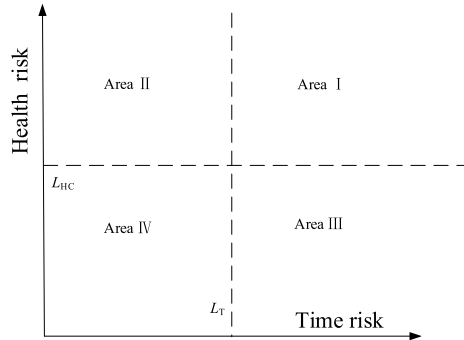
(1) If $v_s \in$ Area I, the time risk as well as health risk during the urgent evacuation of the people located at v_s exceed the acceptable limit.
(2) If $v_s \in$ Area II, the people at V face a time risk that is within allowable levels during the urgent evacuation; however, the health risks are beyond acceptable limits.
(3) If $v_s \in$ Area III, populations located in V are out of bounds experienced acceptable health risks in emergency transfers; however, temporal risk is out of bounds.
(4) If $v_s \in$ Area IV, the people at V face neither time risks nor health risks during the urgent evacuation.

When deciding how to allocate transportation vehicles, urgent rescuer protective devices, as well as other facilities, the above division of the areas can be used as a guide.

4.3   Algorithm for Emergency Route Planning

Models I and II would both be dynamic single-objective models that constructed using a modified Dijkstra method (Yuan and Wang 2009). This part presents a dynamic dual-objective model on the basis of Model III first demonstrates its theoretical correctness, and then presents algorithm. We also perform a plausible transformation on part of the proposed algorithm that prevents the algorithm from looping due to the bidirectionality of the arc and then check the overall reliability of the method.

4.3.1 Model IV

We first normalize the two goal functions before converting the DERS Model III to a single-objective model using the linear weighted sum approach. The following is the specific formula (Mardle and Miettinen 2000):

$$\min F = r_1 \frac{f_1}{f_1^*} + r_2 \frac{f_2}{f_2^*} \tag{4.21}$$

subject to Eqs. (4.5, 4.6, 4.7, 4.8, 4.9, 4.10, 4.11, 4.12, 4.13, 4.14, 4.15, 4.16 and 4.17) where $\vec{f} = (f_1^*, f_2^*)^T$ is the ideal point that is the solution value of the objective functions of Models I and II. The variables r_1 and r_2 are the coeffents related to the weights of the functions f_1 as well as f_2, with $r_1 \geq 0$; $r_2 \geq 0$; $r_1 + r_2 = 1$.

  The revised Dijkstra algorithm by Yuan (2009) could not be utilized to resolve Model IV, and it can be seen from the lemma mentioned below. As a result of this constraint, we created a revised algorithm.

Lemma 4.1 Whenever $t \in [0, +\infty)$, assume that $s_{ij,p}(t)$ is an integrable as well as uniformly declining function of t. Then, t_j is a monotonic as well as growing function in relation to t_i (Yuan 2009).

Lemma 4.2 Obviously, F_j is not a monotonous as well as growing function in relation to F_i in the formula $F_{ij} = F_j - F_i$ if $F_i = r_1 \frac{d_i}{f_1^*} + r_2 \frac{t_i}{f_2^*}$

Proof Let $F_i{}^k$, $d_i{}^k$, and $t_i{}^k$ represent the values of the target function F provided in Eq. (4.21), the estimated dosage, as well as the time at which people arrive at node v_i via the path k separately, $k = 1,2\ldots$ and $d_{ij}{}^k = d_i{}^k - d_j{}^k$, $t_{ij}{}^k = t_i{}^k - t_j{}^k$.

  Suppose that

$$\begin{cases} F_i^1 = r_1 \frac{d_i^1}{f_1^*} + r_2 \frac{t_i^1}{f_2^*} \\ F_i^2 = r_1 \frac{d_i^2}{f_1^*} + r_2 \frac{t_i^2}{f_2^*} \end{cases} \quad i = 1, 2, \ldots, n \tag{4.22}$$

Here,

$$\begin{cases} F_i^1 - F_i^2 > 0 \\ d_i^1 - d_i^2 < 0 \\ t_i^1 - t_i^2 > 0 \\ f_1^* = c \\ f_2^* = c \end{cases} \tag{4.23}$$

v_i to v_j,

$$\begin{cases} F_j^1 = r_1 \frac{d_j^1}{f_1^*} + r_2 \frac{t_j^1}{f_2^*} = \frac{r_1}{f_1^*}(d_i^1 + d_{ij}^1) + \frac{r_2}{f_2^*}(t_i^1 + t_{ij}^1) \\ F_j^2 = r_1 \frac{d_j^2}{f_1^*} + r_2 \frac{t_j^2}{f_2^*} = \frac{r_1}{f_1^*}(d_i^2 + d_{ij}^2) + \frac{r_2}{f_2^*}(t_i^2 + t_{ij}^2) \end{cases} \quad j = 1, 2, ..., n \qquad (4.24)$$

Clearly, as shown in Lemma 4.1, when $t \in [0, +\infty)$, $s_{ij,p}(t)$ is a monotonic as well as continuously decaying function in relation to t, so $t_{ij}^2 > t_{ij}^1$. Here it is assumed that the function $f\{c(x, y, t)\}$ in this case is a value that does not vary with other factors, in other words it is a constant, and thus $d_{ij}^1 > d_{ij}^2$. Then,

$$F_j^1 - F_j^2 = \frac{r_1}{f_1^*}(d_i^1 + d_{ij}^1) + \frac{r_2}{f_2^*}(t_i^1 + t_{ij}^1) - \frac{r_1}{f_1^*}(d_i^2 + d_{ij}^2) - \frac{r_2}{f_2^*}(t_i^2 + t_{ij}^2)$$

$$= F_i^1 - F_i^2 + \frac{r_1}{f_1^*}(d_{ij}^1 - d_{ij}^2) + \frac{r_2}{f_2^*}(t_{ij}^1 - t_{ij}^2) \qquad (4.25)$$

Undoubtedly, Eq. (4.25) could produce a result that is less than zero. Correspondingly, when the value of the function $f\{c(x, y, t)\}$ may not be a fixed value, but varies with a certain factor, the Eq. (4.25) may produce a result less than zero.

4.3.2   The Proposed Method

Yuan (2009) modified parts of Dijkstra's technique, in other words, introduced a variation of the Dijkstra method to resolve the single-objective path finding models underneath the real-time influence of catastrophe expansion. This variation is governed by the value of the target function of the current node, and it will be a monotonic function that is steadily rising in relation to the value of the target function of the upstream node (read Lemma 4.1 for details). Obviously, as shown in Lemma 4.2, this algorithm could not be used to resolve the model IV So, to solve this problem, we partially modified Dijkstra algorithm, creating a new variation of the algorithm that has been validated to determine the shortest path. The following is how this new variation is carried out. The collection of arc weights is denoted by $W_E = \{c_{ij}(x, y, t), t_{ij}, d_{ij}, l_{ij}, \alpha_{ij}, \beta_{ij}, s_{ij}^n, t_s^w\}$.

Label $P(v_j)$ is the minimum value F from node v_s to node v_j in Eq. (4.21), and the designations T_1, T_2 as well as T_F designate the collections of target function values (f_1, f_2 and F are some examples) for the distinct node paths separately. Let $S = \{v_m | m = 1, 2, ..., n\}$ stand for the collection of nodes for which the shortest path has already been discovered. Figure 4.2 depicts the essential processes performed by the suggested approach to resolve Model IV.

N_{max} denotes the number of iterations in Fig. 4.2a. The distribution of solution inside the target area could be used to calculate this variable. The optimum point value of each node in the Eq. (4.21) varies; however, the optimum point value just concerns the known as well as determined nodes: where $P(v_d)$ is just the minimal target value of the function F from node v_s to node v_d, the resulting $W_j, f_1(v_d)$, and $f_2(v_d)$ are the equivalent path as well as the values of f_1 as well as f_2 from node v_s to

Fig. 4.2 DERS algorithm. **a** Main algorithm for DERS, **b** calling algorithm

(a)

(b)
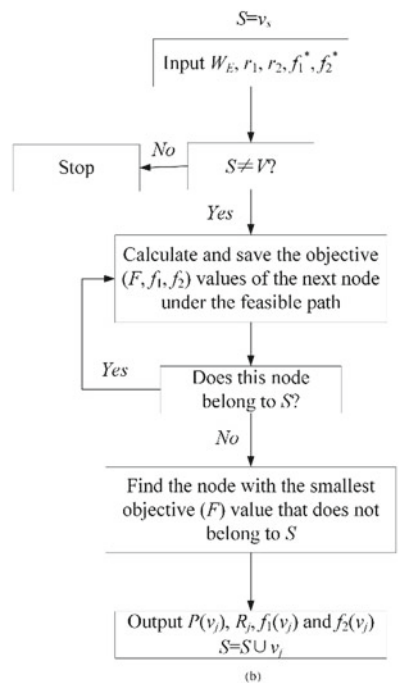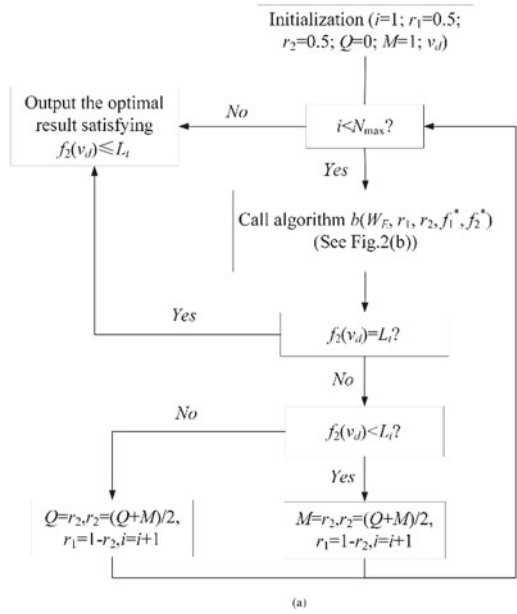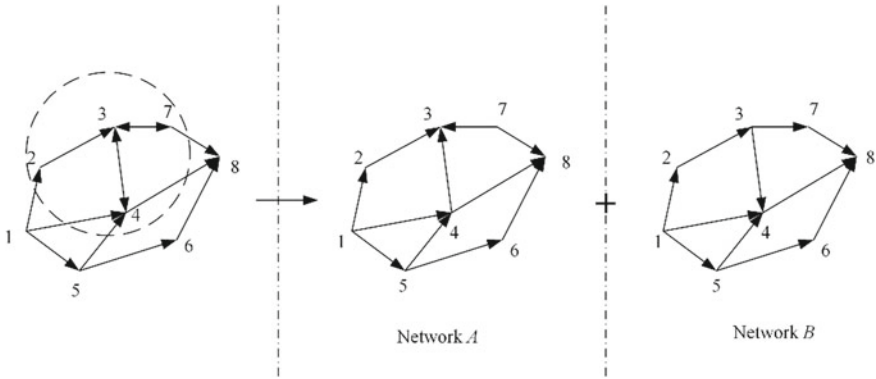
Fig. 4.3 Schematic of solutions for networks with bidirectional arcs

node v_d. The optimum solution underneath Eq. (4.21) with the optimal point values of v_d is allocated for these matching values, for the remaining nodes.

The DERS algorithm is divided into two components, as illustrated in Fig. 4.2. Figure 4.2a depicts the basic algorithm, whereas Fig. 4.2b depicts the activating algorithm. The dual weighting factors of the aforesaid double optimization issue are first determined, and see Fig. 4.3 for details.

In case such issue has only one objective to be optimized, it can be simplified to have $\vec{r} = (r_1, r_2) = (0, 1)$ or $(1, 0)$, and closely related $f_1{}^*$ and $f_2{}^*$ are both 1. The approach presented in Fig. 4.2b could be used straight in this circumstance. In case the issue has two objectives to be optimized, the optimal path would be found at the conclusion of the procedure using a search space built from a set of weight coefficients (as shown in Fig. 4.2a) in a vector.

The basic theory underlying of call algorithm (see Fig. 4.2b) is that whenever the Dijkstra method is used, each succeeding node updates the network's proportion depending on the path that would have been discovered.

4.3.3 Disposal Method in the Presence of a Bidirectional Arc

Providing only safe exits in the initial emergency network if there are any more urgent shelters, nodes in coverage would raise possible routes to emergency shelters. The network could undoubtedly become a two-way system as a result of this condition. Well, now there is a problem that if there are two-way sides, then the proposed algorithm may cause loops, which may result in an incorrect result. We can reasonably split the urgent network into two independent one-way networks to resolve various problems caused by the urgency of urgent response. As a small example, as shown in Fig. 4.3, an emergency shelter is represented by node 3, the coverage area of this emergency shelter is represented by the circle around it, and a safe exit of the

emergency response network is represented by node 8. Now, then, we can solve this problem from the location of the migrating population: We can use network model A (shown in Fig. 4.3) to deduce all nodes inside each shelter's service region; if it were not for the situation we described above, we would be able to use network model B (shown in Fig. 4.3).

4.3.4 Correctness of the Proposed Algorithm

Lemma 4.3 can be used to demonstrate the rationality as well as correctness of our raised algorithm:

Lemma 4.3 If W^* is the shortest path calculated by Model IV, then $f_1(W^*)$ and $f_2(W^*)$ are the decreasing monotonic function and increasing monotonic function, respectively, about the proportion coefficient r_1.

Proof Assuming that the scale coefficient r_1 of the target value f_1 related to the shortest path $W_1{}^*$ is a as well as the scale coefficient r_1 of the target value f_1 related to the shortest path $W_2{}^*$ is b. If a is greater than b as well as $b \geq$ zero, then $(1 - b)$ is greater than $(1 - a)$ as well as $(1 - a) \geq$ zero, then.

$$f_1(W_1^*) \cdot a + f_2(W_1^*) \cdot (1 - a) \leq f_1(W_2^*) \cdot a + f_2(W_2^*) \cdot (1 - a) \qquad (4.26)$$

and

$$f_1(W_1^*) \cdot b + f_2(W_1^*) \cdot (1 - b) \geq f_1(W_2^*) \cdot b + f_2(W_2^*) \cdot (1 - b) \qquad (4.27)$$

which leads to

$$[f_1(W_1^*) - f_1(W_2^*)] \cdot a + [f_2(W_1^*) - f_2(W_2^*)] \cdot (1 - a) \leq 0 \qquad (4.28)$$

and

$$[f_1(W_1^*) - f_1(W_2^*)] \cdot b + [f_2(W_1^*) - f_2(W_2^*)] \cdot (1 - b) \geq 0 \qquad (4.29)$$

Thence, we can deduce that

$$f_1(W_1^*) - f_1(W_2^*) \leq 0 \qquad (4.30)$$

and

$$f_2(W_1^*) - f_2(W_2^*) \geq 0 \qquad (4.31)$$

Next, based on the previous lemma and proof, the method for obtaining model IV is as follows: First, the range of the scale coefficient is set to [0,1] (in other words, this range is the search space), and secondly, it is simple and easy to use to make the obtained range more precise.

Based on the various definitions and Lemma 4.2 mentioned above, it is obvious that the algorithm mentioned above (see Fig. 4.2b for details) can prove its correctness and rationality through recursive thinking. The specific proof process is as follows:

(1)   Clearly, when S is numerically equal to v_s, the conclusions drawn by our model are not wrong.
(2)   We assume that, if $S = S \cup v_n$, the conclusion obtained by our proposed model is without any error, for any node v_j where $v_j \in S$, the minimum target value between node v_j and node v_s can be represented by $P(v_j)$.
(3)   The next thing to do is to show that our proposed algorithm is free of any errors when $S = S \cup v_{n+1}$ hold. As shown in Fig. 4.2b, through the algorithm mentioned in it, there is $F(v_j) = \min_{v_j \notin} T_F(v_j)$ as well as $P(v_x) = \min_{v_j \notin S}\{F(v_j)\}$; obviously, it is easy to get $S = S \cup v_x$.

We can let H be any reasonable path between nodes v_s and v_x. If there is $v_s \in S$ as well as $v_x \notin S$, there must be a special arc along the route H, where the starting node is in S and the destination node is not. There are many arcs along the route H, i.e., $v_r \in S$, we assume (v_r, v_l) is the first of the arcs that appear. As shown in Lemma 4.2, when there is $vl = v_x$, we can assume that the shortest path about v_r can be found, then there will be $P(v_r) = F_r{}^1$. Although there is nothing wrong with the formula $F_r{}^H > P(v_r)$, there is now a problem. Compared with $F_x{}^1$ along the shortest route of v_r, $F_x{}^H$ along this route obviously exists $F_x{}^H < F_x{}^1$, then there is $W_x \neq W_r \cup v_x$. The content mentioned above, on the other hand, also demonstrates that the DERS model cannot be solved by the Dijkstra algorithm modified by Yuan (2009). The specific reason is that when the algorithm involves the selection of nodes, especially the selection of the next node, the algorithm does not find the correct path to calculate the target value, but only uses the shortest path related to the upstream node to calculate the target value; obviously, there is a certain error. When the second loop in Fig. 4.2b (located in the fourth row from the top of the figure) starts running, then according to this algorithm, all the target values calculated along all the routes will be included in the $T_F(v_x)$, in other words, the set S will contain all nodes in all routes. When v_l is not equal to v_x, there is $P(v_x) = \min_{v_j \notin S}\{F(v_j)\} \leq \min_{v_j \notin S} T_F(v_j) < F_j^H + F_{jx}^H$. Since the target value F mentioned above is all greater than or equal to 0, it is obvious that the above-mentioned content is not wrong. In simple terms, the minimum target value between node v_x and node v_s is $P(v_x)$.

4.4   Computational Results

With regard to the following, we describe real-world cases used in our computational experiments that follow, as well as several lemmas used to corroborate. The following

is some calculation and analysis. The main control variables are the situation with the risk of secondary disaster and the situation without secondary risk.

4.4.1 Introduction and Description

As shown in Fig. 4.4, the emergency network we use has a total of 20 nodes (see Table 4.1 for detailed coordinates); Table 4.2 gives the size of the speed decay parameter α_{ij}, the speed decay parameter β_{ij}, as well as the initial travel speed $s_{ij}{}^{n}$. We assume that the accident point of liquid ammonia leakage is located at node 1 in Fig. 4.4. Some important parameters of spill scenarios are described in Table 4.3, including a range of spill parameters as well as some meteorological conditions. When calculating the time-varying concentration of ammonia, we use the Gaussian plume model because of its simplicity and convenience when calculating the diffusion of toxic gases (Ding et al. 2007). The dose of poison gas encountered by evacuees through a certain arc during the evacuation process can be calculated by the human vulnerability model (OGP 2010). The specific formula is as follows:

$$d_{ij} = \int_{t_i}^{t_j} \left(\frac{C_i + C_j}{2} \right)^n \tag{4.32}$$

In the formula, C_i is the ammonia concentration at point v_i as well as C_j is the ammonia concentration at point v_j, both in ppm. n is the value measured through experiments, in the case of ammonia leakage, $n = 2$.

The probit function we used was published by a well-known research institution in the Netherlands (the Netherlands Organization for Applied Scientific Research).
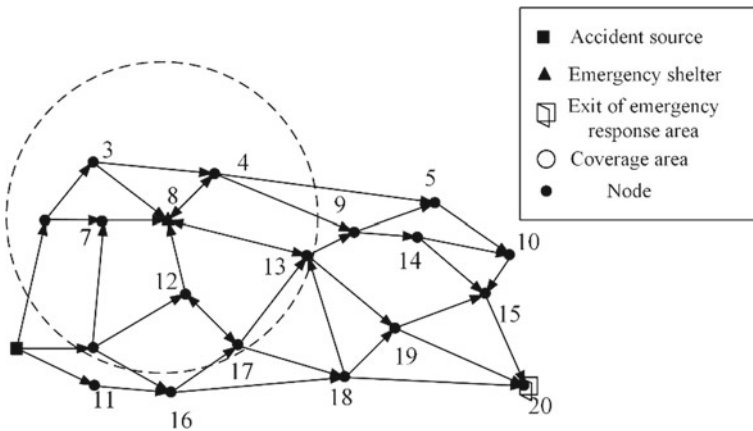

Fig. 4.4 Emergency network structure

Table 4.1 Coordinates of nodes

Node	(x, y)	Node	(x, y)	Node	(x, y)	Node	(x, y)
1	(0, 0)	6	(130,0)	11	(135, −65)	16	(265, −76.123)
2	(50, 221.02)	7	(150,220)	12	(290, 94.893)	17	(380.46, 4.433)
3	(130, 320)	8	(260,220)	13	(500, 160)	18	(565, −50)
4	(340, 300)	9	(580,200)	14	(690, 191.575)	19	(650, 35)
5	(720, 250)	10	(850,160)	15	(805, 92.861)	20	(875, −65)

Table 4.2 Evacuation network structure and speed parameters

(v_i, v_j)	$(s_{ij}^{n}, \alpha_{ij}, \beta_{ij})$	(v_i, v_j)	$(s_{ij}^{n}, \alpha_{ij}, \beta_{ij})$	(v_i, v_j)	$(s_{ij}^{n}, \alpha_{ij}, \beta_{ij})$
(1, 2)	(100,0.85,0.07)	(6, 16)	(75,0.86,0.09)	(14, 10)	(115,1,0)
(1, 6)	(60,0.83,0.07)	(7, 8)	(90,0.89,0.08)	(14, 15)	(105,1,0)
(1, 11)	(115,0.84,0.09)	(8, 4)	(85,0.92,0.03)	(15, 20)	(30,1,0)
(2, 3)	(60,0.88,0.09)	(8, 13)	(75,0.92,0.01)	(16, 17)	(115,0.85,0.06)
(2, 7)	(70,0.82,0.06)	(9, 5)	(65,1,0)	(16, 18)	(70,0.83,0.05)
(3, 4)	(100,0.98,0.01)	(9, 14)	(90,1,0)	(17, 13)	(80,0.91,0.02)
(3, 8)	(95,0.95,0.01)	(10, 15)	(35,1,0)	(17, 18)	(75,0.95,0.04)
(4, 5)	(120,0.99,0.01)	(11, 16)	(70,0.89,0.07)	(18, 13)	(45,0.99,0.02)
(4, 9)	(85,0.98,0.02)	(12, 8)	(65,0.99,0.02)	(18, 19)	(110,0.97,0.01)
(5, 10)	(50,1,0)	(12, 17)	(100,0.95,0.03)	(18, 20)	(120,0.93,0.04)
(6, 7)	(65,0.85,0.05)	(13, 9)	(40,0.98,0.05)	(19, 15)	(75,1,0)
(6, 12)	(105,0.82,0.06)	(13, 19)	(120,0.98,0.04)	(19, 20)	(100,1,0)

Note The unit of s_{ij}^{n} is m/min

Table 4.3 Parameter specification

Leakage parameters		Meteorological parameters	
Volume/m^3	50	Average temperature/°C	25
Cleft diameter/mm	100	Average wind speed/(m/s)	3.5
Cleft shape	Circular	Prevailing wind direction	East wind
Cleft height (from the ground)/m	2.4	Solar radiation intensity	Weak
Cleft height (from liquid level)/m	1.3	–	–
Internal pressure/Pa	1,000,000	–	–
Height measured/m	1.67	–	–
Density/(kg/m^3)	608	–	–

Then, in Eq. (4.18), the value of A is -16.33, and the value of B is 1. We can synthesize health risk and time risk to define high- and low-risk areas, and after our calculation, the high-risk area threshold is $L_{HC} = 2.51$ as well as the low-risk area threshold is $L_T = 8.0$.

4.4.2 Illustration of Lemmas 4.2 and 4.3

We will now analyze the results discussed above with a case study. The model and data of our computational experiments are consistent with the model and data in Yuan (2009) in order to be able to compare with their improved Dijkstra algorithm. These algorithms are compiled on the Java platform and run on a PC with 32 GB RAM as well as 3.6 GHZ processor. The solution process of the shortest path between node v1 and node v20 is shown in Table 4.4. As shown in Table 4.4, the conclusions obtained by our proposed algorithm are significantly different from those obtained by the algorithm modified by Yuan (2009). All in all, in terms of optimizing the objective function (see Eq. (4.12) for details), W^1 is shorter when W^2 is compared to W^2.

Furthermore, the F value of the route $1 \to 11 \to 16 \to 18$ (W^3) and the route $1 \to 6 \to 12 \to 17 \to 18$ (W^4) are -0.33042842 and -0.33042841, respectively; obviously, the latter is larger. It is worth noting that the results show that when there is a part of the shortest path is W^4, the destination node is node 20.Obviously, Lemma 4.2 supports this view to a certain extent, and the specific reason is that the objective function mentioned above is not a strictly monotonically increasing function.

In our algorithm, it is worth noting that we collect the target value of path W4 while obtaining the shortest path (the specific location is node 18) and then update the subsequent target values in turn. In contrast, the algorithm revised by Yuan (2009) has certain problems. The specific problem is that their algorithm does not deal with backtracking when searching, so they do not get the real shortest path.

Based on the data shown above, when all parameters except the scaling factor r_1 are kept constant, only when r_1 changes between 0 and 1, Fig. 4.5 shows the changes in the curves for f_1 as well as f_2 condition. And the conclusion of Lemma 4.3 is basically the same as that obtained by our simulation.

Table 4.4 Shortest evacuation route obtained through the method illustrated in Fig. 4.2b and the modified Dijkstra algorithm proposed by Yuan and Wang (2009)

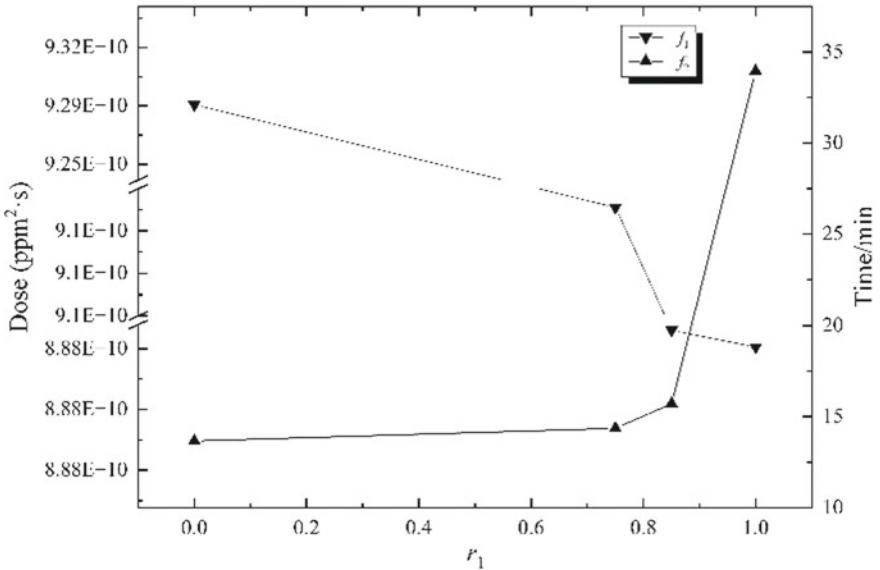| r_1	Route	F	Method
0.77	$1 \to 11 \to 16 \to 18 \to 20$ (W^2)	0.085	The modified Dijkstra algorithm proposed by Yuan and Wang (2009)
	$1 \to 6 \to 12 \to 17 \to 18 \to 20$ (W^1)	0.084	The algorithm illustrated in Fig. 4.2b

**Fig. 4.5** Dose and time by model IV with respect to r_1

4.4.3   Results for Major Accidents Without Secondary Disaster Risks

We will look at what happens if there is no secondary calamity. We make the assumption that there is a parameter $\xi = 1$ which controls the velocity of each person at the source node. When the emergency response command is issued, the evacuees of some nodes take the emergency shelter as the main goal. Of course, there is a premise that their location must be within the coverage of the shelter. However, for persons other than the above-mentioned persons, for safety reasons, the destination of their emergency evacuation should be other locations listed as safe by emergency managers. The specific reasons why these people do not choose to go to emergency shelters are that, firstly, they are far away from the nearest emergency shelter, so they may suffer more toxic gas doses during the journey, and secondly, the emergency shelter is designed with capacity restrictions, so it may not be able to accommodate as many refugees at the same time. We make two simple assumptions here. The first assumption is that everyone involved in emergency evacuation receives disaster warning time $t_s^w = 0$, and the second assumption is that there is no secondary disaster during this emergency response process.

Appendix 1 presents our contingency route planning results. Specifically, on the basis of the first two models, namely Model I and Model II above, the main distinguishing point is that emergency evacuees wear respiratory protective equipment and emergency evacuees do not wear respiratory protective equipment, and then draw emergency route planning results. With people in affected areas evacuating from

many different locations to relatively safe locations, it is clear that what we have mentioned above is critical to the design and operation of an emergency evacuation network. As a comparison and to show the significant difference between Model I as well as Model II, we have produced Fig. 4.6 to show the health consequences of the two models in emergency evacuees after exposure to toxic gases.

When there are many paths from the departure node to the corresponding target node (such as between the departure node 1 and the target node 16), then when solving the optimal emergency route between the same departure point and the target node, as shown in Figs. 4.4 and 4.6, it is clear that the results of Model I and Model II are different. And, although the goal is the same, the health risks obtained are different if different routes are used for emergency evacuation. There is a problem here, that is, the difference in the geographical environment of some nodes between the departure node and the target node will lead to a certain difference in the concentration of
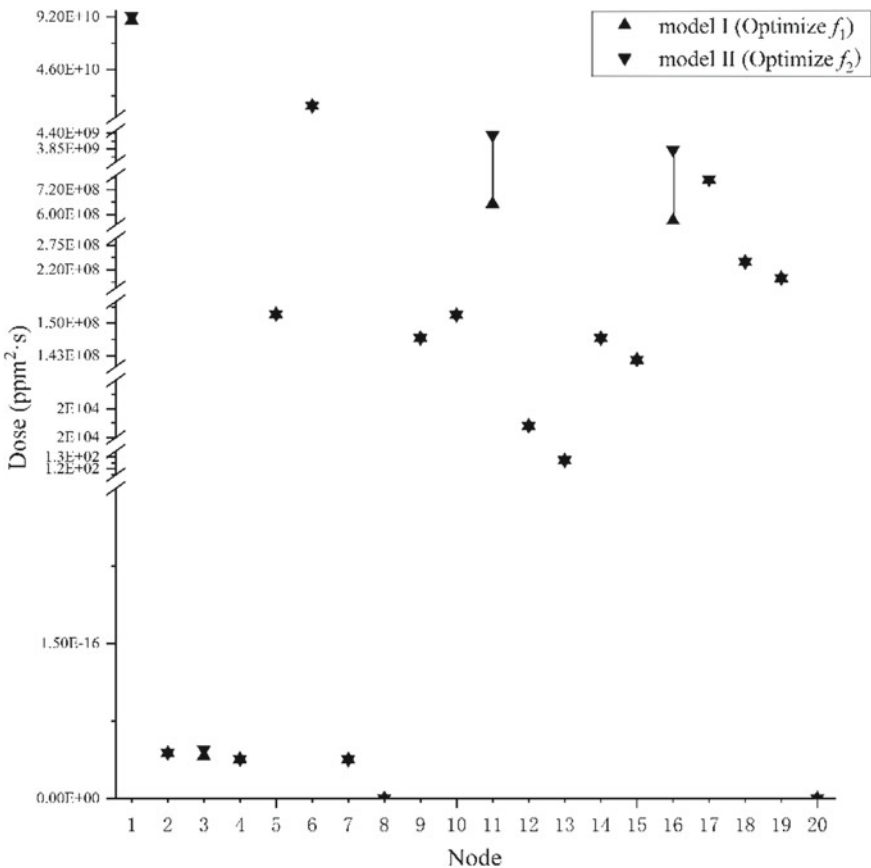

Fig. 4.6 Dose obtained by emergency route planning based on Models I and II for different source nodes

toxic gases and thus a certain difference in the health effects of emergency evacuees. In addition, if the location of the departure node is similar (in other words, the concentration of poisonous gas at the initial node is similar), and the destination node is different, it will also cause a large difference in the health impact of emergency evacuees. Here is a small example. As shown in the figure above, the position of node 13 is very similar to the position of node 9, so the dose of poison gas encountered by emergency evacuation personnel at the beginning of evacuation is also roughly the same, but the emergency of node 13. The evacuees can choose to go to the emergency shelter, so the dose of poison gas they encounter during the transfer process is much smaller than that of the emergency evacuees at node 9. In other words, the health risk of the emergency evacuees at node 9 is much greater than that of the evacuees at node 13. Based on this, it is not difficult to find that if there are a reasonable number of emergency shelters with good gas protection near the gas leakage accident site, the impact of the gas leakage accident will be reduced, and the risk of emergency evacuation will also be reduced. It is worth noting that we cannot blindly increase the number and capacity of emergency shelters, because the probability of toxic gas leakage accidents is very small. If we do this, it will only cause an extremely serious burden on normal urban operations. Therefore, we should maintain a prudent and rigorous attitude to plan emergency shelters reasonably, which will be an important decision to reduce the risk to a tolerable level when disaster strikes. In addition, after sorting out and analyzing the optimal paths obtained by Model I and Model II, we calculated that the health consequences associated with the Model I are significantly lower than those associated with the Model II. Then there is the following situation. When we only consider reducing the evacuation time as the only goal, it is obvious that when the personnel participating in the emergency evacuation do not have the necessary respiratory protection, they may encounter more poisonous gas doses during the emergency evacuation process.

The emergency response region is separated into low-risk as well as high-risk areas based on time to transfer as well as health effects. Figure 4.7a shows our planning as well as evaluation results of emergency routes for each node in the network. The results are obtained through Eq. (4.19) based on Model I. Likewise, Fig. 4.7b shows the evaluation results corresponding to Model II as well as Eq. (4.20). (Of course, it is worth noting that since node 8 and node 20 are destination nodes, they do not participate in the calculation.) Fig. 4.7a shows when the location of emergency evacuees is from a relatively safe node (in this paper, it should be the destination node, such as node 1, node 6, node 11, node 16, node 17, node 18, and node 19) with greater distances, they do not have toxic gas protection equipment, they obviously have a higher risk to their health throughout the emergency response. As shown in Fig. 4.7b, obviously, the nodes located in the high-risk area are node 1, node 5, node 9, node 10, node 11, and node 16.

We calculate the emergency route according to the algorithms of Model I and Model II, and then we discuss the related health risks and time risks, as shown in Fig. 4.7a, b. It can be seen that they have certain similarities, but differences in some details. Node 9, node 17, node 18, node 19, and node 6 describe the following two cases: The first case is that the departure node and the poison gas diffusion direction
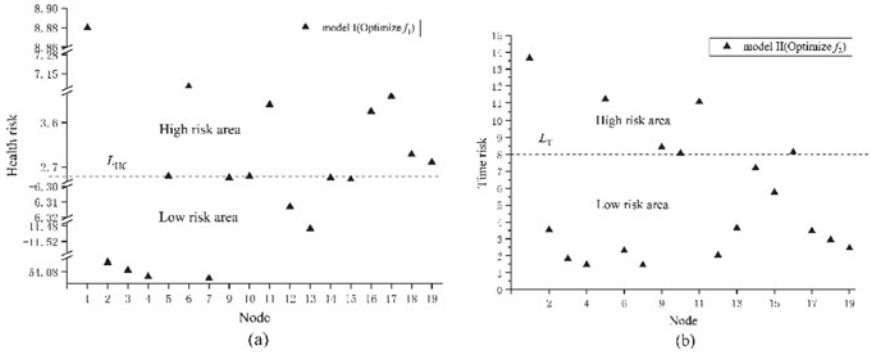
Fig. 4.7 Risk area division based on Models I and II. **a** Optimize f_1, **b** optimize f_2

are not the same, but the departure node and the destination node are far away; the first case is that the distance between the departure node and the destination node is relatively close, but the position of the departure node is close to the direction of the poison gas diffusion. Obviously, Model I and Model II are one sided when it comes to finding the appropriate emergency route for toxic gas leakage accidents, because the emergency routes they get still cannot guarantee the safety of emergency evacuees. And the results of these two models cannot describe the emergency risk level of the entire network. We can give a small example, when the health risk is not considered and only time is the optimization objective, the risk of the evacuation route taken by the emergency evacuation personnel at node 17 during the emergency evacuation is acceptable, but they will suffer unacceptable health risks, that is the downside. Of course, our goal is to find the optimal emergency route. Obviously, the rationality of the results of regional division is crucial. Because it not only determines emergency early warning planning and program design, it also affects the entire emergency operation. When a major chemical accident occurs, the relevant departments should issue an early warning to high-risk areas to ensure that they can escape the accident scene as quickly as possible and go to the nearest emergency shelter or other relatively safe areas to ensure safety. In general, when a major chemical accident occurs, the formulation of a public protection plan should not only consider the number of shelters and facilities in the target area, but also comprehensively consider the protection of personnel.

Figures 4.8 and 4.9 show contingency planning as well as risk evaluation as a function of given parameters, namely warning time as well as speed level. According to the algorithms of Model I as well as Model II, we calculate the risk under the optimal path of node 14 with respect to the parameter t_s^w. The details are shown in Fig. 4.8. As can be seen from Fig. 4.8, when the emergency manager does not issue an early warning in time, whether the emergency evacuation personnel at node 14 carry out self-safety protection will increase the time risk as well as health risk of the transfer process to varying degrees. When the time interval between the occurrence of a

major chemical accident and the warning notice issued by the emergency management personnel reaches one minute, the urgent time risk could gradually grow. The emergency health risk would escalate to an unbearable degree if this time interval approaches three minutes. According to the algorithms of Model I as well as Model II, Fig. 4.9 describes the emergency risk situations corresponding to the optimal paths of different groups of people at node 15. Specifically, as the moving speed of this group of people decreases, as shown in Fig. 4.9, their time risk and health risk increase to varying degrees. When the affected ratio ξ of the moving speed of pedestrians participating in emergency evacuation is reduced to 0.8, the health risk of pedestrians would increase; when the affected ratio ξ of the moving speed of pedestrians participating in emergency evacuation is reduced to 0.6, the time risk of pedestrians would rise. There are not only normal adults in the dangerous area covered by the toxic gas, but also some people are the elderly and children. In the emergency response process of a major gas leak accident, if emergency managers do not pay attention to the elderly as well as children with limited mobility and do not help them through the dangerous time, obviously, compared with normal adults, they may suffer more unacceptable health threat. In other words, the emergency route planning model mentioned in this paper has excellent strength in effectively identifying high-risk persons in the scenario of a major chemical leakage accident. In addition, our proposed algorithm can also reasonably plan emergency resources according to specific accident scenarios, personnel protection conditions, and other factors.

4.4.4 Results of Dynamic Route Selection for Major Accidents with Secondary Disaster Risk

Next, we look at the situation where there are secondary disaster risks. Below we give a series of assumptions: the population velocity influence coefficient of the departure node $\xi = 1$; the available emergency response time $L_t = 16$ min; the warning reception time $t_s{}^w = 0$.

There is also an assumption that we believe that emergency shelters in this scenario cannot provide sufficient protection, that is, all people in the network must be moved to a relatively safe place. Model III can be solved by our proposed algorithm. Then we can get the best emergency evacuation route of any node in the network, then the emergency risk of each area in the network (see Appendix 2 for details) can be calculated. As shown in Appendices 1 as well as Appendices 2, the optimal contingency route calculated by Model III is, in some cases, a compromise between the solutions corresponding to an ideal point (as a small example, Node 1). As shown in Appendices 1 as well as Appendices 2, the optimal contingency route calculated by Model III, in some cases, is not completely accurate, but is just a compromise between solutions corresponding to ideal points (take a small example like node 1). Obviously, in the case of a major chemical accident, if we still insist on using Model I
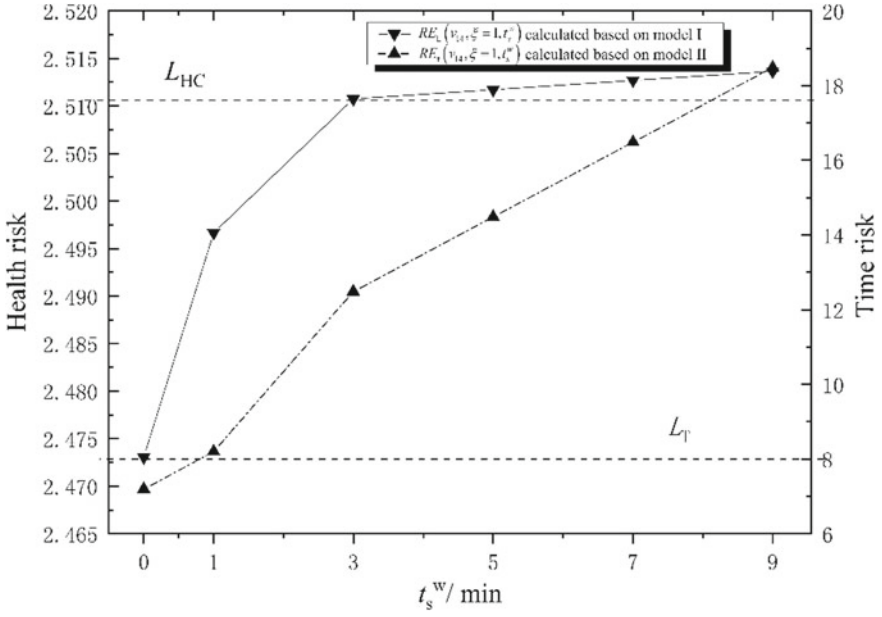
Fig. 4.8 Emergency risk of the optimal routes for node 14 based on Models I and II with respect to t_s^w
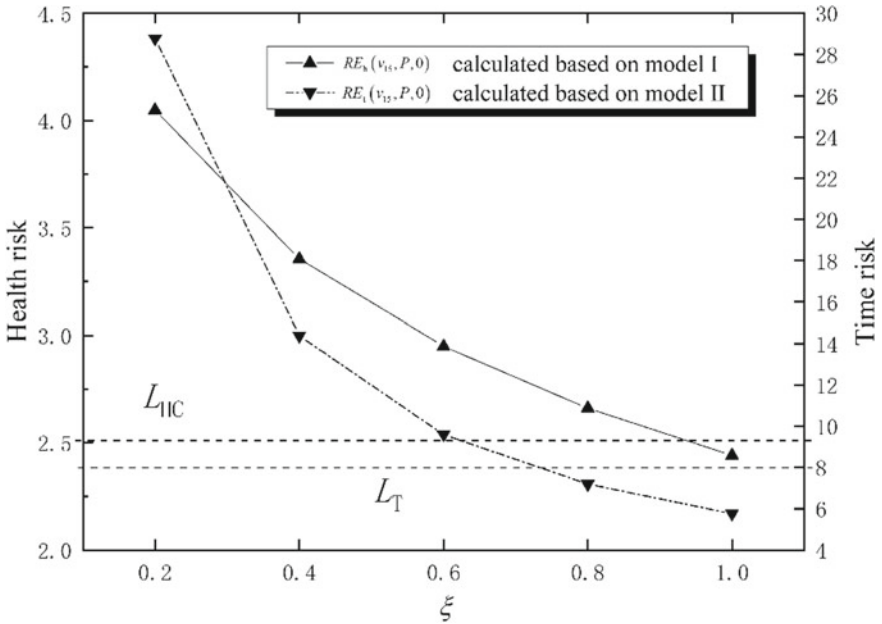

Fig. 4.9 Emergency risk of the optimal routes for node 15 based on Models I and II with respect to ξ

or Model II to solve the emergency route, the emergency evacuees will still encounter unacceptable health risks as well as time risks during the entire evacuation process. Also, when the departure location of emergency evacuees is within the coverage of a well-conditioned emergency shelter in the network, they can have two choices: One is to go to the shelter; the other is to go to the exit of the emergency response area and go to other safe area. There is no doubt that the first option suffers significantly less risk than the second option.

As shown in Fig. 4.10, we divide each node in the network into several different emergency risk areas according to the level of emergency risk. The specific division method is based on the multi-index emergency risk evaluation method mentioned above as well as the appendix 2 results. It is worth noting that this risk classification method enables the time risk and health risk encountered by emergency evacuation personnel in the entire network to be interpreted in detail and accurately. Compared with the risk classification method of the only indicator mentioned above, it has the advantages of higher reliability and more comprehensiveness. As shown in Fig. 4.10, it is obvious that when a major chemical accident occurs, emergency managers should give priority to the safety of personnel located in Area I, because compared with personnel in other areas, these personnel may suffer the highest time risk and health risk. Likewise, as shown in Fig. 4.10, emergency evacuees in Area II will face significantly different risks than Area I, a lower temporal risk and a higher health risk. In order to minimize casualties caused by major chemical accidents, emergency managers should not only update and improve emergency equipment and early warning facilities, but also reasonably plan and build emergency shelters in good condition. Comparing the emergency evacuees in the first two areas, the emergency evacuees in Zone III will suffer a lower health risk, but still suffer a higher time risk, so emergency managers should provide the area with more emergency equipment. Emergency evacuees in Area IV face the lowest time as well as health risks. Then, for the protection of this area, in addition to the necessary emergency management measures, considering the cost, an emergency early warning system should also be improved. To sum up, the research results of this paper can be used to judge the level of risk faced by people in different areas of the disaster area when a major chemical accident occurs. This result will be of great help to the formulation as well as implementation of emergency plans under the scenario.

We take the people to be evacuated located at node 14 in the network as the research object and use the algorithm of Model III as a tool to analyze whether the different population categories have a certain impact on the division of emergency risk areas. We divide the people to be evacuated at node 14 into two groups, one group is the affected people, the coefficient $\xi = 0.5$ related to their being affected, and the other group is the unaffected people, that is, $\xi = 1$. Likewise, the risk assessment method we use here is still the one mentioned in Sect. 4.2.3, as shown in Fig. 4.11, for the risk area division based on $\sigma_{14, \xi = 0.5}$. Figure 4.11 shows that once the proportion of the affected population in the total population increases, it will affect the entire emergency response process, resulting in a substantial increase in emergency risk. It is worth noting that once this ratio is higher than 20%, both the health risk and the time risk may rise to an unacceptable level. In summary, our proposed model can
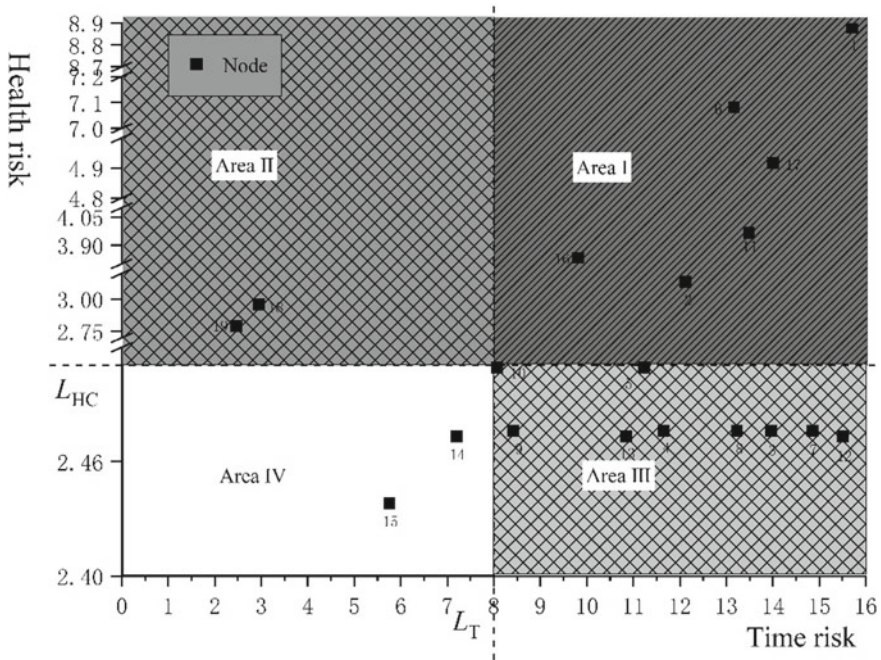
Fig. 4.10 Area division results of the multi-indicator emergency risk

assess the risk to people at the scene of an accident given important factors such as the proportion of people affected and the disaster scenario and finally flag high-risk groups. To put it another way, our proposed method can make the allotment of urgent resources more reasonable.

4.5 Conclusions and Future Research

Compared with the emergency route adopted by traditional and conventional natural disasters, due to the prominent feature of lag in the early warning of major chemical accidents, secondary disasters may be caused, so there are obvious differences in the planning, formulation, and implementation of emergency routes. And there are more factors that need to be considered in the planning, formulation, and implementation of emergency routes. Such as the number and location of emergency shelters, population distribution, the occurrence of secondary disasters, the early and late release of the warning time, and the degree of reduction in the speed of people's movement are some important factors that need to be considered. Then, according to the various characteristics of major chemical accidents, we propose a different emergency route planning model from the previous one, and one of its distinctive
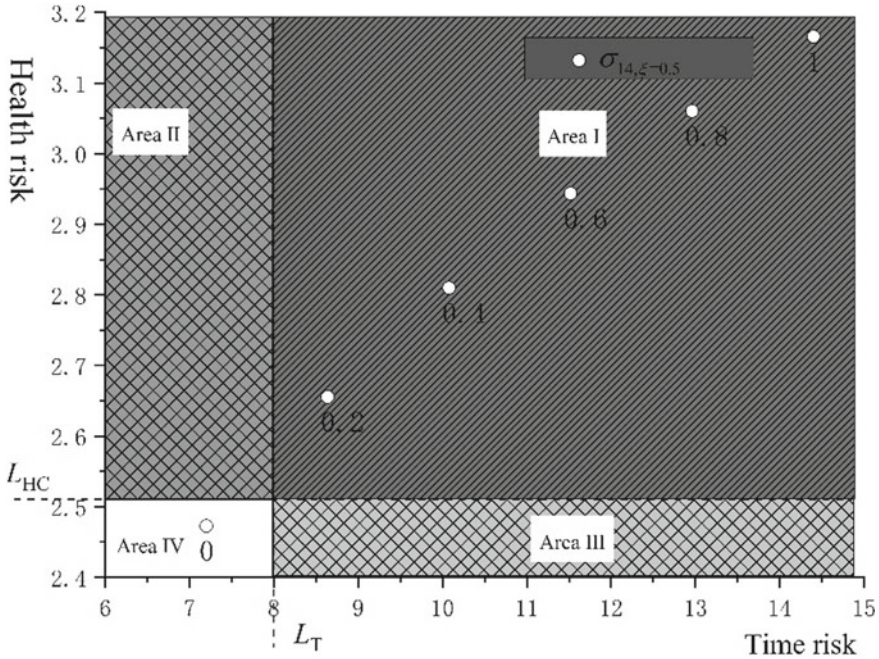
Fig. 4.11 Corresponding risk of node 14 changes with $\sigma_{14,\xi=0.5}$

features is dynamic. Here, we performed single-objective optimization as well as multi-objective optimization, the main optimization goals are transfer time as well as health consequences, and some of the factors mentioned above are the main reference objects. In order to calculate the emergency route more accurately, we simulate the accident expansion situation as accurately as possible in the model and use the modified Dijkstra algorithm to deal with this single-objective optimization as well as multi-objective optimization problem. We also came to a special result that we created a personal risk categorization technique based on time risk as well as health risk, which will greatly increase the probability of survival of victims of significant chemical accidents. From our simulation results, it is clear that our algorithm and model have significant feasibility as well as merits. The following are the main conclusions of this paper.

(1) To begin with, the ideal path depending on various optimization targets might differ. The main reason for this phenomenon is due to an important feature of the emergency network, that is, the emergency network has great complexity. When a major chemical accident occurs, it is worth noting that when the personnel in the dangerous area do not have respiratory protection facilities, when the optimization goal is still to reduce the transfer time, these personnel will suffer higher health risks. Take a small example, the emergency evacuation personnel at node 1, if the evacuation route is obtained according to the algorithm of Model II,

after calculation, the health risk increases $(5.86114 - 3.96556)/3.96556 \times 100\%$ = 47.8%, however, the time risk. It is only reduced by $(11.07 - 13.49)/13.49 \times 100\% = 17.9\%$.

(2) Second, when a major chemical accident occurs, if the emergency manager releases the warning information later, the people in the dangerous area will receive the information later, and the time they will be exposed to poisonous gas will be longer. Obviously, there is a certain increase in the time and health risks they suffer during emergency evacuation. It is worth noting that those who for some reason (e.g., mobility impairment due to own reasons or impaired mobility due to assisting others) had impaired metastatic velocity apparently suffered significantly higher temporal as well as health risks than healthy, normal adults.

(3) Third, we also found that in the event of a major chemical accident, simply adding safety exits will not make people at the accident site safer, but will be safer if they go to the nearest and well-protected shelter. Doing so would not only make major chemical accidents less of a health threat, but would also allow for shorter evacuation times. It is worth noting that this can only be achieved under certain conditions, such as certain requirements for the protection effect of emergency shelters as well as no secondary disasters.

(4) Fourth, we should closely link the composition of the population to emergency risk assessments. The total regional risk in the network is closely related to the degree of impairment of the movement speed of the people at the accident site, and the higher the degree of impairment, the higher the risk.

To sum up, when a major chemical accident occurs, our model can identify people who will suffer unacceptable time risks as well as health risks based on various factors (these factors include, but are not limited to: the degree of damage to the movement speed of people in the disaster area, the early or late issuance of the warning, the situation of individual protection) in the accident scene, so as to facilitate key protection for them. When a major chemical accident occurs, this method may be used as a guide for optimizing resource allocation as well as implementing emergency plans. This research could be expanded in the following ways. (1) In addition to solving the emergency route selection problem in this paper, the algorithm mentioned in this paper can also solve logistics management as well as other constrained optimization problems. It is worth noting that we can calculate the time risk and health risk of each node based on the optimal path of each node. By comparing these two values, we can plan, manage, and allocate emergency resources more reasonably. (2) This chapter also conducts a series of studies on the emergency evacuation behavior of individuals in major chemical accidents. Individual traits as well as time of departure are the most important criteria considered. Nowadays, with the rapid development of smartphone technology, we believe that in the near future, the results of our research can provide personalized evacuation guidance for emergency evacuation personnel who are encountering major chemical accidents through smartphone technology. Future study might look at the constraints of collective variables in emergency response,

such as the effect of crowd movement on personal velocity. (3) In addition, the development of modern technologies such as GIS and big data has become more and more mature in recent years, and we can also combine the risk assessment of major chemical accidents with it. This connection facilitates urban design, building, management as well as service. We will use a residential neighborhood of the Wanhua Group in Yantai as just an instance to investigate the fundamental evacuation strategy in the following chapter.

References

Danial, S.N., J. Smith, B. Veitch, and F. Khan. 2019b. On the realization of the recognition-primed decision model for artificial agents. *Human-Centric Computing and Information Sciences* 9 (1): 36.

Ding, L., J. Ji, and F. Khan. 2020. Combining uncertainty reasoning and deterministic modeling for risk analysis of fire-induced domino effects. *Safety Science* 129: 104802.

Ding, X.Y., J.C. Jiang, and Q. Huang. 2007. Simulation analysis on release and dispersion process of liquefied ammonia tank. *Journal of Safety Science and Technology* 3 (3): 7–11 (in Chinese).

Gai, W.M, Z.A, Jiang, Y.F Deng, J Li, Y, Du. 2015. Multiobjective route planning model and algorithm for emergency management. Mathematical Problems in Engineering (pt.2) 1–17

Gai, W.M., Y.F. Deng, Z.A. Jiang, J. Li, and Y. Du. 2017. Multi-objective evacuation routing optimization for toxic cloud releases. *Reliability Engineering & System Safety* 159: 58–68.

Georgiadou, P.S., I.A. Papazoglou, C.T. Kiranoudis, and N.C. Markatos. 2007. Modeling emergency evacuation for major hazard industrial sites. *Reliability Engineering & System Safety* 92 (10): 1388–1402.

Hong, L., J. Gao, and W. Zhu. 2018. Self-evacuation modelling and simulation of passengers in metro stations. *Safety Science* 110: 127–133.

Hosseinnia, B., N. Khakzad, and G. Reniers. 2018. Multi-plant emergency response for tackling major accidents in chemical industrial areas. *Safety Science* 102: 275–289.

Khakzad, N. 2018. Which fire to extinguish first? a risk-informed approach to emergency response in oil terminals. *Risk Analysis* 38 (7): 1444–1454.

Mardle, S., and K.M. Miettinen. 2000. Nonlinear multi objective optimization. *Journal of the Operational Research Society* 51 (2): 246.

Menz, H.B., M.D. Latt, A. Tiedemann, M.M. San Kwan, and S.R. Lord. 2004. Reliability of the GAITRite® walkway system for the quantification of temporo-spatial parameters of gait in young and older people. *Gait and Posture* 20 (1): 20–25.

Norafneeza, N., K. Faisal, V. Brian, and M.K. Scott. 2018. Dynamic risk assessment of escape and evacuation on offshore installations in a harsh environment. *Applied Ocean Research* 79: 1–6.

Norazahar. N, F. Khan, Veitch, B, Mackinnon, S. 2015. Assessing evacuation operation performance in harsh environments. In ASME 2015 34th international conference on ocean, offshore and arctic engineering, 1: vol. 1–6

OGP. 2010. Risk assessment data directory: Vulnerability of humans. *International Association of Oil and Gas Procedures, Report* 434–14: 1.

Reniers, G., and K. Soudan. 2010. A game-theoretical approach for reciprocal security-related prevention investment decisions. *Reliability Engineering and System Safety* 95: 1–9.

Shi, C., M. Zhong, X. Nong, L. He, J. Shi, and G. Feng. 2012. Modeling and safety strategy of passenger evacuation in a metro station in china. *Safety Science* 50 (5): 1319–1332.

Shimbel, A. 1953. Structural parameters of communication networks. *The Bulletin of Mathematical Biophysics* 15 (4): 501–507.

Smith, J, M. Musharraf, B. Veitch. 2017. Data informed cognitive modelling of offshore emergency egress behaviour. In Proceedings of the 15th international conference on cognitive modeling. Vol. 146–151. Coventry, United Kingdom: University of Warwick

Sorensen, J.H., B.L. Shumpert, and B.M. Vogt. 2004. Planning for protective action decision making: Evacuate or shelter-in-place. *Journal of Hazardous Materials* 109 (1/3): 1–11.

Stepanov, A., and M.G. Smith. 2009. Multi-objective evacuation routing in transportation networks. *European Journal of Operational Research* 198 (2): 435–446.

Xiao, G.Q., L.M. Wen, B.Z. Chen, and H. Wang. 2001. Shortest evacuation path on toxic leakage. *Journal of Northeastern University (natural Science)* 22: 674–677.

Yadav, K., and R. Biswas. 2010. An intelligent search path. *International Journal of Intelligent Systems* 25 (9): 970–980.

Yoo, B., and S.D. Choi. 2019. Emergency evacuation plan for hazardous chemicals leakage accidents using GIS-based risk analysis techniques in South Korea. *International Journal of Environmental Research & Public Health* 16 (11): 1948.

Yuan, Y., and D. Wang. 2009. Path selection model and algorithm for emergency logistics management. *Computers and Industrial Engineering* 56 (3): 1081–1094.

Zhang, J.H., H.Y. Liu, R. Zhu, and Y. Liu. 2017. Emergency evacuation of hazardous chemical accidents based on diffusion simulation. *Complexity* 2017: 1–16.

Zhang, X., Z. Zhang, Y. Zhang, D. Wei, and Y. Deng. 2013. Path selection for emergency logistics management: a bio-inspired algorithm. *Safety Science* 54: 87–91.

Zhou, Y., and M. Liu. 2012. Risk assessment of major hazards and its application in urban planning: a case study. *Risk Analysis* 32 (3): 566–577.

Chapter 5
Simulation and Analysis on Characteristics of Subregional Evacuation Based on Individual Behaviors

5.1 Introduction

5.1.1 Evacuation Time

In the previous chapter, we studied the path planning model and method in regional evacuation. But in a specific case, how does the effect of regional evacuation change under the effect of evacuation time, evacuation speed, personnel density, and other factors? In this chapter, we will take a residential area of Wanhua Group in Yantai as an example to simulate and analyze them.

Considering that community residents are not decision-makers in regional evacuation, their evacuation time mainly consists of evacuation notification time, preparation time, and evacuation time (Lindell 2008). Among these, evacuation notification time and preparation time can be decided according to this chapter (Hou et al. 2020). The evacuation time refers to the actual time evacuees need to evacuate to a safer place (Wang 2007), and the spatial path can be separated into line segment before calculating the result of each segment and summing them up:

$$t_{ev} = t_{0,1} + t_{1,2} + t_{2,3} + \cdots t_{n,s} \tag{5.1}$$

in the formula

suffixes 0, 1, 2,…, n indicate nodes of different road sections;
suffix s indicates safe places/locations;
$t_{n-1,n}$ indicates the time series of evacuation between two adjacent nodes of the paths.

The time series of personnel evacuation on each section can be calculated independently, and the total evacuation time is obtained by summing up the individual egress time. And the evacuation time of personnel evacuating can be obtained through both the empirical formula to calculate the evacuation time and the simulation of evacuation dynamics.

5.1.2   Empirical Calculation of Evacuation Time

Previously, evacuation scholars have accumulated large quantities of calculation formulas for evacuation time, which include the Melink and Booth formula (Melinek and Booth 1975), the Togawa formula and the Paul empirical formula (Togawa 1995; Pauls 1999). In this chapter, a brief introduction of the former two formulas will be given.

(1)   The Melink and Booth formula

This empirical formula focuses more on calculating the overall evacuation time of a multi-story building. The formula is shown below:

$$t_r = \left(\sum_{i=r}^{n} N_i \right) \bigg/ (f' \, b_{r-1}) + rt_s \qquad (5.2)$$

in the formula

t_r indicates the maximum time for personnel above the rth $[r \in (1, \ n)]$ floor to evacuate to a safer place downstairs, and n refers to the number of stories;
f' refers to the flow of people passing through a unit width floor, number of people/(m s);
b_{r-1} refers to the width of floor from $(r - 1)$th floor to rth floor, m;
t_s refers to the time of people descending from a unit floor when it is not crowded, and often it is set as 16 s.

From the equation, we can obtain n values of $t_r (r = 1, 2, \cdots, n)$. The minimum evacuation time of the building equals to the maximum value of t_r. When the number of people on each floor and the width of staircase are all equal, respectively, then $N_i = N$, and $b_{r-1} = b$ is true for all r floors. Equation (5.2) can be simplified into:

$$t_r = \frac{(n - r + 1)N}{(fb)} + rt_s \qquad (5.3)$$

in which

N refers to the number of people on each floor;
r denotes the story number;

f refers to the passing rate of a unit width staircase, number of people/(m s);
b refers to the total effective width of the staircase, m.

If $N/(fb) \geq t_s$, a maximum t_1 can be obtained when $r = 1$, and the overall time of evacuation shall be $t_1 = nN/(fb) + t_s$; if $N/(fb) \leq t_s$, a maximum t_n can be obtained when $r = n$, and the total egress time can be obtained through $t_n = N/(fb) + nt_s$.

(2) The Togawa formula

The Togawa formula can calculate the time for evacuees to move to the exit of each residential area. The formula is shown below:

$$t_e = \frac{1}{fb'}\left[N_t - \sum_{i=1}^{n_e}\int_0^{t_0} f_i(t)b_i\phi_i(t)\mathrm{d}t\right] + t_0 \tag{5.4}$$

in which

t_e refers to the time needed to make to the exit, s;
N_t denotes the total number of evacuees inside the building;
$f_i(t), f$ denotes, respectively, the flow of people at the ith exit and at the final exit;
n_e refers to the total number of the exits;
b_i refers to the width of the ith exist, m;
t_0 refers to the time when a constant population flow appears, s;
$\phi_i(t)$ denotes the coefficient of people detaining at the ith exist, also the percentage of people gathering in this place.

The right side of the equation describes the evacuation time after the constant population flow appears, and it is only related to the evacuation capacity of the final exit; and the integral item refers to the number of people getting out from each exit from the start of the evacuation till the constant flow occurs. And the formula can be simplified into:

$$t_e = \frac{N_t}{bf} + \frac{k_s}{\upsilon} \tag{5.5}$$

in which

k_s refers to the distance between the final exit to the initiating terminal of the flow of people.
υ denotes the speed of flow.

The distance between the final exit and the initiating terminal of the flow of people can be taken as the distance of the first evacuee moving from his spot to the final exit. If we assume, after the first personnel arrive at the exit, the line behind him is in coherent order, obviously, according to the simplification, the shortest overall

evacuation time can be obtained assuming the evacuation speed unchanged, since the other evacuees will not follow closely with the first evacuee in real practice.

5.1.3 Simulation Modeling of Evacuation

In this chapter, LEGION software is selected to analyze the evacuation time of residences from the target community and the dynamic features in the evacuation.

(1) LEGION vector model

The model LEGION software employed is a vector model. And based on the individual behavior simulation technology and two-dimensional vector continuous spatial analysis, it takes into account individual behavior description, staff size, and spatial area. The model is most suitable for analog simulation for areas with large population and large scale. In this example, the model is based on individual pedestrians, and the plane route and direction of each step are calculated by computer algorithm, whereas each individual pedestrian has the right to determine his own action. Pedestrians will consider the surrounding environment (buildings and obstacles, etc.) and to interact, communicate with others to change information before making decisions. "Minimum effort" is often employed into the decision-making process (Zipf 1949), that is, when an individual chooses his next move, he will manage to minimize his dissatisfaction, which is possibly caused by physical and mental factors that slow down his speed, including obstacles, inconveniences, and uncomfortable feelings. And the LEGION vector model is mainly employed to study evacuation behavior of the crowd, evacuation time, and evacuation strategies and techniques.

(2) Components and functions of LEGION software

The LEGION software mainly consisted of three parts: modeler, simulator, and analyzer (Zhu 2006).

The modeler creates a precise and favorable model for space simulation, for example, to lead in a map of the building, which defines its physical space; to specify the demand of pedestrians for spaces; to designate the area of activities, such as a queuing area or a waiting area; to consider different routes; to link the data to the model; and to lead out the model files to the simulator.

The simulator can simulate how pedestrians move or cycle in the model space defined in the modeler. Through using the simulator, you can lead in the model files, play and view the simulation process, and record the relevant part of the simulation in the result file to be analyzed and to record all or part of the simulation through demo video file.

The analyzer can carry out a series of analyses in the analog space, through which files and the model file are able to be leaded in. Also, it can show the selected part of the recorded simulation or a set of new simulation, present the important measurement information in the form of a map to enable detailed analysis, showcase the results of the analysis through a times series, a stack bar chart or a column, and lead-out

analysis dialog in the form of graphics, documents, videos, pictures, or forms to help insert it to the presentation files, reports, or spreadsheets. Also, the analyzer has other functions, including data analysis of the density of people, the time of walking, the evacuation time, the maximum time of queuing, and also the maximum waiting time. And it supports data output into graphics, data, and charts.

5.2 The Evacuation Simulation of the Residential Community

5.2.1 The General Introduction of the Residential Community

In this chapter, a residential community in Qindao, belonging to Wanhua Group, which is of northeast orientation, is selected. In Fig. 5.1, the plane plan of the typical residential community we select is shown, from which readers can notice that there are 51 buildings in the whole community, mostly multi-storied. Most of them are households, small businesses, and shops. There are three main roads in the community. A hedge or plants separated the roads and the residential buildings. There are all in total ten exits in the area.
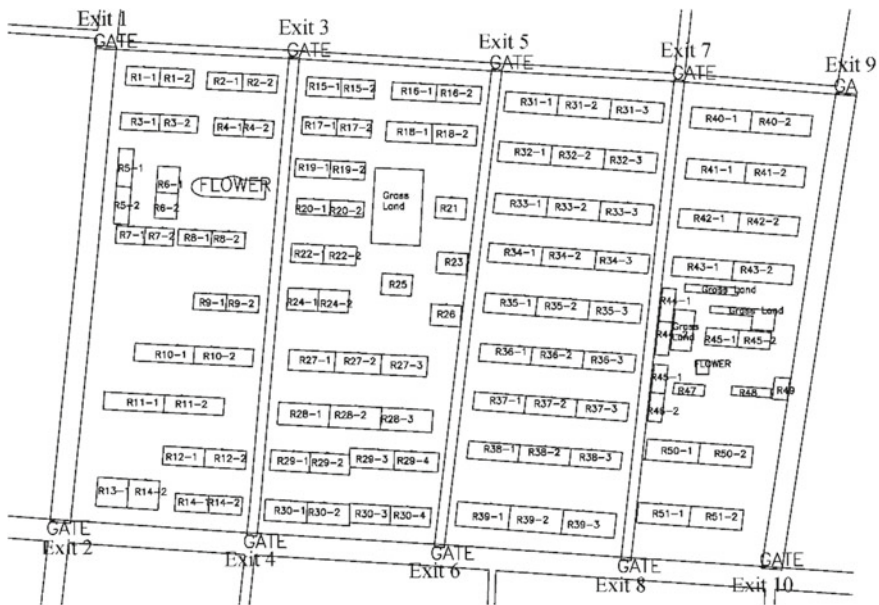

Fig. 5.1 Detailed plan of the residential community

The number of residents inside the community can be estimated according to the per capita floor space. For households, according to domestic statistics (Yantai Bureau of Statistics 2008), the average per capita area of the community is 25 m^2/person; for commercial shops, the initial estimation is 2.8 m^2/person. As shown in Table 5.1, according to the number of people on different floors, the plane area, and building types, the total number of residences inside the community can be estimated, which is around 14,832 people.

5.2.2   The Selection and Setting of Analog Parameters

(1)   Directions of evacuation

The residents inside the community will choose the exit based on the shortest path method during evacuation (Gloor et al. 2004), and the directions of evacuation from different buildings are shown in Fig. 5.2. For those inside the building, they will first leave their doors, descend through staircases to the ground floor to make to the entrance of the building, get out of the building and get to the secondary roads or main roads of the community, and reach the exit of the whole residential community when they receive the evacuation notice; and for those who are outside the building walking, they need to get directly from the secondary roads to the main ones and then reach to the exit of the building.

(2)   Evacuation options

We assume that all the residents receive the evacuation notification at the same time, and all of those inside the buildings take fast action once they get informed. The time of residents leaving the buildings shall be calculated, taking into consideration the total number of people, the number of floors, and the width of the entrance of each building, and parameters shall be set at the exit of the buildings as well as the time people need to get out of the building. The evacuation strategy shall be set, including the emergency plan for the escape, the shortest path selection, and the pre-action time.

(3)   The distribution of initial personnel

Decision-makers should take into consideration that different types of residents may vary in gender, age, and items they carry. The difference in resident types may cause differences in parameters, including reaction time, the area they occupied, maneuverability, and the speed of movement. Figure 5.3 shows the distribution of personnel at the initial moment, and it uses dots to indicate people.

Table 5.1 Estimation of people in the community

No.	Floor number	Area/m²	The building type	Density of people/(m²/people)	Number of people	Number of people inside the passage of the building
1	5	790	Household	25	158	79
2	5	746	Household	25	149	75
3	5	805	Household	25	161	81
4	5	628	Household	25	126	63
5	1	686	Shop	2.8	245	123
6	1	711	Shop	2.8	254	127
7	1	611	Shop	2.8	218	109
8	1	655	Shop	2.8	234	117
9	6	658	Household	25	158	79
10	6	1285	Household	25	308	154
11	6	1289	Household	25	309	155
12	6	945	Household	25	227	113
13	6	1112	Household	25	267	133
14	6	725	Household	25	174	87
15	4	781	Household	25	125	62
16	4	949	Household	25	152	76
17	4	743	Household	25	119	59
18	4	1091	Household	25	175	87
19	5	765	Household	25	153	77
20	4	640	Household	25	102	51
21	7	395	Household	25	111	111
22	6	754	Household	25	181	90
23	7	395	Household	25	111	111
24	6	834	Household	25	200	100
25	7	395	Household	25	111	111
26	7	395	Household	25	111	111
27	7	1726	Household	25	483	161
28	7	2109	Household	25	591	197
29	7	2039	Household	25	571	143
30	7	2058	Household	25	576	144
31	7	1952	Household	25	547	182
32	7	1952	Household	25	547	182
33	7	1952	Household	25	547	182
34	7	1872	Household	25	524	175
35	7	1879	Household	25	526	175

(continued)

Table 5.1 (continued)

No.	Floor number	Area/m^2	The building type	Density of people/(m^2/people)	Number of people	Number of people inside the passage of the building
36	7	1696	Household	25	475	158
37	7	1723	Household	25	482	161
38	7	1659	Household	25	465	155
39	7	2408	Household	25	674	225
40	6	1552	Household	25	372	186
41	7	1495	Household	25	419	209
42	7	1399	Household	25	392	196
43	7	1436	Household	25	402	201
44	1	561	Shop	2.8	200	100
45	1	688	Shop	2.8	246	123
46	1	487	Shop	2.8	174	87
47	1	210	Shop	2.8	75	75
48	1	220	Shop	2.8	79	79
49	1	205	Shop	2.8	73	73
50	7	1368	Household	25	383	192
51	7	1325	Household	25	371	186
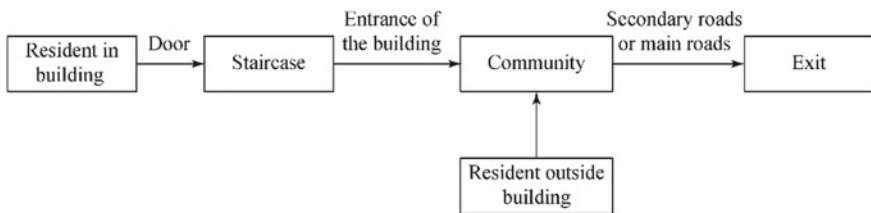
Fig. 5.2 Map of evacuation directions

5.2.3 Analysis of Evacuation Simulation Results

(1) Evacuation time

Through the simulation, we can obtain the evacuation time for all residents in to get evacuated into safer places outside the exit of the residential area. The dynamic change curve of the evacuee numbers in this calculation is shown in Fig. 5.4, from which we can notice that the cumulative curve is in a S-type. At about 82 s after the evacuation starts, evacuees start to move and get out of the exit. And at 474 s after the evacuation starts, all 14,832 evacuees have been successfully evacuated outside their community.
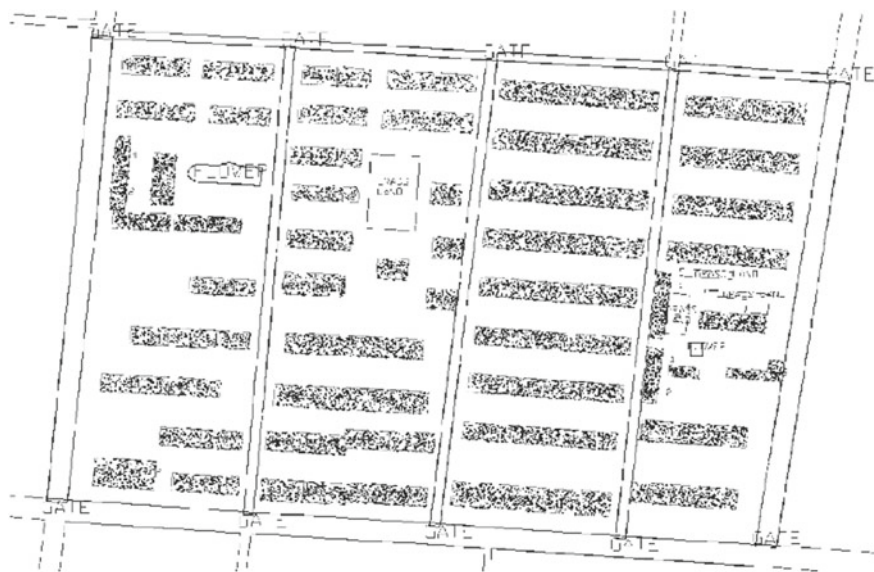
Fig. 5.3 Personnel distribution at the initial moment

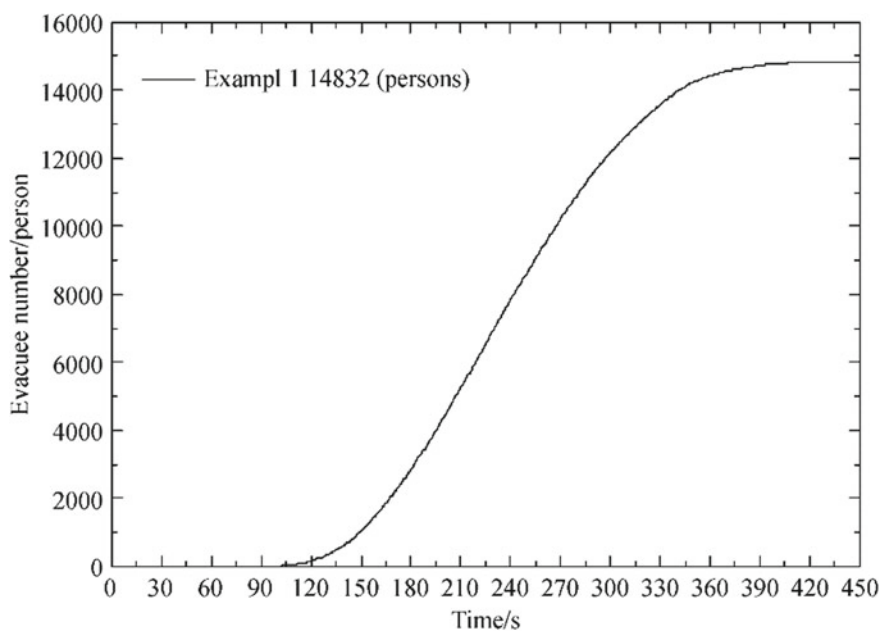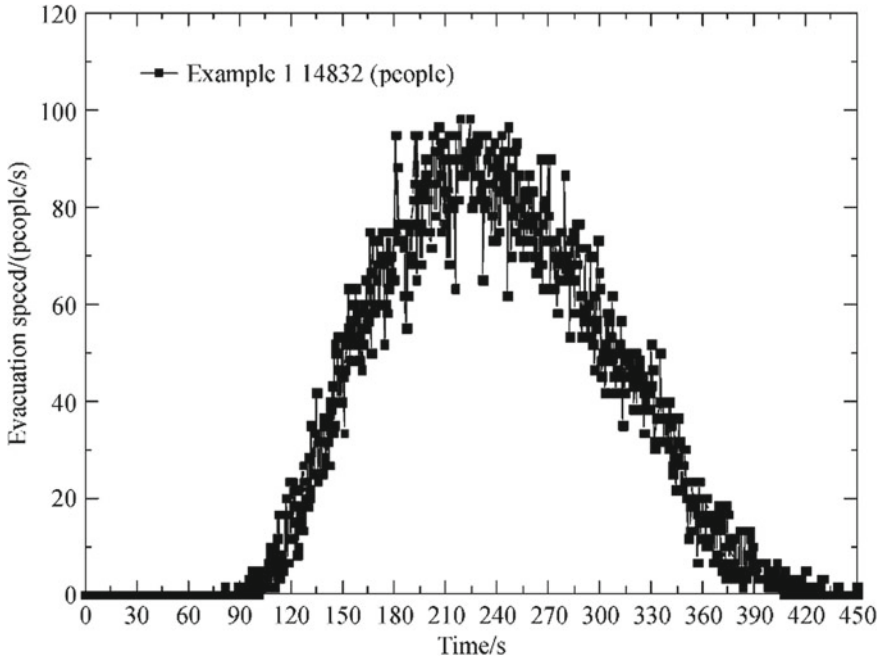**Fig. 5.4** Dynamic change curve of the evacuation

Fig. 5.5   Evacuation speed change chart

(2)   Evacuation speed

The variation curve between the total evacuation speed and time is given in Fig. 5.5, from which we can notice that the total evacuation speed has an increase tendency before its dropping and the maximum evacuation speed comes at 230 s since the evacuation starts. The change is likely to be caused by the density of people outside the exit of each residential area.

(3)   Statistics of evacuees evacuating through the exit of the community

Figure 5.6 shows the number of evacuees evacuating through the exit of the community, and it reveals the dynamic change of the amounts of evacuees from different exits. Since the way to Exit 1 is much longer, people tend to avoid choosing it. And from Fig. 5.6, we can notice the number of people evacuating from Exit 1 is 0, indicating no one takes the exit. Thus, in the simulation, the optimal path algorithm should be adopted: Inhabitants will choose the exit by the shortest path from their own locations, and thus, the numbers of people evacuating through different exits vary. Under such parameter, Exit 3, Exit 5, and Exit 6 are three main evacuation exits in this example, and they have relatively more people passing through.

(4)   Dynamic characteristics in the evacuation process

The typical simulation of evacuation process can be seen in Fig. 5.7a, b, c, d, e, f, g, h, i, j, from which we can notice at around the 50th s, people start to move out
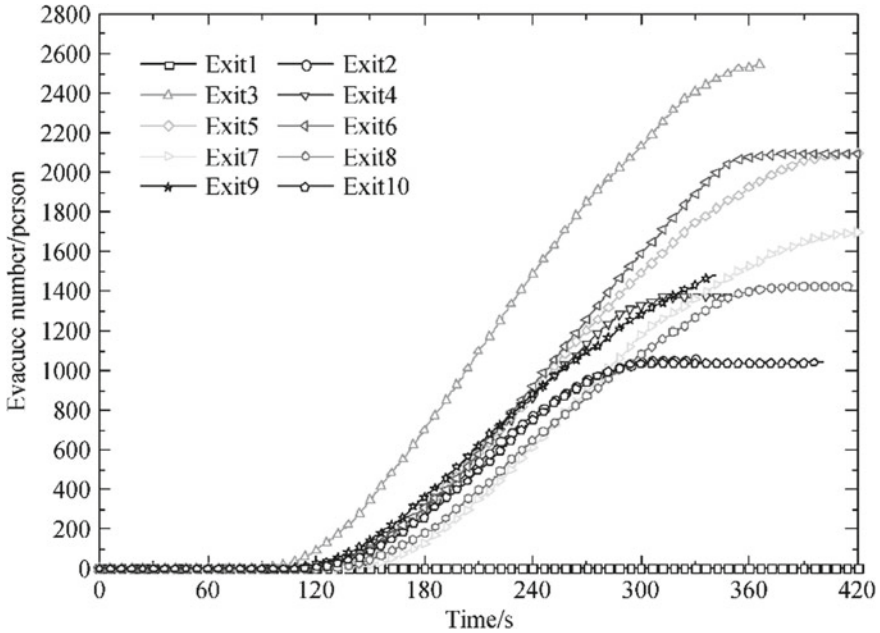
Fig. 5.6 Dynamic change curve of number of evacuees at each exit

of the building, and this has included the time people spend for actions that delay their evacuation process, for example, locking the doors. Since the types of building and the numbers of floor vary, the time they need to get out of the building differs accordingly. For those who have been outside the building, they will select the exit based on their distance to each exit and choose the routes based on their habits or comfortable degree of each road. Around the 2nd min, most residents are already out of the building. At around the 3.5–4th min, the density of people around the exit reaches a maximum, and the passing rate climbs to the maximum accordingly. At around the 7.5th min, almost all residents have been evacuated to the external road network of the residential area.

5.3 Comparison of Simulation Results of Different Evacuation Scale

In this chapter, we have studied the evacuation scale of the residential community, also the influences of evacuee numbers have on evacuation time and other evacuation dynamic characteristics. We conduct three simulations under different circumstances within one community, and name them, respectively, by Examples 2, 3, and 4, the evacuation population of which are 10,004, 5019, and 1020 accordingly, while we keep other simulation parameters unchanged. According to the examples, this chapter makes a comparative analysis of the simulation results.
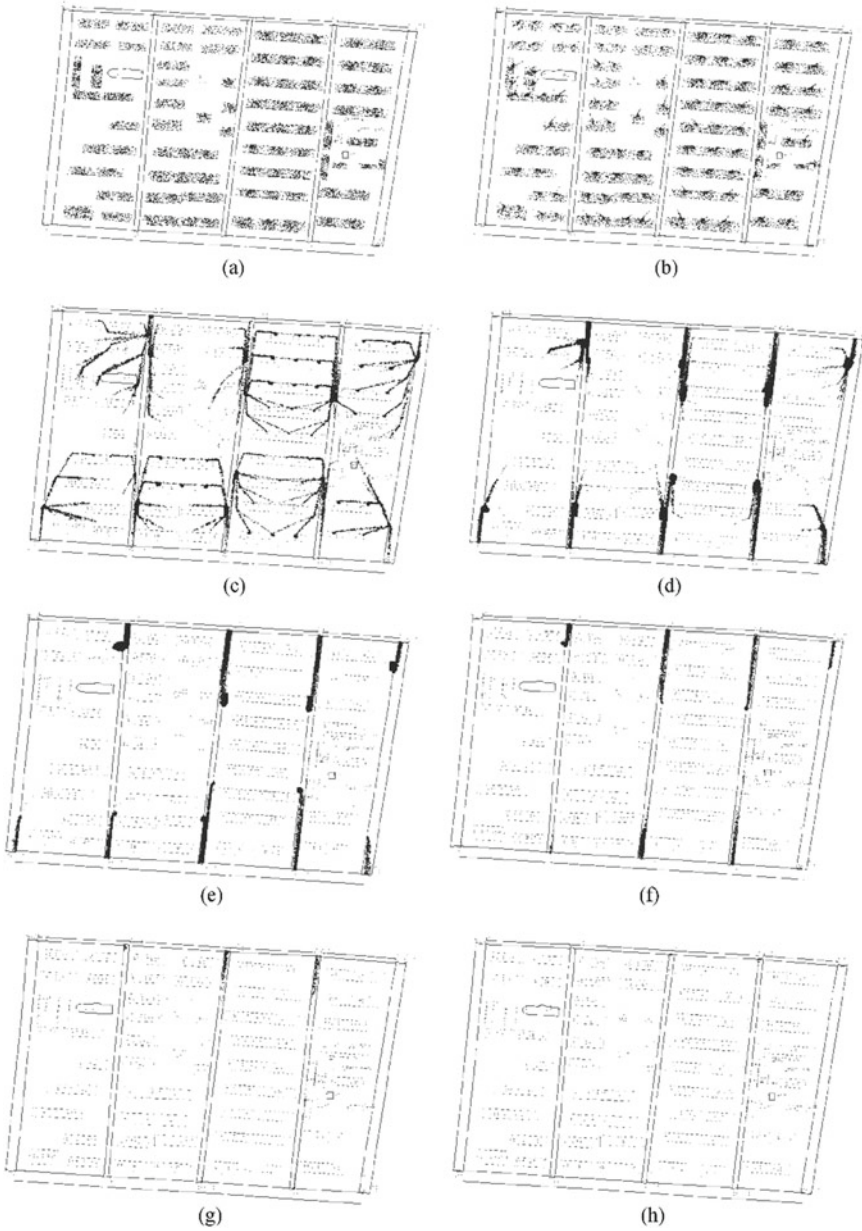
Fig. 5.7 Typical simulation of evacuation process. **a** Evacuation scene at the 0.5th min, **b** evacuation scene at the 1st min, **c** evacuation scene at the 2nd min, **d** evacuation scene at the 3rd min, **e** evacuation scene at the 4th min, **f** evacuation scene at the 5th min, **g** evacuation scene at the 6th min, **h** evacuation scene at the 7th min, **i** evacuation scene at the 7.5th min, **j** evacuation scene at the 8th min
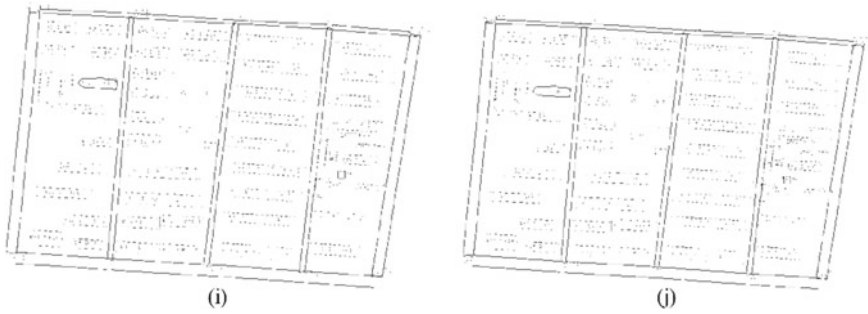
(i)   (j)

Fig. 5.7 (continued)

5.3.1 Comparison and Analysis of the Different Evacuation Time

The comparison diagram of different evacuation time curves for the four examples is shown in Fig. 5.8, and the overall time for all residents to get out of the community in each example is shown in Table 5.2. From Fig. 5.8 and Table 5.2, we can notice the relationship between the evacuation time of residents and the number of evacuees. When the evacuation population is 14,832, the time for evacuees to get out through the exit reaches 474 s; when the number of residents is 1020, it takes 363 s, which suggests the overall evacuation time grows with the increase of the evacuee number.

Table 5.2 also carries out the comparison of change rate of evacuees and that of evacuation time. From Fig. 5.1, we can notice that when the number of evacuees drops to 6.88%, the evacuation time drops to 76.58%, which suggests the drop in change rate of evacuation time is much lower than that of evacuee numbers. When the number of evacuees inside the community increased 14.54 times, the evacuation time only increased by 31%.

5.3.2 Comparison of Evacuation Rate

The trend of evacuation speed changing with the evacuee numbers is shown directly in Fig. 5.9. Although there are only 5000 more people in Example 1 compared with that in Example 2, their maximum evacuation speeds are almost the same. But in Example 3 and Example 4, although the former has nearly 4000 people more than the latter, the maximum evacuation speed rises from about 22 people/s to almost 68 people/s, a growth of 3.5 times. The increase pattern of evacuation speed is related to the design of internal road network, the width of the community entrance, and its passing capacity.
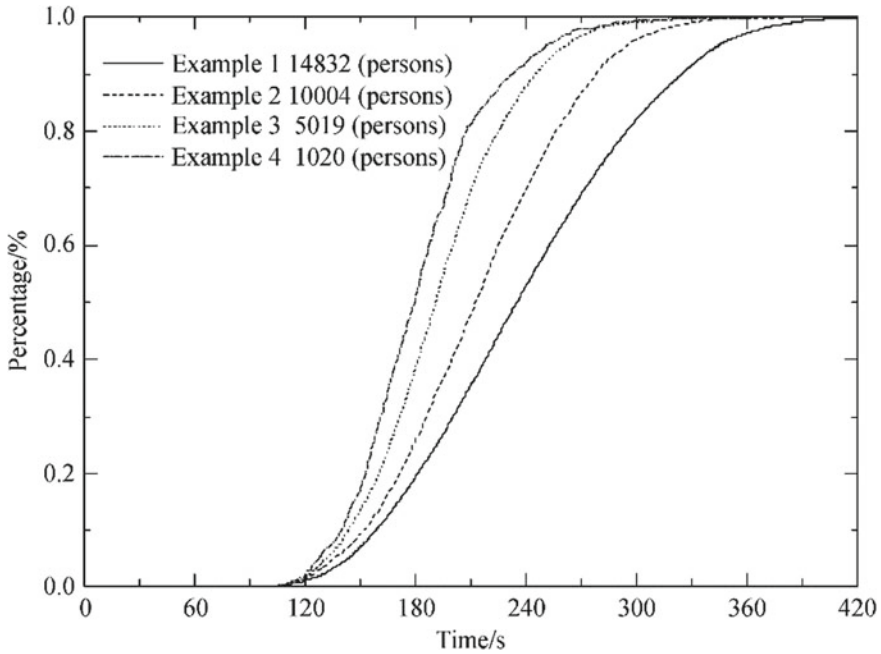
Fig. 5.8 Comparison of change curves of evacuation dynamics of each example

Table 5.2 Comparison of overall evacuation time from various examples

Serial number	The number of evacuees	The evacuation movement time/s	The change in the number of evacuees/%		The change in evacuation time/%	
			Based on the data of example 1	Based on the data of example 4	Based on the data of example 1	Based on the data of example 4
Example 1	14,832	474	100	14.54	100.00	1.31
Example 2	10,004	432.6	67.45	9.81	91.27	1.19
Example 3	5019	385.8	33.84	4.92	81.39	1.06
Example 4	1020	363	6.88	1.00	76.58	1.00

5.3.3 Comparison and Analysis of Space Utilization

Through LEGION evacuation simulation, we can observe the space utilization inside
the residential community during the evacuation. Figures 5.10, 5.11, 5.12 and 5.13
show the space utilization during the evacuation in Examples 1, 2, 3, and 4, respec-
tively, and their colors change from dark gray to light gray, indicating the utilization
rate changing from low to high. Also, the white parts denote the spaces when evac-
uees have not utilized. Judging from the four figures, we can notice that with the
increase of evacuee numbers, people have obviously utilized more space during
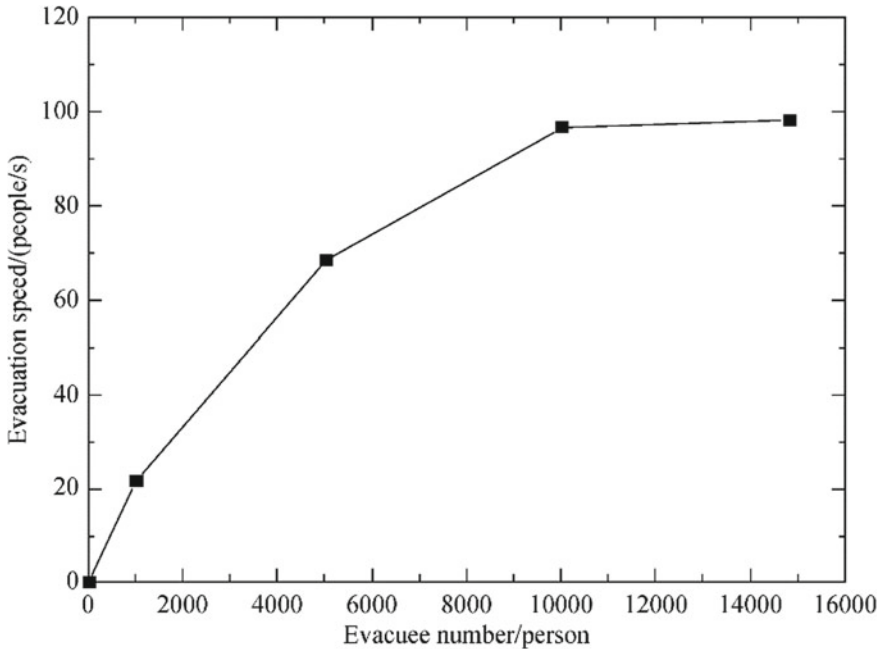
Fig. 5.9 Trend of maximum evacuation speed changing with the number of evacuees

evacuation (dark gray parts), especially around the secondary roads, main roads, and the community exits.

5.3.4 The Comparison and Analysis of the Densities of People

Through LEGION evacuation simulation, we can notice the density of people both inside the community and around the exit. Figures 5.14a, b, 5.15a, b, 5.16a, b and 5.17a, b show the mean density and the maximum density in Example 1, Example 2, Example 3, and Example 4, respectively, in which the colors changing from light gray to dark gray denote the density changing from low to high, whereas the white parts denote the space with no evacuees. From these figures, we can notice the following:

(1) The number of evacuees increases, and congestions inside the community occur. In Example 1, congestions occur mainly around the breach of hedge (the intersection of secondary and main road) of the main roads and near the main roads, especially near the intersections of main and secondary roads. In Example 2, although the mean density and the maximum density are all lower than their counterparts in Example 1, there are still congestions happened near the breach and the main roads of the community. In Example 3, there is a reduction in congestions, while in Example 4, there is hardly any congestion.
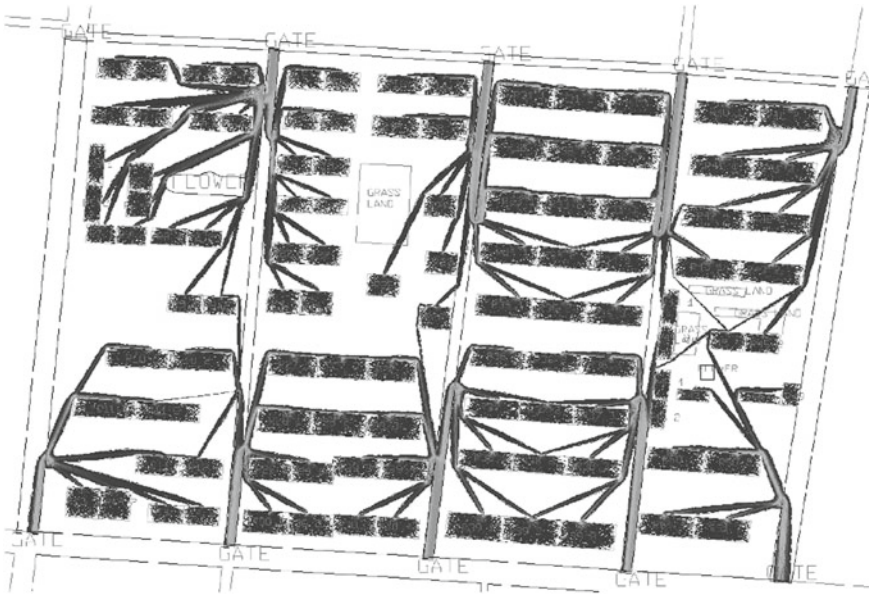
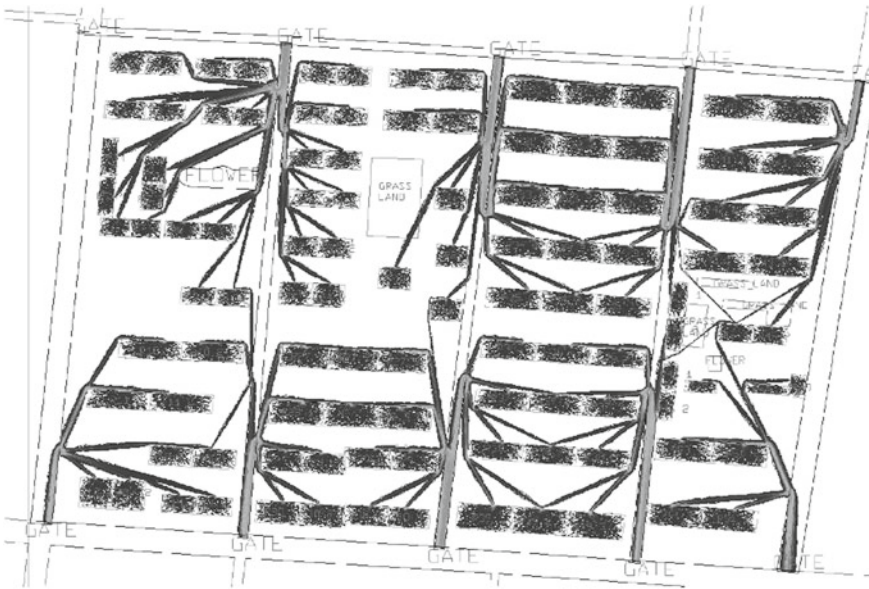**Fig. 5.10** Evacuation space utilization rate in Example 1

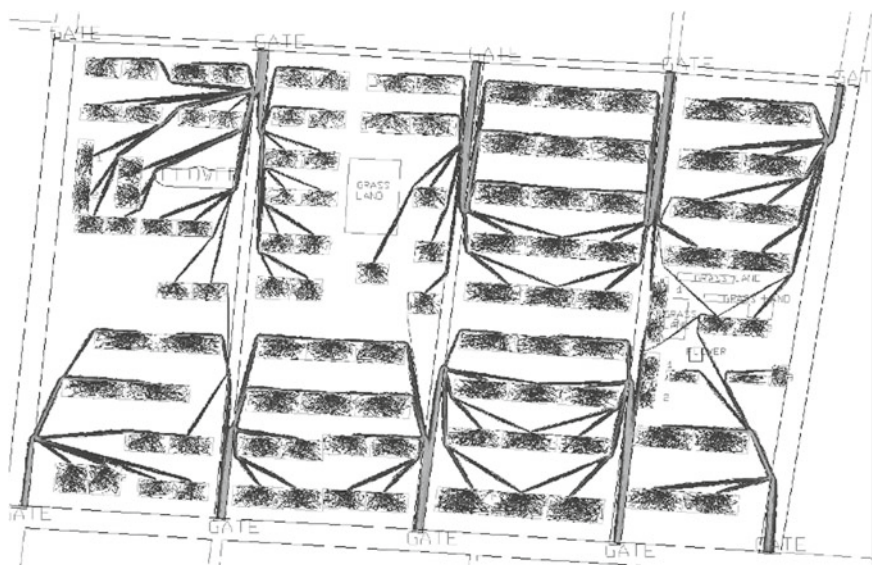
Fig. 5.11 Evacuation space utilization rate in Example 2
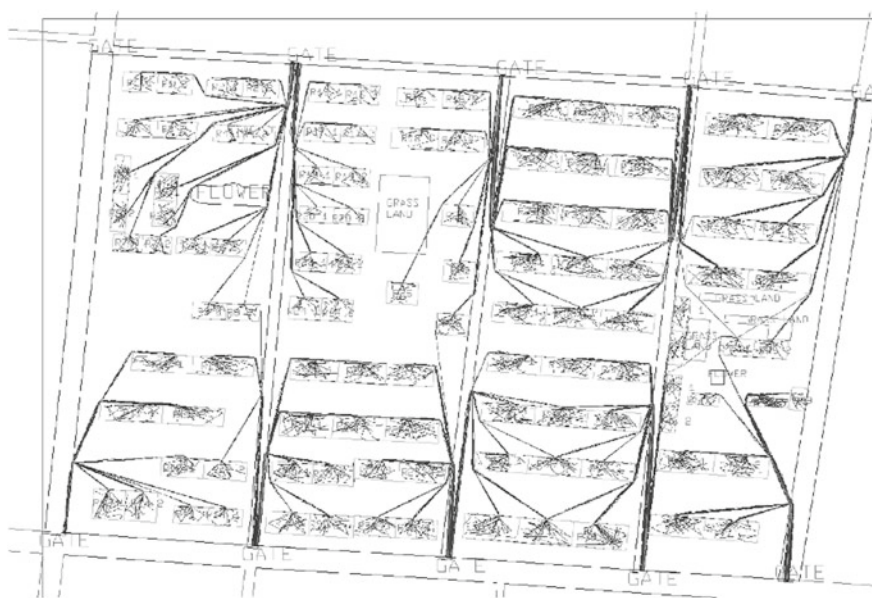
Fig. 5.12 Evacuation space utilization rate in Example 3
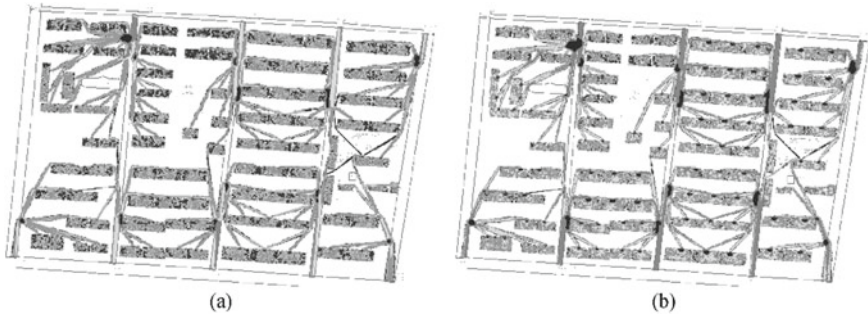

Fig. 5.13 Evacuation space utilization rate in Example 4

Fig. 5.14 Density of people in Example 1. **a** Mean density and **b** maximum density
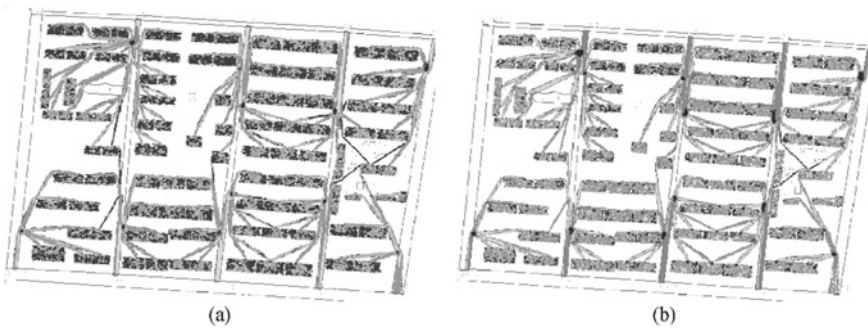
Fig. 5.15 Density of people in Example 2. **a** Mean density and **b** maximum density
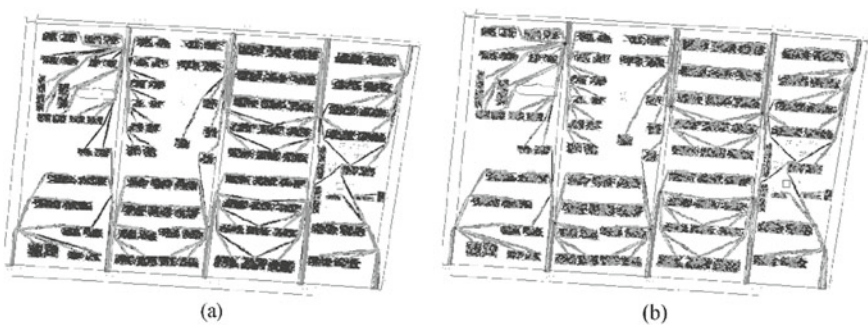
Fig. 5.16 Density of people in Example 3. **a** Mean density and **b** maximum density

(2) The most serious congestion occurs surprising not around the exit of the community. Comparing the four examples, we can find out that the mean density and the maximum density do not often occur near the exit of the community in both Examples 1 and 2, but around the breach of hedge near the main road, which is the intersection of the main road and the secondary road. A plausible
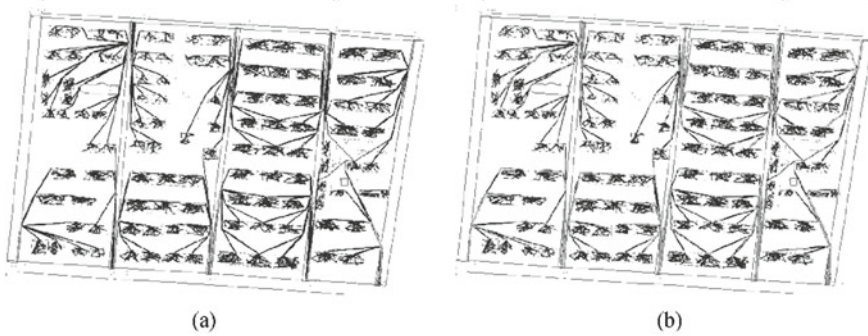
Fig. 5.17 Density of people in Example 4. **a** Mean density and **b** maximum density

reason for this circumstance is, the capacity of the intersection is not able to hold so many people, worse than that of the community. With the decrease of evacuee numbers, the congestion will be gradually eased. In Examples 3 and 4, the congestions mainly occur around the main road and near the exit of the community.

5.4 Study on the Loading Characteristics of Evacuation Network in Subregions

5.4.1 Influence Factors on the Loading Time in Urban Evacuation Road Network

In order to carry out regional evacuation analysis of the gas leak accident, it is necessary to know the time for residents from each subregion of the affected area to get loaded outside the region, which is also the time to get into the city road network. Assuming the residences receive the evacuation notification simultaneously, the previous part of this chapter employs LEGION vector simulation to analyze the evacuation time of a chosen residential community and other dynamic characteristics during evacuation.

According to the simulation, although the evacuee number varies, the evacuation time for the first evacuee to get to the exit is basically the same, and the total evacuation time increases with the number of evacuees. This linear increase is shown in Fig. 5.18, in which the regression of the linear increase is carried out. The slope of the line reflects the change in overall evacuation time with the increase of evacuee number, and the constant reflects the intrinsic properties of the residential area, closely related to the attributes of the internal road, the width of the community exit, and the passing capacity.
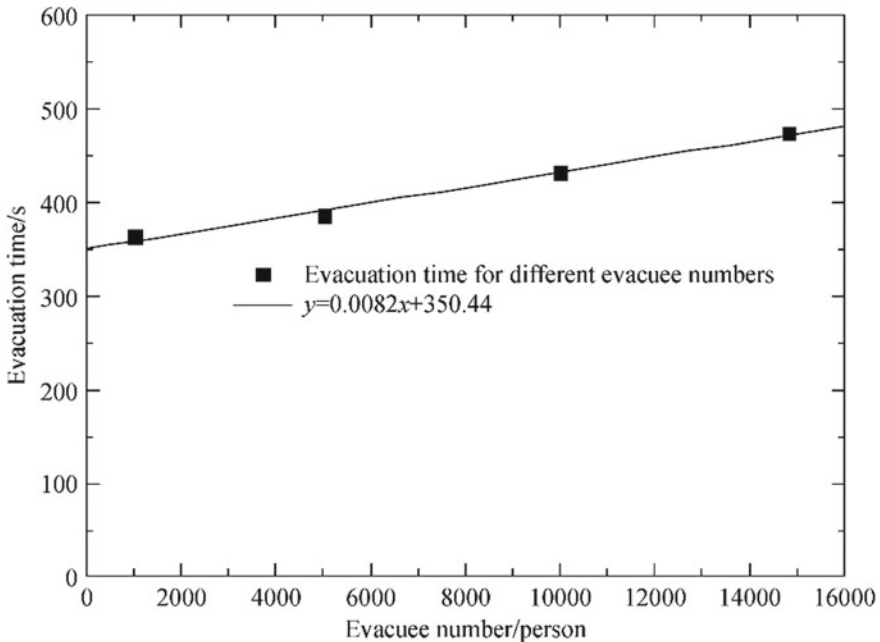
Fig. 5.18 Linear relation between evacuation time and the number of evacuees

However, judging from Fig. 5.18 and the comparisons of evacuation speed, space utilization rate, and the density of people in previous chapters, we can notice that although parameters, including space utilization rate and the density of people, change obviously with the increase of people, the overall evacuation time does not show such a clear change, as the characteristic shown in the comparison of Fig. 5.1. This characteristic suggests that the number of evacuees in subregions is not a crucial element in the time analysis of people evacuating from inside the residential area to the city road network in regional evacuation analysis. Therefore, it is not necessary to accurately calculate the number of residences.

Although an accurate calculation of evacuee number is not necessary, the time of people evacuating to the road network is still closely related to the intrinsic properties of the community, including its patterns and forms. Therefore, it is necessary to consider the evacuation time inside each residential area or each subregion, which is also the differences in loading time.

5.4.2   The Estimation Method of Evacuation Time in Subregions

Individual analysis is employed in LEGION vector simulation process, and the simulation involves detailed information of building types, specific buildings, and the mesoscopic parameters of the section. Since the method considers all individual information of every evacuee, the calculation process is very complex and time-consuming, unable to support a fast simulation and optimal analysis in subregion evacuation. Therefore, we need a better approach to estimate the overall evacuation time of the subregions as well as the evacuation time for the first evacuee to reach the exit of the community.

In most cases, it is difficult to get detailed information of the residence number inside each building and the construction type within a community or city. However, it is still possible to estimate the overall evacuee number within one community or a subregion. In this character, a time model to calculate the loading time for people to get into the city road network is proposed, which is only based on the following parameters: the characteristics of buildings (high-rise, multi-story, or low-level buildings), exit number, the width of entrance, and overall number of people.

Suppose the time people need to pass the exit of subregion and get loaded to the city road network $t_{loading}$ is between t_0 and t_{ev}, that is

$$t_0 \leq t_{loading} \leq t_{ev} \tag{5.6}$$

in which

> t_0 denotes the time when the first evacuee arrives at the subregion exit, s;
> t_{ev} denotes the overall evacuation time, also the time duration till the last evacuee leaves the exit of subregion, s.

The overall evacuation time mainly consists of the time evacuees need to get out of the building and the time to reach the subregion exit:

$$t_{ev} = t_1 + t_2 \tag{5.7}$$

in which

> t_1 denotes the overall time for a person to get out of the building, s;
> t_2 denotes the time a person needs to get to the subregion exit, s.

Based on empirical formula for overall time calculation, the time of people moving out of the building, the time for moving to the exit of the subregion, and the time the first evacuee needs to get to the exit of subregion can be obtained.

(1)   Time calculation of evacuees to get out of the building

The time an evacuee needs to leave the building is closely related to various parameters, including the number of people inside the building, the total area of the building, its plane area, the number of floors, plot radio, and the types of building (e.g., residential building, shopping malls, etc.), and it can be obtained through Melink and Booth formula.

If we assume a same number of people on each floor and a same width of floor, when taking the time of other actions evacuees may take (such as locking the door) into consideration, the formula can be changed into:

$$t_1 = N \big/ (f b) + n t_s + t_a \tag{5.8}$$

in which

> n refers the floor number of the building, and if it is a single-story building, $n = 0$;
> N refers to the number of people on a unit floor inside a unit block;
> f denotes the unit width flow or passing rate through the entrance of the building;
> b denotes the width of a unit entrance of the building;
> t_s denotes a person descending to a lower floor, usually takes around 16 s;
> t_a denotes the time other actions may take during the evacuation, for example, locking the door, which can be estimated at around 30 s.

(2)   Time calculation of evacuees to move to the exit of the community

The time residences need to get to the community exit from outside the building is closely related to the size of subregions, the width of roads and the density of road network, as well as the walking speed of residents, and it can be calculated through Togawa formula. We take the subregion in Fig. 5.19 as an example, and suppose the overall population inside the building is P. When the evacuees come out from the building, they may choose different subregion exit according to their judgment of distance and degree of familiarity. Suppose the number of people at Exits 1, 2, 3 and 4 of the subregion is P_1, P_2, P_3, and P_4, respectively, and the distance of the building to each exit is L_1, L_2, L_3, and L_4. Based on the shortest path selection, we take that evacuees choose their exit only based on the distance. In this case, people from one building are highly possible to choose the same exit of the community, as shown in Fig. 5.19, all the evacuees choose Exit 1. If other influence factors are considered, such as degree of familiarity and other social causes, people might choose other exits. Therefore, the time duration for evacuees to move from building j to get to exit I of subregion can be calculated according to Eq. (5.9).

$$t_e = \frac{P_{i,j}}{b_i f_i} + \frac{L_i}{\upsilon} \tag{5.9}$$
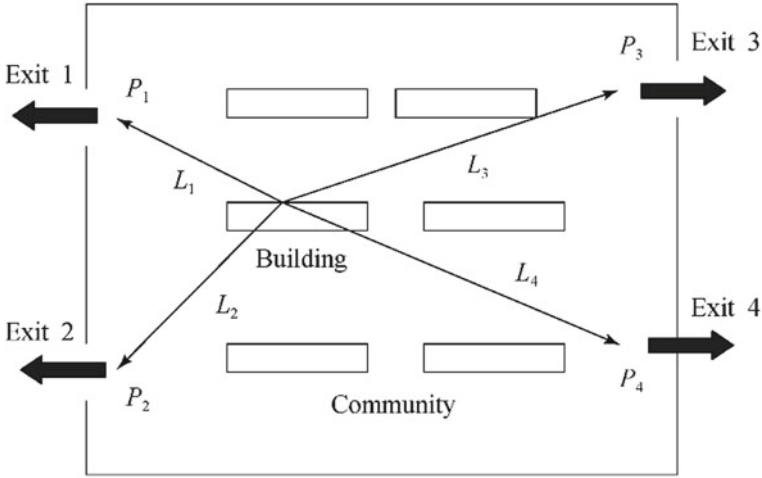
Fig. 5.19 Evacuation paths and exits inside a subregion

in which

> $P_{i,j}$ denotes the time of an evacuee getting to exit i from the entrance of the jth building;
> b_i denotes the exit width of the ith subregion;
> f_i denotes the flow of evacuees passing through the exit of the ith subregion;
> L_i denotes the distance between the building and the exit of the ith subregion;
> υ denotes the flow speed of people.

If ergodic is employed to all the buildings, the maximum evacuation time can be obtained as follows:

$$t_2 = \max\left(\frac{P_{i,j}}{b_i f_i} + \frac{L_i}{\upsilon}\right) \tag{5.10}$$

If there is no individual characteristic analysis, and only overall parameters of the subregional are employed, we need to simplify Eq. (5.10) to get the duration of evacuating residences to reach the exit of the subregion:

$$t_2 = \phi_1 \frac{N_t}{bf} + \phi_2 \frac{L}{\upsilon_0} \tag{5.11}$$

in which

> N_t refers to the total number of evacuees in the subregion;
> b refers to the total width of the subregion, m;

f refers to the flow or passing rate of people from a unit width, number of people/(m s);

L refers to the characteristic length of the subregion, and if the area is a rectangle, we take its characteristic length as half of its diagonal length, m.

(3) Time calculation of the first evacuee to reach the exit

The time first evacuee to reach the exit of the community can be calculated through the following formula:

$$t_0 = \frac{L_{\min}}{\upsilon_0} + t_a \tag{5.12}$$

in which

$L_{\min}$ denotes the shortest path from the ground floor entrance to the subregion exit;

υ_0 denotes the moving speed of evacuees, when it is not crowded, usually around 1.2–1.4 m/s.

The speed of the flow, the unit width flow, and other parameters should be determined using empirical formula to calculate the duration of evacuation, which could be obtained through referencing to existing empirical formulas or technical standards.

5.5 Conclusion

This chapter summarized the theoretical basis of evacuation study and chose a residential area of Wanhua Group, located in Yantai, as an example, which is of northeast orientation. The change of evacuation characteristics, including evacuation time, evacuation speed, space usage, and personnel density in this residential area, was simulated and analyzed through using the LEGION vector simulation under the four evacuation scales. The following conclusions have been drawn: In regional evacuation analysis, the number of residents from subregions should not be taken as a crucial factor in analyzing the evacuation time for urban road network; therefore, it is not necessary to estimate the residents number accurately. However, decision-makers should take into consideration the differences in forms and attributes of the subregions, as well as the time needed for each area to evacuate. Moreover, basic approaches for a fast estimation of subregional evacuation time based on empirical formula were proposed.

References

Gloor, C, P, Stucki and Kai, N. 2004. Hybrid techniques for pedestrian simulations. In: *4th Swiss transport research conference.*

Hou, J., W. Gai, W. Cheng, and Y. Deng. 2020. Prediction model of traffic loading rate for large-scale evacuations in unconventional emergencies: a real case survey. *Process Safety and Environmental Protection* 144: 166–176.

Lindell, M.K. 2008. EMBLEM: An empirically based large-scale evacuation time estimate model. *College Station TX: Texas A and M University Hazard Reduction and Recovery Center* 42 (1): 140–154.

Melinek, S.J, S Booth. 1975. An analysis of evacuation times and the movement of crowds in buildings. *Building Reseach Establishment, Fire Reseach Station, Borehamwood.*

Pauls, J.A. 1999. Personal perspective on research, consulting and codes/standards development in fire-related human behaviour, 1969–1999, with an emphasis on space and time factors. *Fire and Materials, Fire Material* 23: 265–272.

Togawa, K. 1995. Study of fire escapes basing on the observation of multitude current. Report No. 14, Building Research Institute, Ministry of Construction, Tokyo.

Wang, C. 2007. *Study on safety evacuation during the fire at a subway station.* Beijing Jiaotong University (in Chinese).

Yantai Bureau of Statistics. 2008. *Statistical bulletin of national economic and social development of Yantai in 2007.*

Zhu, X. 2006. Summary of passenger flow simulation software for rail transit station. *Underground Engineering and Tunnel* (04): 44–45 + 49 + 53 (in Chinese).

Zipf, G.K. 1949. *Human behavior and the principle of least effort.* Cambridge MA: Addison-Wesley.

Appendix A
Optimal Route Planning Results for Each Node Based on Model I and Model II

Optimization model	Model I			Model II		
Optimization objectives	Mitigation of health consequences			Minimizing transfer time		
Optimization goals	Route	Dose	Transfer time/min	Route	Dose	Transfer time/min
	1 → 11 → 16 → 18 → 13 → 9 → 14 → 15 → 20	8.88E+10	33.94	1 → 11 → 16 → 17 → 18 → 19 → 20	9.29E+10	13.65
	2 → 7 → 8	4.41E−17	3.54	2 → 7 → 8	4.41E−17	3.54
	3 → 4 → 8	4.09E−17	3.76	3 → 8	4.75E−17	1.83
	4 → 8	3.83E−17	1.48	4 → 8	3.83E−17	1.48
	5 → 10 → 15 → 20	1.52E+08	11.23	5 → 10 → 15 → 20	1.52E+08	11.23
	6 → 12 → 8	1.44E+10	2.31	6 → 12 → 8	1.44E+10	2.31
	7 → 8	3.77E−17	1.45	7 → 8	3.77E−17	1.45
	8	0	0	8	0	0
	9 → 14 → 15 → 20	1.47E+08	8.43	9 → 14 → 15 → 20	1.47E+08	8.43
	10 → 15 → 20	1.52E+08	8.07	10 → 15 → 20	1.52E+08	8.07
	11 → 16 → 18 → 20	6.52E+08	13.49	11 → 16 → 17 → 18 → 19 → 20	4.34E+09	11.07
	12 → 8	224	2.04	12 → 8	224	2.04
	13 → 8	127	3.65	13 → 8	127	3.65
	14 → 15 → 20	1.47E+08	7.20	14 → 15 → 20	1.47E+08	7.20
	15 → 20	1.42E+08	5.76	15 → 20	1.42E+08	5.76
	16 → 18 → 20	5.68E+08	9.81	16 → 17 → 18 → 20	3.82E+09	8.13
	17 → 12 → 8	7.71E+08	3.47	17 → 12 → 8	7.71E+08	3.47
	18 → 20	2.37E+08	2.95	18 → 20	2.37E+08	2.95
	19 → 20	2.02E+08	2.46	19 → 20	2.02E+08	2.46
	20	0	0	20	0	0

Appendix B
Multi-objective Optimization Results of Emergency Route Selected Based on Model III

Route	Dose	Transfer time/min	Route	Dose	Transfer time/min
1 → 11 → 16 → 18 → 19 → 20	8.88E+10	15.71	11 → 16 → 18 → 20	6.52E+08	13.49
2 → 7 → 8 → 13 → 19 → 20	2.84E+08	12.12	12 → 8 → 4 → 9 → 14 → 15 → 20	1.47E+08	15.51
3 → 4 → 9 → 14 → 15 → 20	1.47E+08	13.97	13 → 9 → 14 → 15 → 20	1.47E+08	10.85
4 → 9 → 14 → 15 → 20	1.47E+08	11.65	14 → 15 → 20	1.47E+08	7.20
5 → 10 → 15 → 20	1.52E+08	11.23	15 → 20	1.42E+08	5.76
6 → 12 → 8 → 13 → 19 → 20	1.47E+10	13.16	16 → 18 → 20	5.68E+08	9.81
7 → 8 → 4 → 9 → 14 → 15 → 20	1.47E+08	14.86	17 → 13 → 9 → 14 → 15 → 20	1.69E+09	14.00
8 → 4 → 9 → 14 → 15 → 20	1.47E+08	13.23	18 → 20	2.37E+08	2.95
9 → 14 → 15 → 20	1.47E+08	8.43	19 → 20	2.02E+08	2.46
10 → 15 → 20	1.52E+08	8.07	20	0	0